STUDIES ON NUCLEAR INSTRUMENTATION FOR PULSED REACTORS

by

Toshiyuki IIDA

Department of Nuclear Engineering,

Faculty of Engineering,

Osaka University

Suita-shi, Osaka

1978

Contents

Chapter I Introduction

1-1 Intense Pulsed Neutron Sources

The availability of a device for generating either single or repetitive intense bursts of neutrons is the basic requirement for a wide variety of experiments for fundamental and applied researches in the field of nuclear engineering. The extensive application of time-of-flight methods in the field of neutron spectroscopy is the typical example of this. Another example is found in the study of transient thermal processes in reactor fuel elements, where the requirement for an effectively instantaneous heat input of given intensity under the selected test conditions can be adequately satisfied by an intense neutron pulse whose width is comparable to the characteristic relaxation time of the effect caused by a reactivity accident.

Methods used for generating such intense bursts of neutrons include the following ways; 1) the use of neutron beams, which are supplied by the conventional steady high flux reactor, in combination with choppers, 2) the use of intense accelerators such as an electron linear accelerator, with a target appropriate for the (p,n), (d,n), (α,n) or (γ,n) reaction , 3) the use of pulsed reactors designed either for repetitive or single pulsing and 4) the use of intense accelerators in combination with pulsed reactors.

A survey of intense pulsed neutron sources in operation or under development shows a wide variety of types, designs and pulsing characteristics, which make the classification difficult. However, it is safe to say that such a device can be operated

with the pulse width from 100 ms to a few nano seconds and at the neutron intensity higher than 10^{14} neutrons/cm^2 sec (pulse peak value).

1-2 Pulsed reactors in Japan

In general, the definition of " a pulsed reactor " is the followings: a nuclear reactor designed for producing intense bursts of neutrons for a short interval of time by means of the insertion of positive reactivity exceeding the prompt critical during a very short time.

In Japan, the first one-shot thermal pulsed reactor, HTR-P[1] (Hitachi Training Reactor - P) served with 100 ms pulse width to experiments on self-limiting power excursion characteristics of light water reactors since 1967. The second one-shot thermal pulsed reactor, NSRR [2] (Nuclear Safety Research Reactor), has been operating as the highest peak power pulsed reactor in the world since August 1975. This reactor is an ACPR type reactor and has contributed to the investigation of fuel behaviour under the reactivity initiated accident conditions with the pulse width of 5 ms.

The first one-shot fast pulsed reactor, the YAYOI-P [3], which went over the prompt critical in 1975, has been operated with the two pulse widths of about 100 μsec and a few seconds. Additional mechanisms of six different reactivities for pulsing in various ways make it possible to be used for researches in reactor kinetics, safety, detector development, radiation effects etc.. The JLB (Japan Linac Booster), a planning facility is a repetitive pulsed fast reactor. The JLB is a Linac-driven,

boosted system and will be used for studies in nuclear physics, solid state physics, neutronics, radiation chemistry, etc.. The summary of JLB designed characteristic is the followings.

Effective thermal neutron flux	= 1×10^{16} n/cm^{2}sec
Pulse width of fast neutron flux	= 10 μsec
Pulse width of thermal neutron flux	= 10 ~ 30 μsec
Repetition rate	= 5 ~ 200 pps
Reactivity insertion	= -4$ subcritical to 1$ supercritical
Average power	= 2 MW
Peak pulsed power to back ground power	= 10^4

The JLB project was adopted by Science Council of Japan as one of the major university nuclear research programs for future. The basic researches have been carried out at Osaka University and other institutes. The major parts of this work are carried out as contributions to the researches and developments for this JLB project. In addition, there is a plan of developing an intense pulse neutron source by the use of a proton synchrotron with uranium booster at KEK (National Laboratory for High Energy Physics). This neutron source is also expected to be able to produce about one tenth of a peak power of the pulsed reactor JLB.

1-3 Required Instrumentation for Pulsed Reactors.

A rapid response and stable neutronic power monitor system with wide measuring ranges has clearly become the most important nuclear instrumentation for pulsed reactors. For safe operations and versatile applications of intense sources, the accurate measurement of pulsed output shapes is essential. Even for a conventional steady reactor, the rapidness and the stability of electronic instruments in a neutronic transient power monitor are very favourable.

Precise reactor powers are generally determined by instantaneous measurement of the intensity of radiation generated from reactors. There are two fundamental systems for measuring the intensity of radiation and they have been both used for nuclear instrumentation of conventional steady reactors. One is composed of a pulse counter such as a fission counter or a BF_3 proportional counter, pulse amplifier equipments to shape current signals from the counter, a scaler and a recorder. The block diagram of this system is shown in Fig. 1-1. This system is excellent in the removal of gamma ray background and external electronic noises. It has been employed at low power level, where the level of gamma ray background is very high due to delayed gamma rays generated from fission products in fuels. But, excessively high counting rate distorts the linearity of this system, since this system has inherently a dead time. The other system is composed of a current-type ionization chamber, an electrometer to amplify the chamber current and a

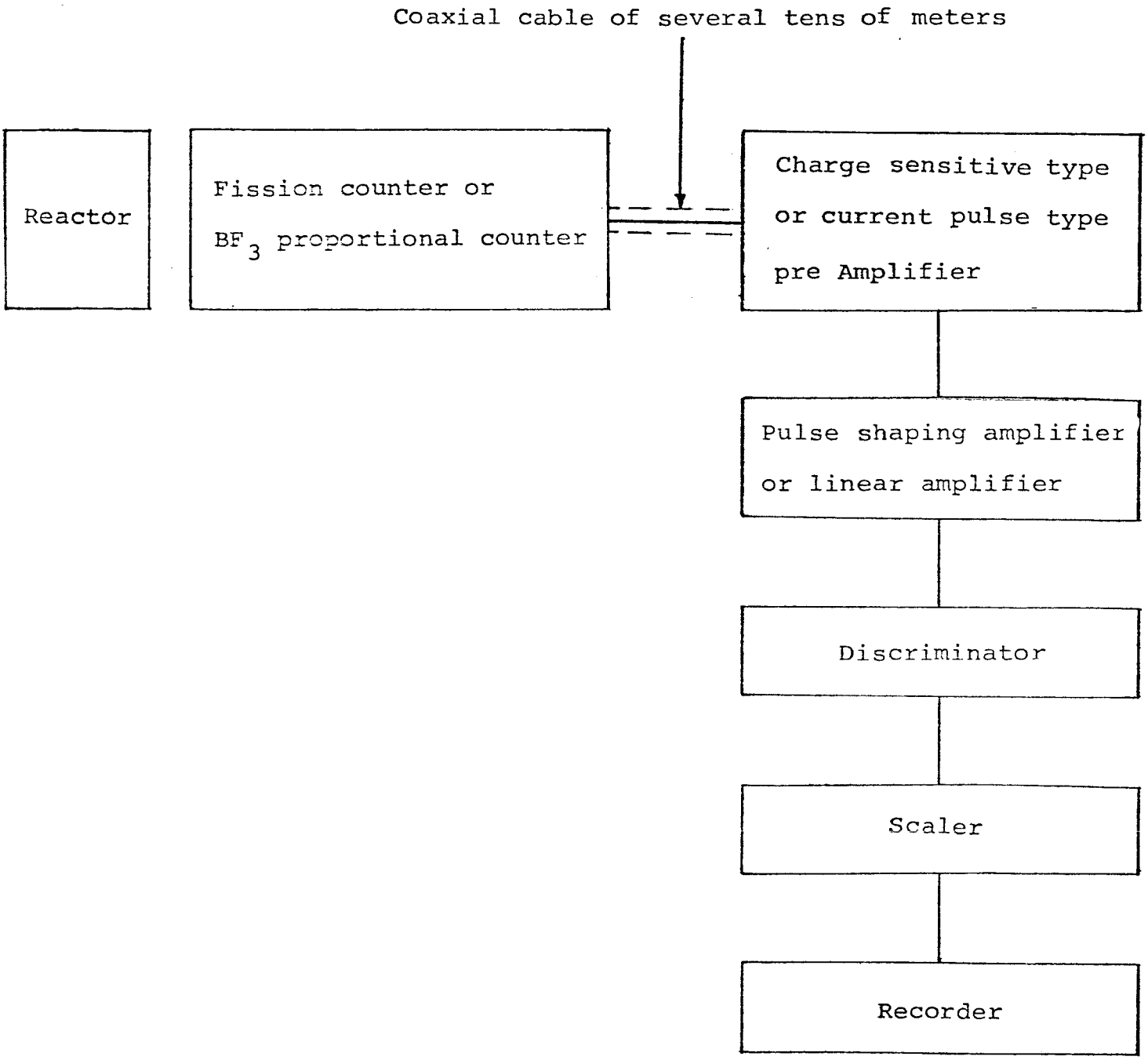

Fig. 1-1 Pulse counting system of nuclear instrumentation for reactors.

recorder. The block diagram of this system is shown in Fig. 1-2. The output current of the ionization chamber is the result of the pile of many elementary current pulses induced by detection of radiation, so that the ionization chamber can be used in the range of very high counting rate. This system has disadvantage of slow response time in comparison with that of the pulse counting system. The response time of this system is mainly determined by that of the electrometer to amplify the low output current of the chamber. Table 1-1 gives the rise times and the available counting rates of the main amplifiers of these two systems.

Now let us consider nuclear instrumentation for pulsed reactors. In order to observe the precise power shapes of pulsed reactors, it requires fast responsiveness and sufficiently statistical accuracy based on high counting rate. Figure 1-3 [5] shows the measured results of power shapes of the pulsed reactor YAYOI by the two systems . Both shapes in Fig. 1-3 are normalized at the low power level. There is also no time lag between both shapes since they were measured by the use of the same trigger signal from the pulse operation system of the reactor. It is evident from the comparison of the two shapes that statistical inaccuracy at low power level and saturating effect due to counting loss at high power level are found in the pulse counting system. Even if the fastest and very expensive pulse amplifier equipments are introduced into the pulse counting system, the available counting rate of this system should be limited to 10^8 cps. Hence it is difficult for even this fast

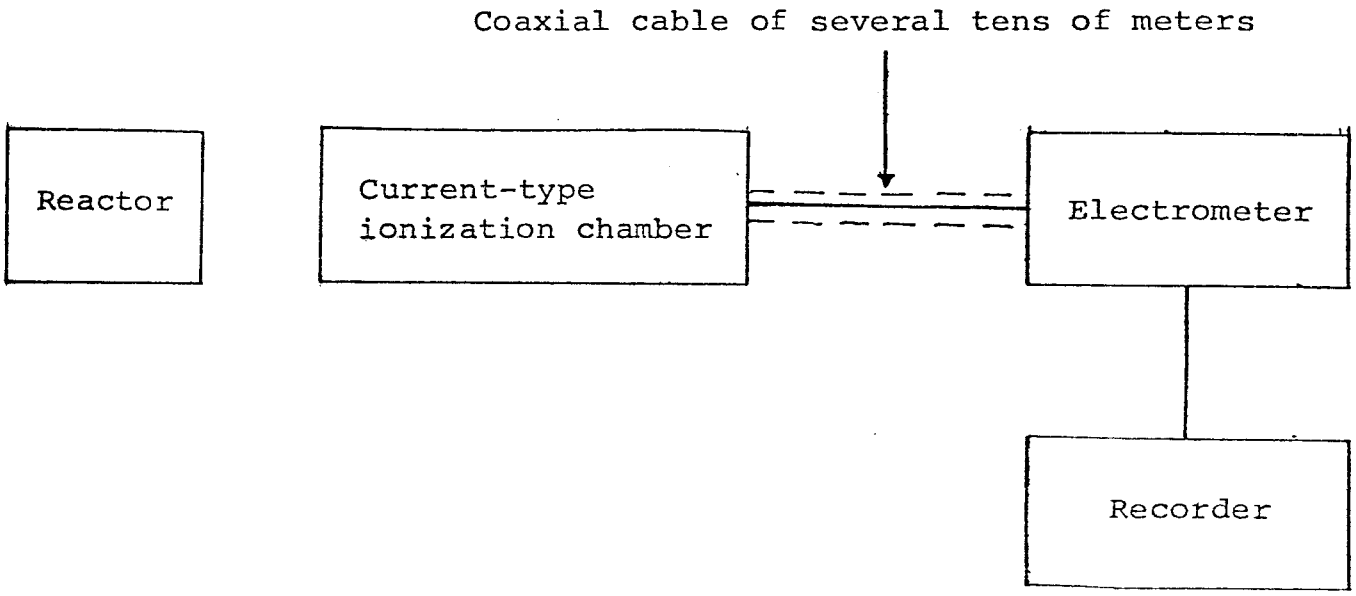

Fig. 1-2 Ionization Chamber-Electrometer System of Nuclear Instrumentation for reactors.

Table 1-1 The rise times and available counting rates of the main amplifier of nuclear instrumentation for reactors.

System	Amplifier	Rise time	Available counting rate
Pulse counting system	Current pulse amplifier	$\approx$ 5 nsec	$< 10^7$
	Charge sensitive amplifier	$\approx$ 30 nsec	$< 10^4$
Ionization chamber system	Electrometer	$>$ 0.5 μsec	$< \infty$

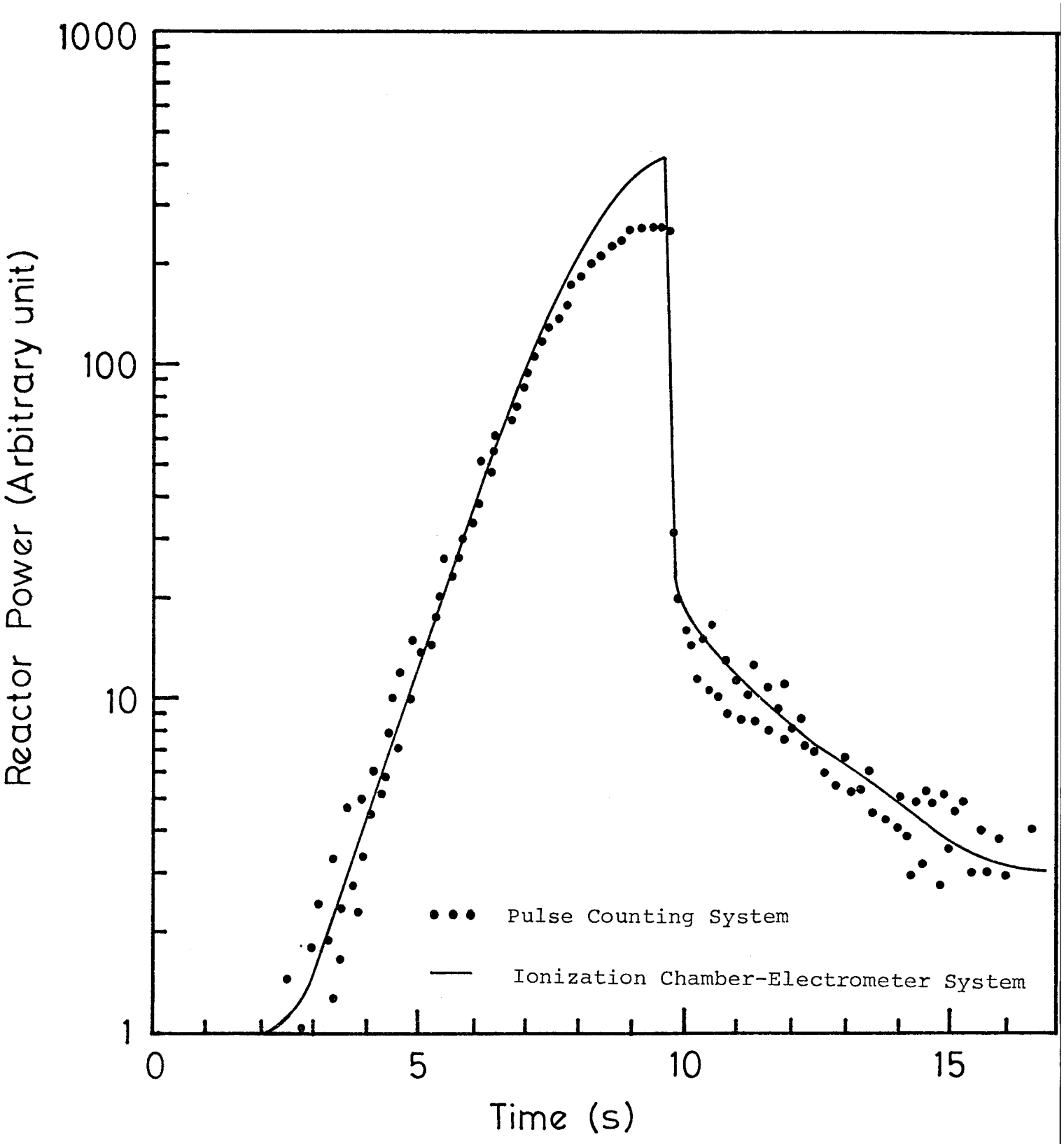

Fig. 1-3 An example of the measured results of power shapes of the YAYOI.

system to measure the precise one-shot power shape of which pulse width is narrower than 1 msec. Thus, the pulse counting system suffers from the statistical inaccuracy in the measurement of power shapes of the one-shot pulse reactors. On the other hand, an ionization chamber easily permits obtaining a very high counting rate of 10^{12} cps, which is equivalent to an output current of about 1 mA. The ionization chamber-electrometer system is much superior to the pulse counting one in point of counting rate, and hence the former system should be mainly applied to the nuclear instrumentation for the pulsed reactors.

Remarkable improvements can be expected in reliability and rapidness by increasing the neutron detection effeciency of an ionization chamber. For fast pulsed reactors, the neutron detecting efficiency of an ionization chamber with the 1/v type neutron energy response is improved largely by introducing a suitable neutron moderator layer. The sensitibity can be improved by reducing the incident neutron energy through the neutron moderator, within the permissible broadening in the observed pulse width of the reactor power. Figure 1-4[6] gives the experimental result of the detection efficiency and the pulse width versus the moderator thickness in the case of a hydrogenous moderator with B^{10} coated detector.

The purpose of this paper is to clarify factors in the determination of the response time of the ionization chamber-electrometer system and, moreover, to design a fast response nuclear instrumentation for pulsed reactors. First, the transfer function of an ionization chamber is discussed in

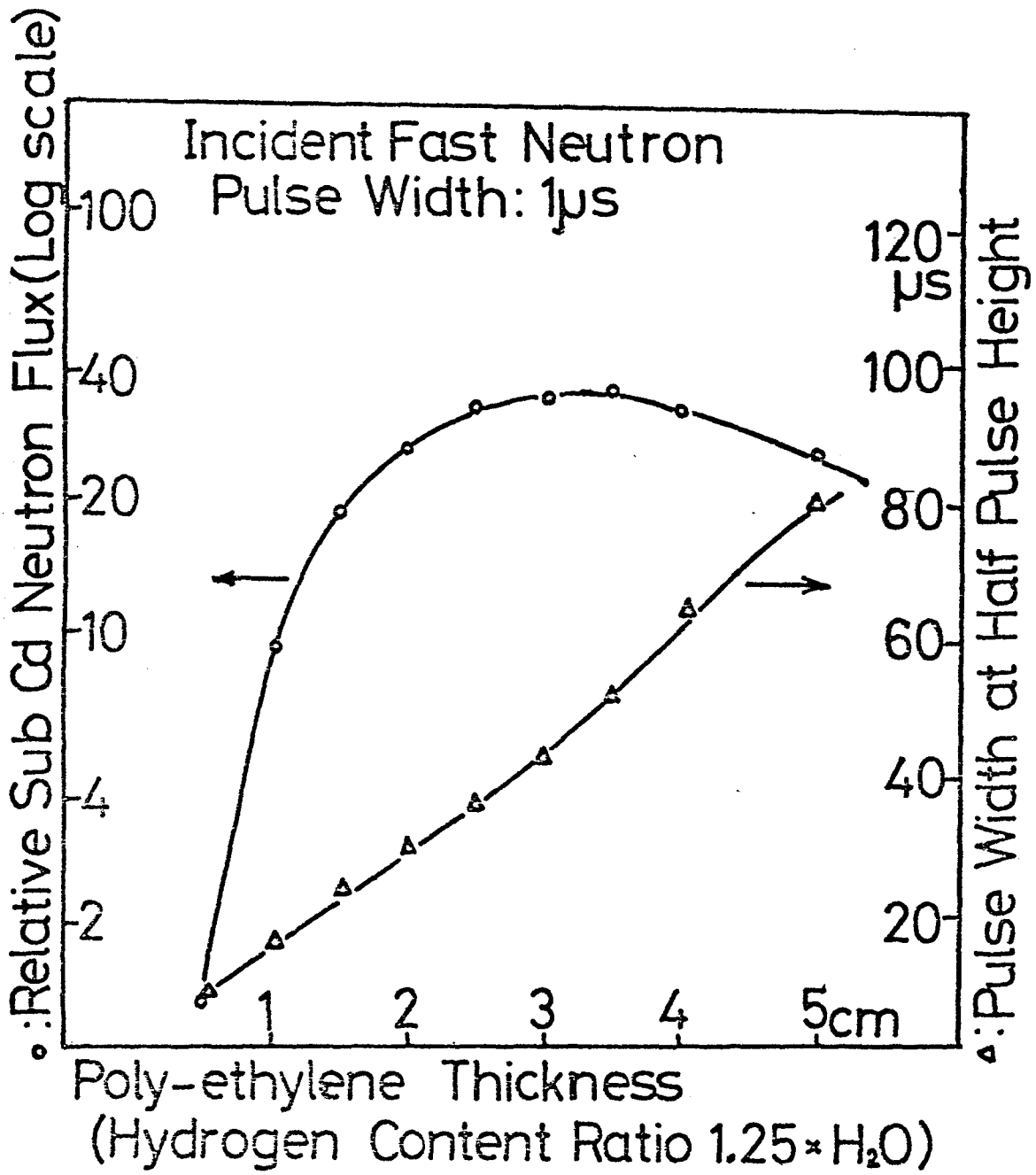

Fig. 1-4 An example on increase of neutron detection efficiency and pulse width broading with a moderator layer (poly-ethylene)

Chapter II and the relation between the transfer function and the transit times of positive ions and electrons is clarified from the results obtained by the use of a linear accelerator. This will be useful for the development of a fast response ionization chamber for pulsed reactors. Chapter III describes the response speed of a linear electrometer to amplify a chamber current. The relations between the response speed and measuring conditions, that is, the length of a detector cable, current sensitivity and so on , are obtained from the equivalent circuit analysis. Moreover, a fast response linear electrometer circuit with a new technique for reducing a cable capacitance is illustrated and it has been successfully applied to the measurements of power shapes of the YAYOI. Chapter IV shows that the response time of a logarithmic electrometer is severely limited due to the strong current dependency of the resistance of a logarithmic element. A new technique of using a current-dependent impedance element for the phase compensation of a logarithmic electrometer is discussed to cope with this problem, and a newly designed logarithmic electrometer has been also successfully applied to the measurements of power shapes of the YAYOI. In chapter V, the instantaneous measurement of a reactor period which is closely related to the reactivity inserted to a pulsed reactor is described. A fast response log N & period meter circuit which has been developed in order to measure a time-dependent reactor period is shown. Some examples of the measured results of the instantaneous prompt periods of the NSRR and the YAYOI are illustrated.

In the last chapter, the whole of this work is summarized. It is also shown that the newly designed power monitering system with above techniques has been adopted as the nuclear instrumentation for the NSRR and the YAYOI, and that it is moreover necessary to develope a fast response ionization chamber for that of the JLB.

References

1) M. Imai, et al., J. Nucl. Sci. Technol. 6 [2], (1969) 69.

2) S. Saito, et al., J. Nucl. Sci. Technol. 10 [12], (1973) 739.

3) H. Wakabayashi, et al., Proc. US/Japan Seminar on Fast Pulse Reactors I-2 (1976).

4) J. Wakabayashi, ibid., I-3 (1976).

5) T. Iida, N. Wakayama and K. Sumita, Proc. for Symp. on Intense Pulsed Neutron Sources in Japan, Py-5 (1975).

6) K. Sumita, T. Iida, et al., Proc. US/Japan Seminar on Fast Pulse Reactors III-1 (1976).

Chapter II Transfer Function of Ionization Chambers [1)]

2-1. Introduction

Many experiments have been made for the investigation of reactor safety at the pulsed reactors of the NSRR , the YAYOI[2)] and others. In order to obtain precise data in those transient experiments, measuring systems for radiation require fast responsiveness and sufficiently statistical accuracy based on high counting rate. There are two typical systems for measuring the intensity of radiation. One is composed of a current-type ionization chamber and an electrometer to amplify the chamber current, and the other composed of a pulse counter such as a fission counter or a proportional counter, pulse amplifier equipments to shape current pulses from the counter and a scaler. The former system permits obtaining very high counting rate but the latter one has inherently a dead time resulting in counting loss. Therefore, ionization chamber systems have been used preferably for measuring narrow pulse of intense radiation.

The response of the ionization chamber is distorted by the effect of the positive ion transit time, which is the time taken for positive ions to move the interval between the electrodes, in the case that pulse width of radiation is smaller than several hundreds of microseconds. Hence it has become important in recent pulsed reactor experiments to determine the precise response time of the ionization chamber.

With respect to the determination of the transfer function of the ionization chamber, R. Subramaniam and R. Vedam [3)] measured the frequency response by beam modulation and also S. Gotoh [4)] obtained that by utilizing uncorrelated reactor noise. These measurements

can contribute to obtaining general frequency characteristics like break frequency of the ionization chamber, but those methods are not sufficient to determine the precise transfer function in very high frequency region. Those measurements in frequency domain cannot give effective data on the transit times which are expected to be closely related to the transfer function. The precise data on these transit times should be obtained by measurement in time domain rather than in frequency one. This chapter analyzes the impulse response of the ionization chamber measured using intense gamma ray pulses produced by a linear accelerator and clarifies the relation between the transfer function and the transit times of positive ions and electrons. Moreover the fluctuation current induced by random detection of radiation is also discussed based on the measured transfer function.

2-2. Transfer Function

A current pulse of the ionization chamber is formed whenever a charged particle passes through the gap between the electrodes and the resultant electron-ion pairs are swept to the electrodes by an applied electric field. From the principle of the conservation of energy, the external current induced by point electronic charge $\pm Q_0$ moving toward each electrodes is given by the following equation after A. H. Snell [5].

$$i_0 = \frac{1}{V}\left(Q_0 E W_i - Q_0 E W_e\right) , \qquad (2\text{-}1)$$

where V is the applied voltage,

E the strength of the electric field,

w_i the drift velocity of positive ions and

w_e the drift velocity of electrons.

Hence, taking the numbers of positive ions and electrons produced by a single detection of radiation in a unit volume $d\mathbf{r}$ at a location $\mathbf{r}$ and time t to be $n_i(\mathbf{r},t)d\mathbf{r}$ and $n_e(\mathbf{r},t)d\mathbf{r}$ respectively, we obtain the following equation for the elementary current pulse of the ionization chember.

$$i(t) = \frac{1}{V}\int_R \left\{ q_0 n_i(\mathbf{r},t) E(\mathbf{r},t) w_i(\mathbf{r},t) - q_0 n_e(\mathbf{r},t) E(\mathbf{r},t) w_e(\mathbf{r},t) \right\} d\mathbf{r}, \quad (2\text{-}2)$$

where R is the total space of the ionization chamber and q_0 the elementary electronic charge. Ionization chambers used in reactor instrumentation are generally cylindrical in shape but the electrode structure is considered to be approximately of parallel-plate, since the interval d between the electrodes is much smaller than the radii of the electrodes. Consequently, the strength of the electric field between the electrodes becomes

$$E = \frac{V}{d} \quad . \quad (2\text{-}3)$$

As is well known, the drift velocities of positive ions and electrons are also given by

$$w_i = \mu_i \frac{E}{P} = \mu_i \frac{V}{Pd} \quad , \quad (2\text{-}4)$$

$$w_e = \mu_e \frac{E}{P} = \mu_e \frac{V}{Pd} \quad , \quad (2\text{-}5)$$

where p is the pressure of the enclosed gas, μ_i the mobility of positive ions and μ_e that of electrons. Here it is assumed that the density distributions of positive ions and electrons produced directly after a single detection of radiation are uniform along a track. When the ionization chamber is operated under saturated condition, the effects of the recombination and the electron attachment are negligible. Then taking the total charge produced by the detection of radiation to be $\pm \frac{Q}{2}$, we obtain a simplified expression as a substitute for Eq.(2-2).

$$\left.\begin{aligned} i(t) &= \frac{Q}{T_i}\left(1-\frac{t}{T_i}\right)+\frac{Q}{T_e}\left(1-\frac{t}{T_e}\right) && \text{for } 0 \le t \le T_e \\ &= \frac{Q}{T_i}\left(1-\frac{t}{T_i}\right) && \text{for } T_e \le t \le T_i \\ &= 0 && \text{for } T_i \le t \end{aligned}\right\}, \tag{2-6}$$

where

$$T_i = \frac{p d^2}{\mu_i V}, \tag{2-7}$$

$$T_e = \frac{p d^2}{\mu_e V}, \tag{2-8}$$

The value of Q varies according to the direction of a track and it is therefore expected to be statistically distributed. In the case that the direction of a track is nearly parallel to the electrodes, the elementary current pulse cannot be expressed by Eq. (2-6). However such cases seldom take place and are therefore ignored in this chapter. Here T_i is the transit time of positive ions and T_e that of electrons. These times are not zero, so that the response

of ionization chamber must be evaluated with distortion to the narrower radiation pulses than these transit times.

Now let us consider the output current of the ionization chamber set up in a radiation field. The output current is the result of the pile of many elementary current pulses. Though all shapes of elementary current pulses are not practically equal, it is assumed that they are all represented as the expression (2-6) with Q replaced by average charge $\bar{Q}$ to simplify the determination of the transfer function of the ionization chamber for the following reasons and experimental results in next section. First the transit times of positive ions and electrons are constant except in the special case that the direction of a track is nearly parallel to the electrodes. Secondly the total electronic charge is fixed independently of the intensity of incident radiation and time. Taking radiant flux density at time t to be $\phi(t)$, we can obtain the output current of the ionization chamber as follows.

$$i_c(t) = \int_0^t \varepsilon \phi(t-t') \frac{\bar{Q}}{Q} i(t')\, dt' \qquad (2\text{-}9)$$

where ε is the detection efficiency, which is determined by the total cross section of the reaction materials of the ionization chamber. Then we can take the Laplace transform of both sides with respect to t and the transfer function of the ionization chamber is given by

$$G(S) = \frac{I_c(S)}{\Phi(S)} = \varepsilon \bar{Q} \left\{ \frac{1}{T_i^2 S^2}(T_i S - 1 + e^{-T_i S}) + \frac{1}{T_e^2 S^2}(T_e S - 1 + e^{-T_e S}) \right\}, \qquad (2\text{-}10)$$

where $I_c(S)$ is the Laplace transform of $i_c(t)$, $\Phi(S)$ that of $\phi(t)$ and S the Laplace transform variable. This equation shows that the transfer function of the ionization chamber is mainly expressed by the transit times of positive ions and electrons.

2-3. Transit Time Measurement

It is evident from Eq.(2-9) that the impulse response of the ionization chamber is expressed by Eq.(2-6). The impulse response is characterized by the two functions of the first degree with respect to time as shown in Fig. 2-1. One is based on the positive ion component and the other based on the electron one. Hence the measurement of the impulse response of the ionization chamber should clarify the relation between these transit times and the transfer function.

Figure 2-2 shows the instrumentation for measuring the impulse response of the ionization chamber. As is well known, the drift velocity of positive ions is much slower than that of electrons and hence the impulse response due to the positive ion component was first measured. The ionization chamber used in this experiment was a gamma ray compensated type Westinghouse model 8074 and the compensating electrode was grounded. The specification of the ionization chamber are given in Table 2-1. Gamma ray pulses of about 2 μsec produced by the linear accelerator KUR-LINAC [6] were used for input signals. The pulses were regarded as impulses for the positive ion component since the pulse width was much narrower than the positive ion transit time.

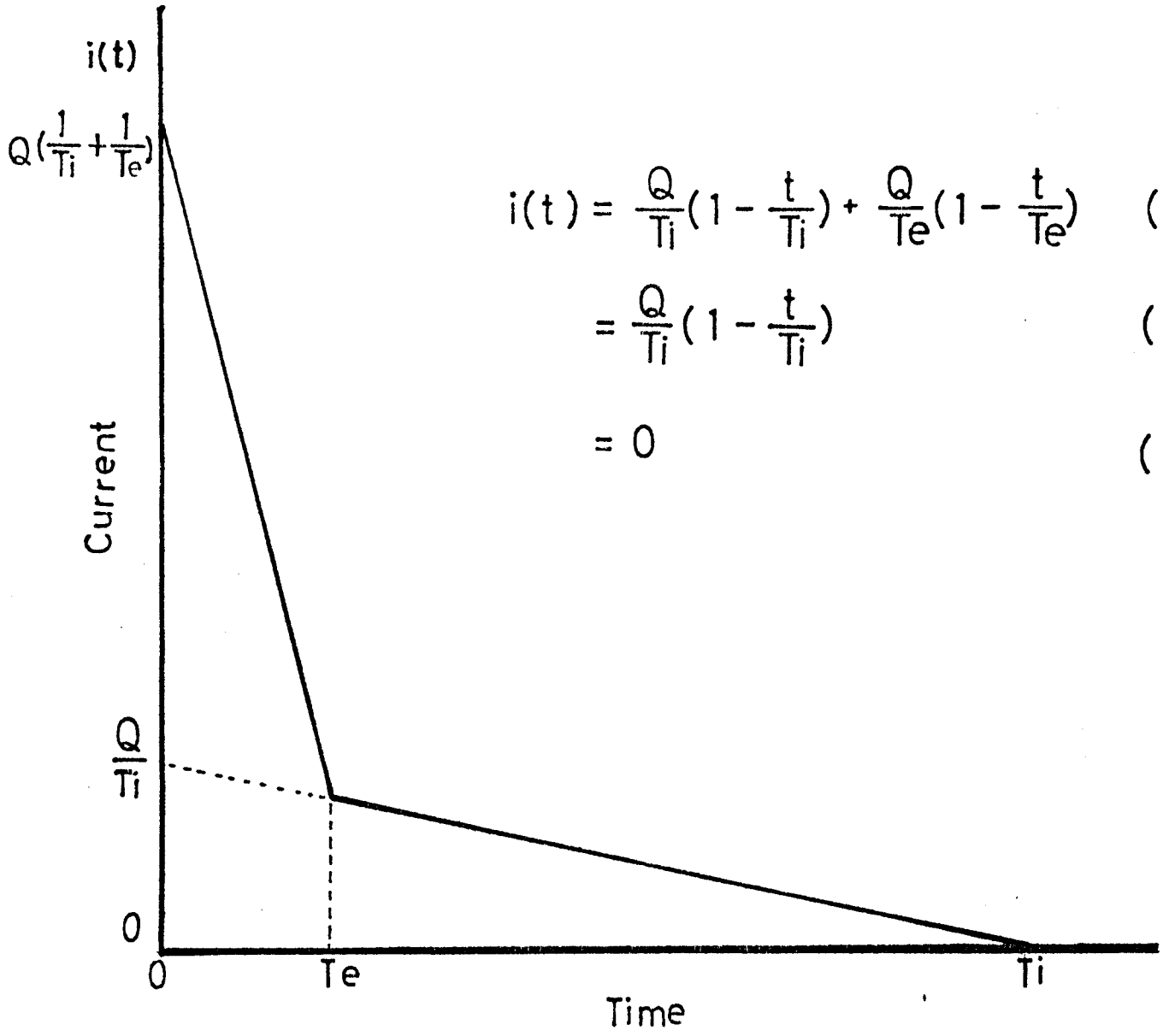

$$i(t) = \frac{Q}{Ti}(1-\frac{t}{Ti}) + \frac{Q}{Te}(1-\frac{t}{Te}) \quad (0 \le t \le Te)$$

$$= \frac{Q}{Ti}(1-\frac{t}{Ti}) \quad (Te \le t \le Ti)$$

$$= 0 \quad (Ti \le t)$$

Fig.2-1 The elementary current pulse shape

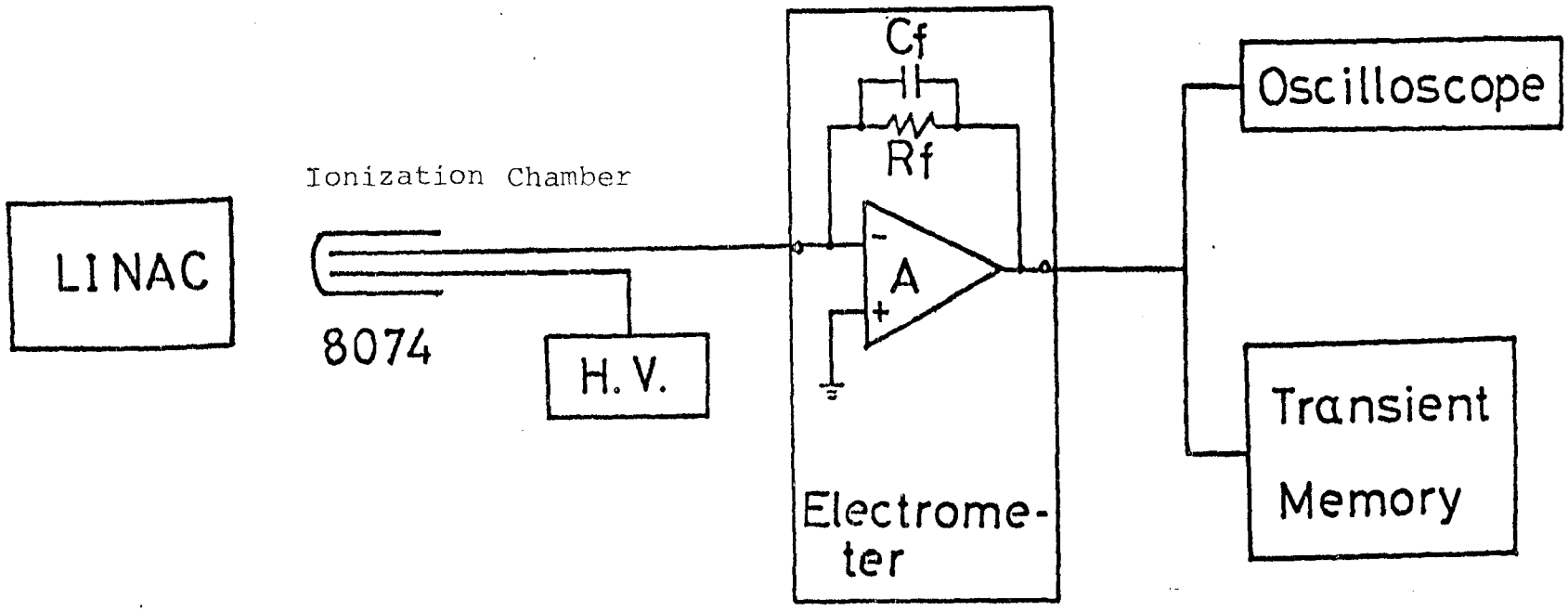

Fig.2-2 Block diagram of the equipment for measuring the impulse response.

Table 2-1 Specifications of the detector used in this experiment.

Westing house *Type 8074*

Overall length	$23 \cdot \frac{13}{16}$ *inches*	
Outer diameter	$3 \cdot \frac{3}{16}$ *inches*	
Sensitive length	*14 inches*	
Weight	$5 \cdot \frac{3}{8}$ *pounds*	
Coating	*Boron enriched in* ^{10}B	
Filling gas	N_2	
Operating voltage	*300 - 800 V*	
Compensating voltage	*-10 - -80 V*	
Neutron sensitivity	4×10^{-14} *A/nv*	
Neutron flux range	$2.5 \times 10^{2} - 25 \times 10^{10}$ *nv*	
Uncompensated gamma	*Sensitivity*	3×10^{-10} *A/R/hour*

A fast response electrometer was manufactured for this measurement[7]. The time constant of the electrometer containing a detector cable was about 3 μsec in 10^{-6} A range. This was much smaller than the positive ion transit time, so that the time lag of the electrometer was negligible.

Figure 2-3 shows an example of results observed by the use of an oscilloscope. The response shape due to the electron component is too sharp to be visible together with that due to the positive ion component in the screen of an oscilloscope. Concerning the positive ion component, the observed pulse is apparently linearly falling to zero. This agrees quite well with Eq.(2-6) and it is therefore proved that the transfer function of the ionization chamber is expressed by Eq.(2-10). The output voltage of the current amplifier was led not only to the oscilloscope but also to a transient-memory Iwatsu model DM 701, by which the transit time of positive ions was precisely measured, varying the applied voltage as a parameter. The results of the positive ion transit time and its reciprocal versus the applied voltage are shown in Fig. 2-4. The positive ion drift velocities indicated by the reciprocals are represented as relative values since the precise value of the interval between the electrodes is not obtained. It is, however, evident from the results shown in Fig.2-4 that the drift velocity of positive ions is directly proportional to the applied voltage and the transit time of positive ions inversely porportional to that. These agree quite well with Eqs.(2-4) and(2-7) respectively.

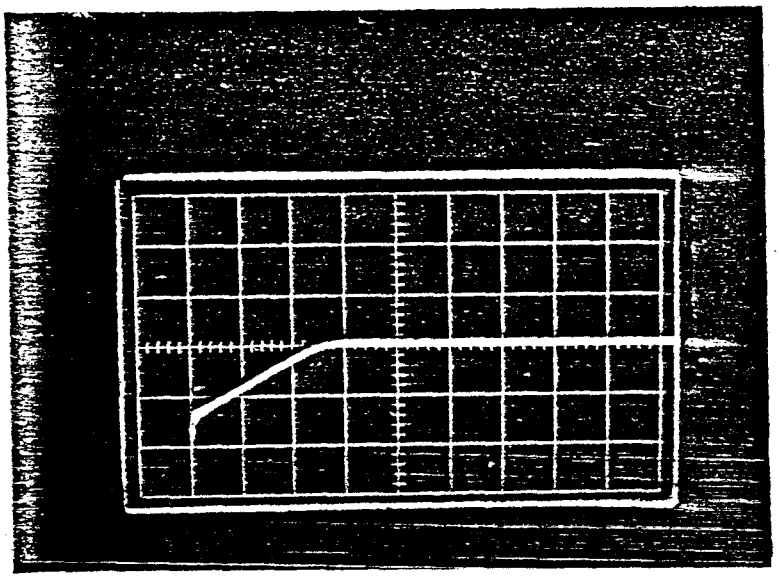

Fig.2-3 An example of measured impulse responses concerning the positive ion component (the applied voltage = 300 V) . Horizontal scale : 100 μsec/div. Vertical scale : 2×10^{-6} A/div.

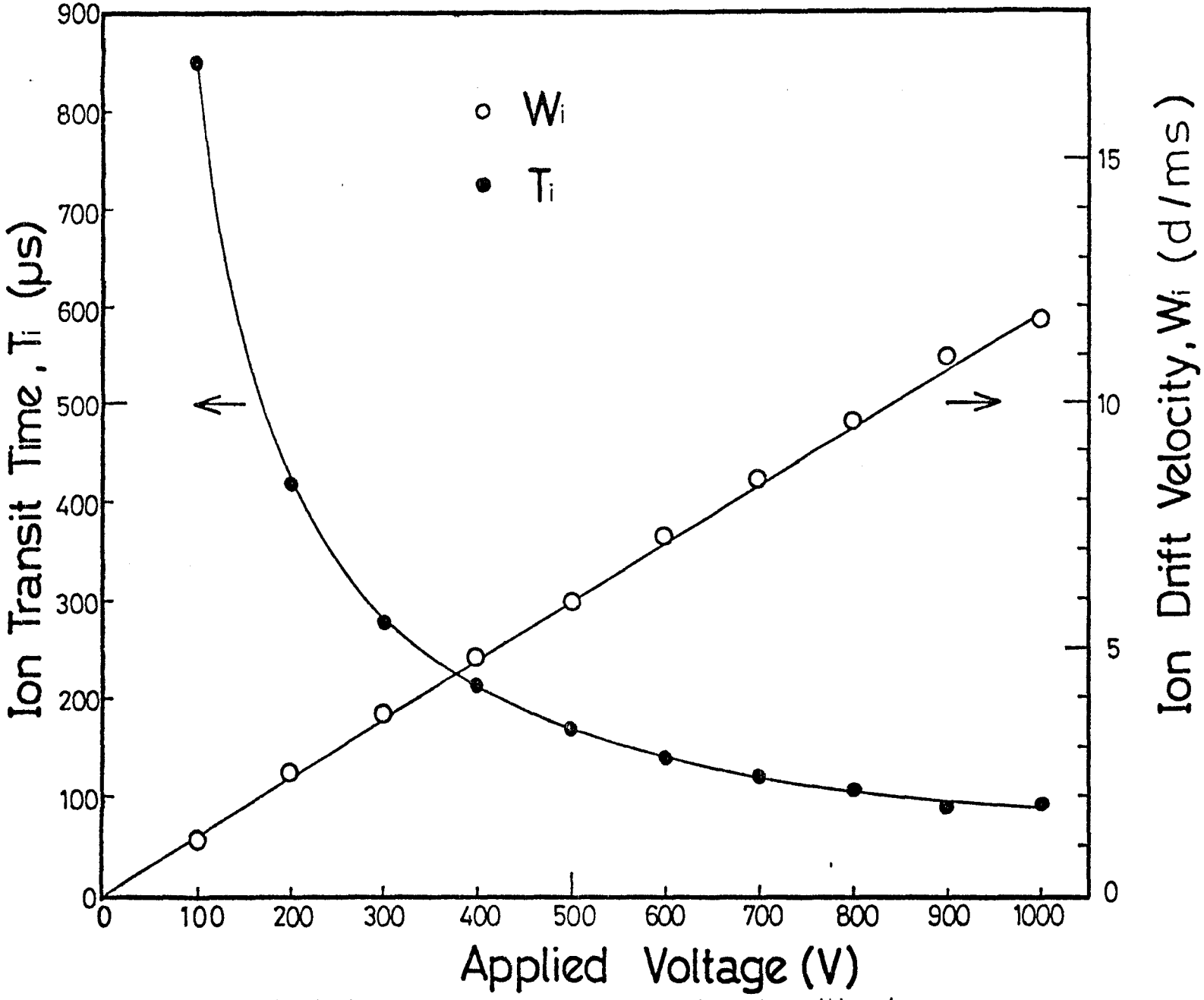

Fig. 2-4 Transit time and drift velocity of positive ions.

Now let us consider the response due to the electron component of the ionization chamber. If a sufficiently narrow pulsed radiation source and a current amplifier of which time constant is much smaller than the electron transit time are available, the same simple experiment as on the positive ion component might be possible. However, it is very difficult to obtain such a fast response current amplifier so far, so that we have to take account of the time lag of a current amplifier in analysis of the response of the ionization chamber. From equivalent circuit analysis the transfer function of the current amplifier is approximately given by

$$G_a(S) = -\frac{R_f}{1+\tau S} \quad , \tag{2-11}$$

where τ is the time constant, which is determined by the product of a current range resistor R_f and a feedback capacitance C_f. Here, it is assumed that the transfer function of the ionization chamber is expressed by Eq. (2-10). Then, if we measure the time T_p from a square pulse change of input to the time the corresponding output arrives to the peak value as shown in Fig. 2-5, the electron transit time is obtained by

$$T_e = T_o \cdot \frac{\exp\left(\frac{T_p}{\tau}\right)}{\exp\left(\frac{T_o}{\tau}\right)-1} - \tau \qquad \text{for } \tau,\ T_e \ll T_i \ , \tag{2-12}$$

where T_o is the pulse width of input.

In the experiment, gamma ray pulses of 100 nsec were applied to the same ionization chamber. An example of measured results is shown in Fig. 2-6. The time constant of the electrometer was about

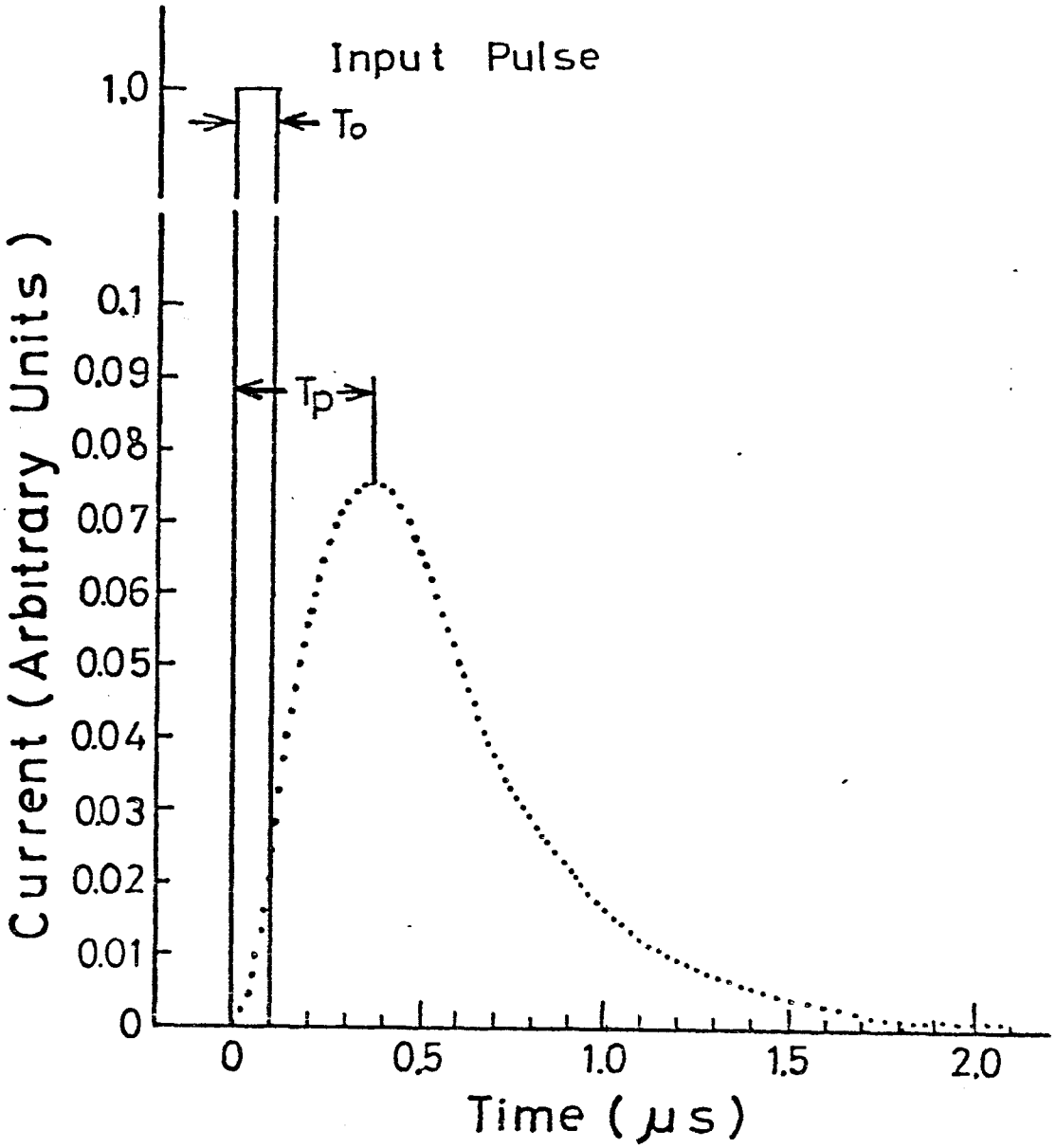

Fig.2-5 Response to square pulse change of input.

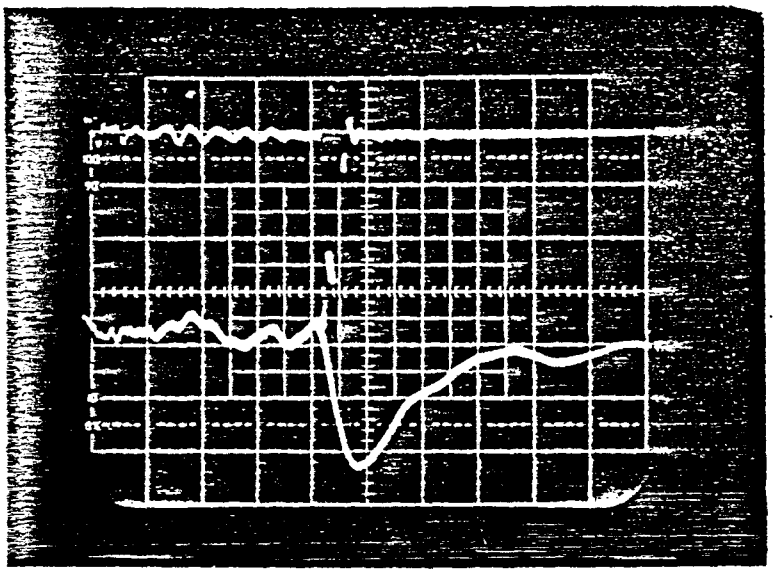

Fig.2-6 An example of measured responses to gamma ray pulses of 100 nsec. The upper trace is an injection current of the accelerator and the lower one an output voltage of the electrometer. Horizontal scale : 0.5 μsec/div. Vertical scale : 0.2 A/div. (upper) and 2×10^{-9} A/div. (lower).

350 nsec ($Rf=10^4\Omega$, $Cf=35pF$). Since a transient memory with a sufficiently small resolving time in comparison with the electron transit time was not available, we took photographs of the responses from a storage oscilloscope and magnified them about four times to measure the time T_p. In Fig 2-7 the response calculated based on the transfer functions of the ionization chamber and the current amplifier is compared with the measured one shown in Fig. 2-6. The calculated response is normalized by the peak value of the measured one. Both response shapes are in good agreement although there are many external noise sources in the accelerator room. Figure 2-8 shows the results of the electron transit time and its reciprocal versus the applied voltage alike on the positive ions. The electron drift velocities are also represented as relative values because of the obscurity of the interval between the electrodes. Although the results apparently differ from Eqs. (2-5)~(2-8), the tendency that the electron drift velocity increases linearly with applied voltage appears to agree with experimental results reported by L.Colli[8] and T.E.Brotner[9].

2-4. Fluctuation Current

In order to measure precise power shapes of pulsed reactors by the use of ionization chambers, it is necessary not only to determine the response time of the ionization chamber but also to evaluate the error due to the fluctuation current induced by random detection of radiation. From Campbell's theory[10] the value of the average current and the mean square value of the fluctuation current of the ionization chamber set up in a steady radiation field are given by

$$\langle i_a \rangle = N \cdot \frac{\bar{Q}}{Q} \cdot \int_{-\infty}^{\infty} i(t)\, dt = N\bar{Q} \quad , \qquad (2\text{-}13)$$

$$\langle i_n^2 \rangle = N \cdot \left(\frac{\bar{Q}}{Q}\right)^2 \int_{-\infty}^{\infty} \{i(t)\}^2 dt \quad , \qquad (2\text{-}14)$$

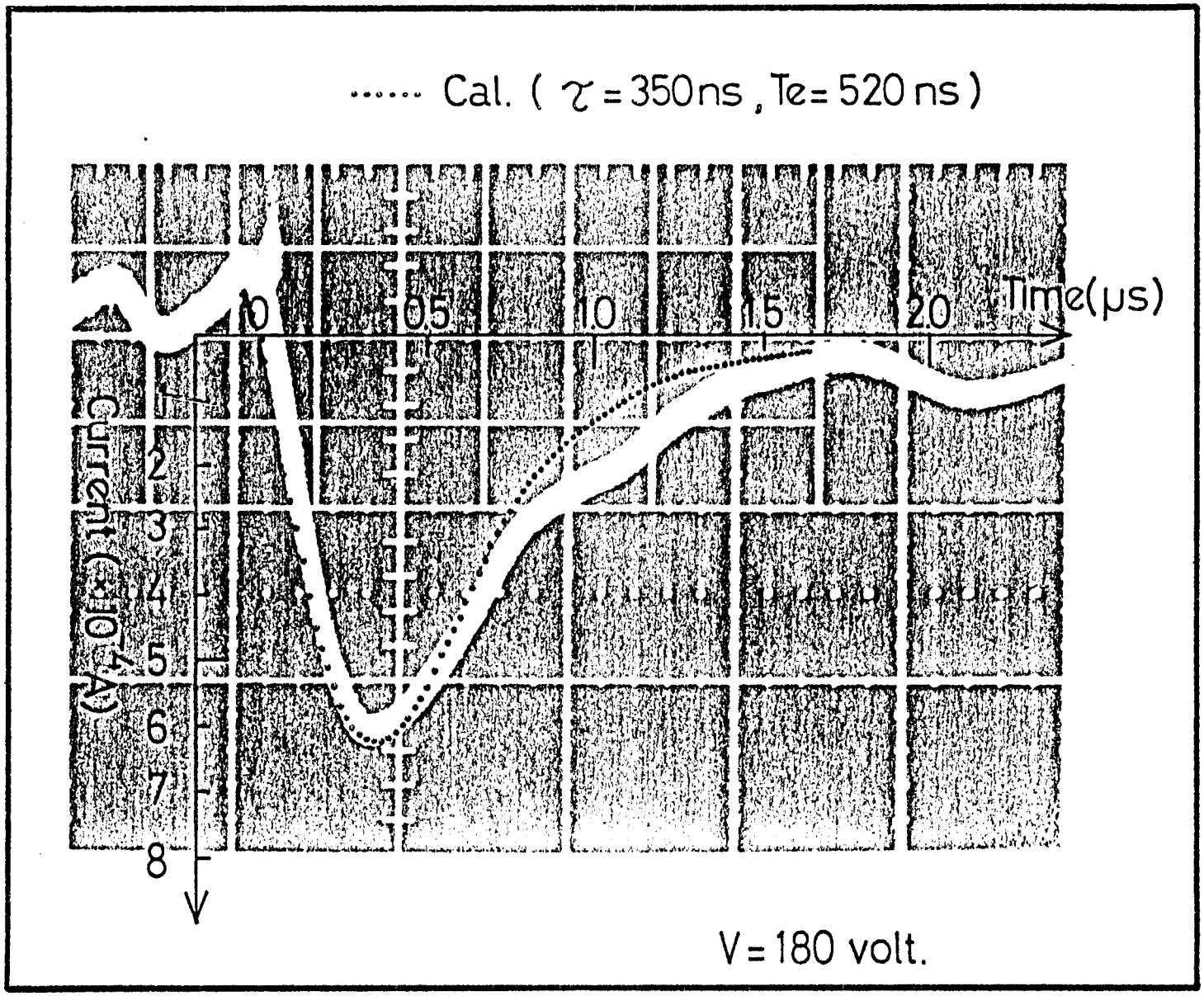

Fig.2-7 Comparison between calculated response and measured one.

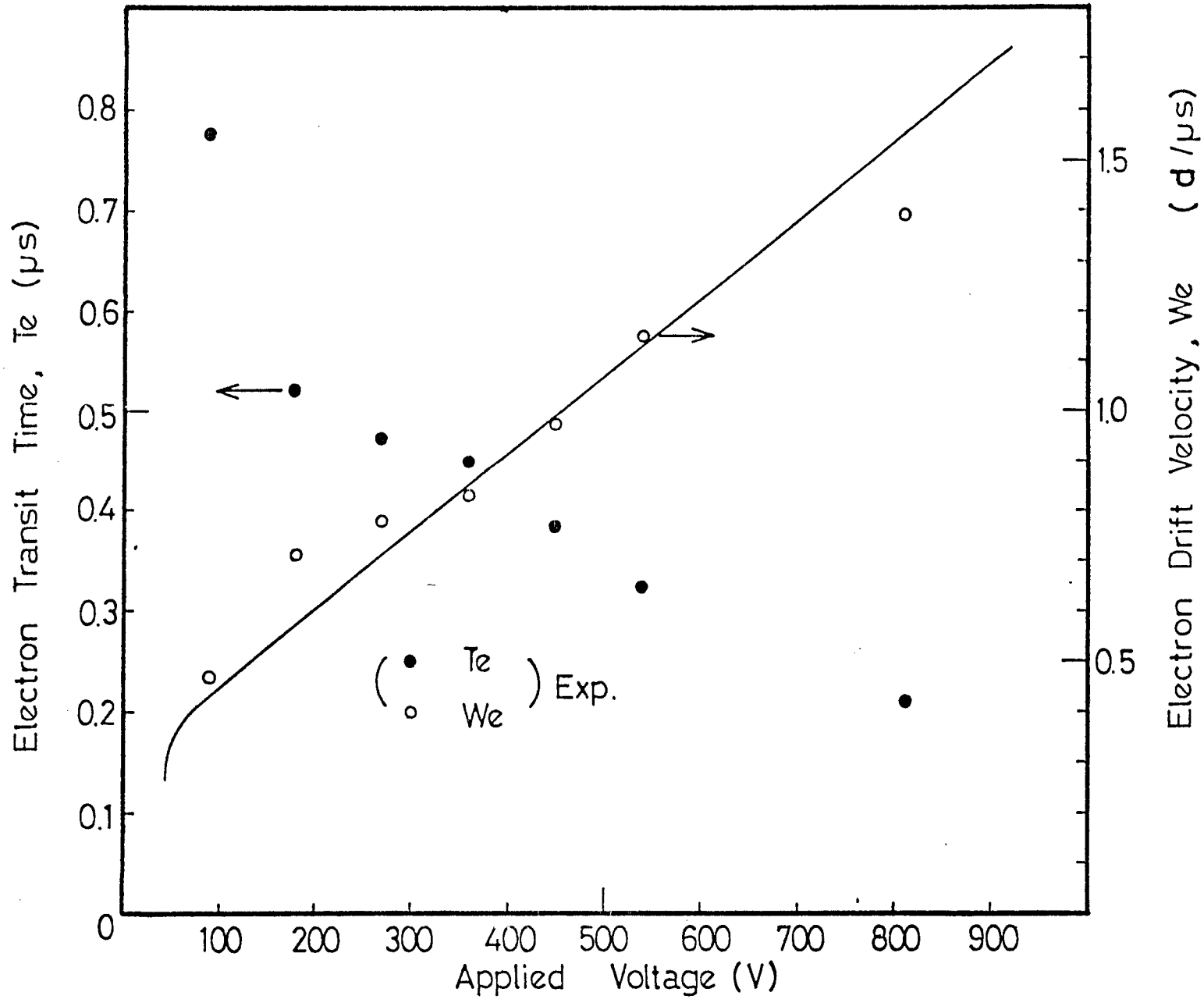

Fig.2-8 Transit time and drift velocity of electrons.

where N is the average counting rate of radiation. In practical measurements of the output current of the ionization chamber, a current amplifier system acts as a low pass filter, so that the mean square value of the fluctuation current is estimated smaller than is expected from Eq.(2-14). Then taking the transfer function of such a low pass filter to be $H(s)$, we can rewrite Eq.(2-14) as follows.

$$\langle i_n^2 \rangle = N \bar{Q}^2 \int_{-\infty}^{\infty} \{h(t)\}^2 dt \quad , \qquad (2\text{-}15)$$

where $I(s)$ is the Laplace transform of $i(t)$ and $Q \cdot h(t)$ the inverse Laplase transform of $I(s)H(s)$.

Consequently, the ratio of the average current to the root mean square value of the fluctuation current, in other words, the ratio of signal to noise is given by

$$\frac{\langle i_a \rangle}{\sqrt{\langle i_n^2 \rangle}} = \sqrt{\frac{N}{\int_{-\infty}^{\infty} \{h(t)\}^2 dt}} \quad . \qquad (2\text{-}16)$$

It is naturally expected from this that the larger the value of N (in other words, the average current) is, or the smaller the value of $\int_{-\infty}^{\infty} \{h(t)\}^2 dt$ (in other words, the bandwidth of the current amplifier system) is, the better the ratio of signal to noise is. From Eqs.(2-13) and(2-15) the average electric charege is given by

$$\bar{Q} = \frac{\langle i_n^2 \rangle}{\langle i_a \rangle} \cdot \frac{1}{\int_{-\infty}^{\infty} \{h(t)\}^2 dt} \quad . \qquad (2\text{-}17)$$

2-5. Measurment of Average Charge Caused per Absorbed Neutron

This section describes the measurement of the average charge caused by absorption of a neutron in the ionization chamber . The average

charge is one of the important factors that determine the magnitude of the fluctuation current of a neutron sensitive ionization chamber.

C. E. Cohn [11] described the average current and the power spectral density of the fluctuation current of a neutron sensitive ionization chamber set up in a reactor as follows.

$$\langle i_{ar} \rangle = \frac{n}{\ell} \varepsilon_D \bar{Q} \quad , \tag{2-18}$$

$$\langle |i_{nr}(j\omega)|^2 \rangle = 2 \frac{n}{\ell} \varepsilon_D \bar{Q}^2 \left\{ 1 + \varepsilon_D \cdot |G_R(j\omega)|^2 \cdot \left(\frac{\bar{\nu}^2 - \bar{\nu}}{\bar{\nu}} \right) \right\} \quad , \tag{2-19}$$

where ε_D : Detector efficiency (= $\frac{\text{Mean frequency of neutron reaction in the detector}}{\text{Mean frequency of fission in the reactor}}$)

n : Total neutron in the reactor

ℓ : Effective neutron lifetime

$G_R(j\omega)$: Transfer function of the reactor

$\bar{\nu}$: Number of neutrons generated per fission

$\bar{\nu}^2$: Mean square value of number of neutrons generated per fission

Consequently, in the case that ε_D is sufficiently small, the fluctuation current only due to the random detection can be observed in the neutron field of a reactor since the contribution of reactor noise (the second term of Eq. (2-19) is negligible.

Figure 2-9 shows the block diagram of the equipment for measuring the average charge $\bar{Q}$ caused by absorption of a neutron in the ionization chamber. The thermal column of the swimming pool type reactor KUR was utilized as a neutron field and there the same ioni-

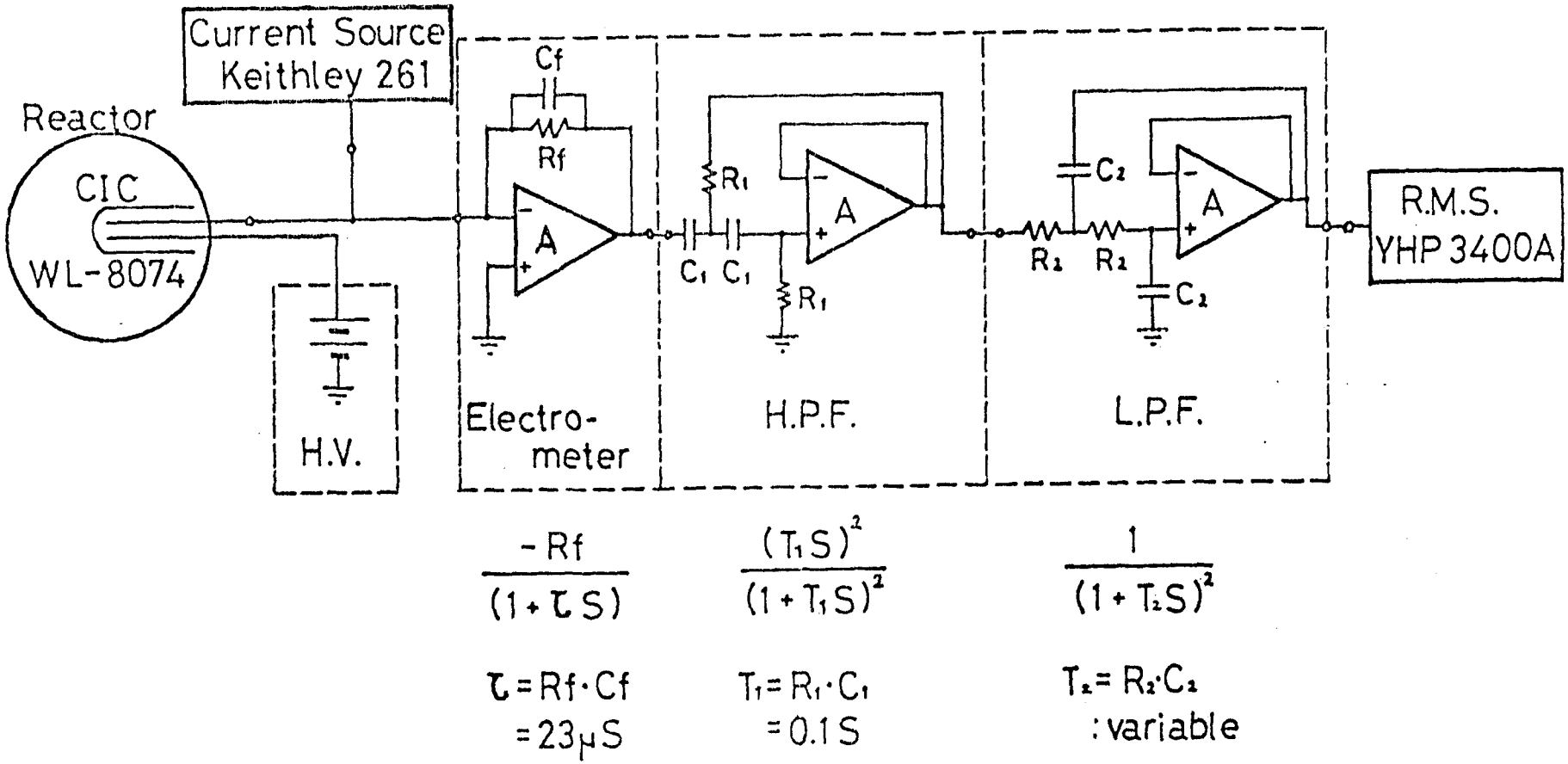

Fig.2-9 Block diagram of the equipment for measuring the average electronic charge.

zation chamber as used in the transit time measurement was set. The values of the average current and the root mean square values of the fluctuation current were measured at a reactor power of 5MW, varying the time constant of the low pass filter as a parameter. The value of the average current was nearly constant during the measurements ($=1.12\times 10^{-6}$ A). A current source Keithley model 261 was employed to cancel the average current. Thus the sensitivity to the fluctuation current was raised tenfold. The equivalent fluctuation current due to the internal noise sources of the equipments was also measured for the shut-down reactor. It was much smaller than the fluctuation current measured at the operating reactor (power level= 5MW) and therefore ignored. In analysis of data obtained the transfer function of the measuring equipment was approximated by the product of the following three expressions :

The electrometer : $\dfrac{-Rf}{1+\tau S}$

The high pass filter : $\dfrac{(T_1 S)^2}{(1+T_1 S)^2}$

The low pass filter : $\dfrac{1}{(1+T_2 S)^2}$

Here the time constant τ of the electrometer containing a detector cable was found to be 23 μsec in 10^{-7}A range from the response simulated by the use of a step current source. The time constant T_1 of 0.1 sec was also fixed for the high pass filter. The transit times T_i and T_e had been found to be 145 μsec and 0.35 μsec respectively from the experimental results by ultilizing the linear accelerator (the applied voltage = 580 V).

Table 2-2 shows the values of the average charge caluculated from Eq. (2-16) using the value of the average current and the measured root mean square values of the fluctuation current. These measured values of the average charge in various T_2 conditions show good agreement altogether.

In Fig. 2-10 the root mean square values calculated from Eq. (2-16) using the relation $\bar{Q} = 3.7 \times 10^{-15}$ A·sec are compared with the measured ones. Both results are in good agreement and also show the effect of the transit time of positive ions.

By the way, ε_D was also found to be about 7.9×10^{-10} and sufficiently small from Eq. (2-18) using the relations, $\frac{n}{l} = 3.1 \times 10^{10} \times 5 \times 10^{6} \times 2.47$ /sec, $\bar{Q} = 3.7 \times 10^{-15}$ A·sec and $\langle i_{ar} \rangle = 1.12 \times 10^{-6}$ A.

2-6. Conclusion

In order to obtain precise power shapes in pulsed reactor experiments, it is important to determine the response time of not only an amplifier system but also an ionization chamber used for a radiation detector and moreover to evaluate the statistical error due to the fluctuation current caused by the random detection of radiation. With respect to the determination of the transfer function of the ionization chamber, the impulse response was measured using intense gamma ray pulses produced by a linear accelerator since the transit times of positive ions and electrons. The results obtained made it clear that the transfer function is mainly expressed by the transit times of positive ions and electrons and that the positive ion transit time decreases proportionately with increasing applied voltage and the

Table 2-2 Average electronic charge caused per absorbed neutron.

T_2 (μs)	$\bar{\bar{Q}}$ ($\times 10^{-15}$ A·sec)
1000	3.8
300	3.6
100	3.7
30	3.6
10	3.7
3	3.8

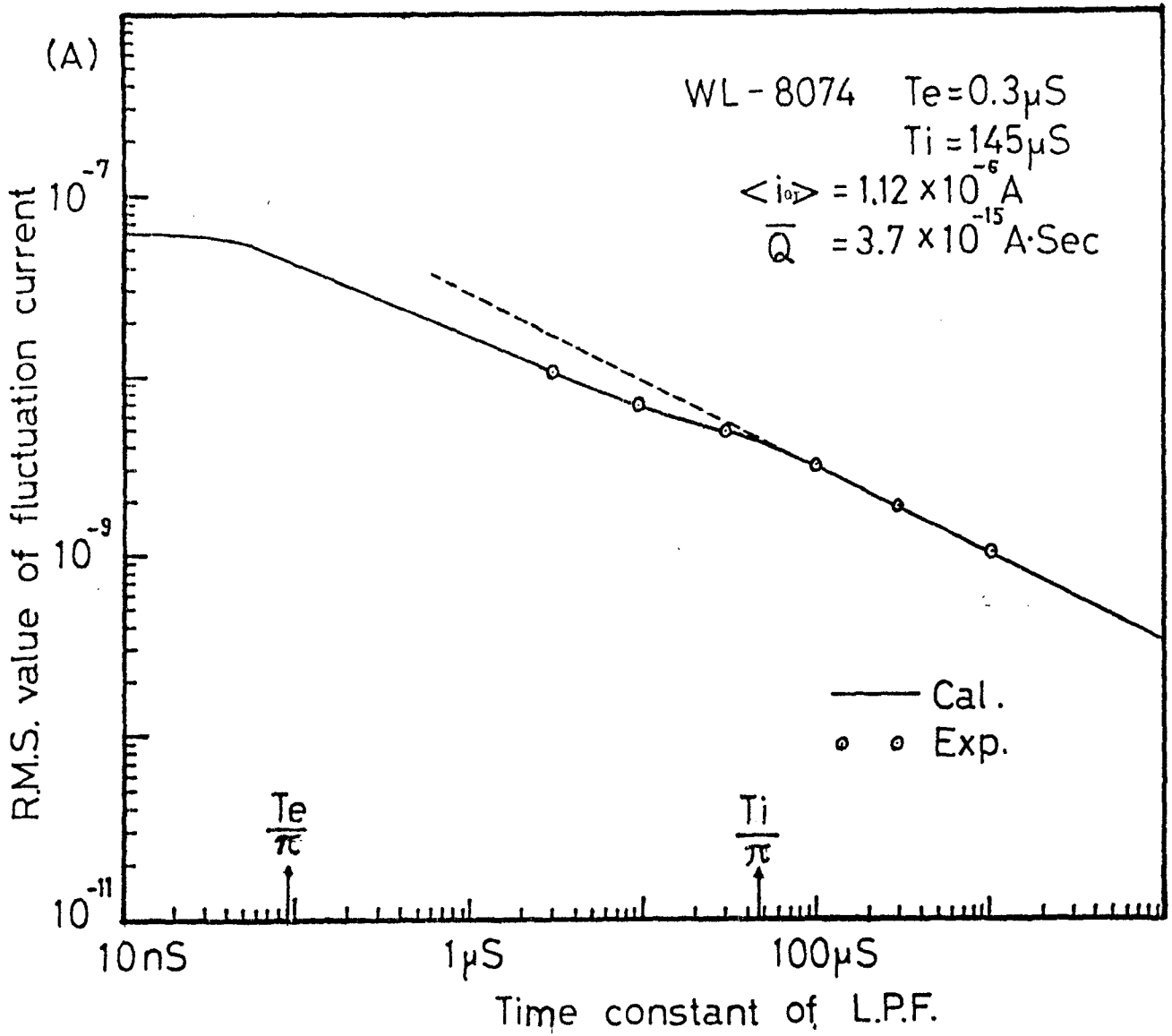

Fig. 2-10 Root mean square values of fluctuation current.

electron one consistently with that. From the measurements of the fluctuation current utlizing the neutron field of a reactor, the power spectral density of the fluctuation current was found to be not perfectly white but dependent on these transit times. This is explained from the fact that the elementary current pulse of the ionization chamber is not δ -function but expressed by Eq.(2-6). In the past, current-type ionization chambers have been considered to be unsuited to the measurements of pulsed radiation because of the slow responsiveness attributed to the positive ion component. However the electron component of the ionization chamber permits measuring a radiation pulse of which width is considerably smaller than the positive ion transit time, although the response is accompanied by a little error due to the slow component of positive ions.

As a successful example of this proposal, the observed result of the same ionization chamber to a gamma ray pulse of about 1 μsec is shown in Fig. 2-11. This response shape is mainly based on the electron component and the positive ion one is scarcely contributive to it. This will be examined in detail for the instrumentation of a fast pulsed reactor like the JLB[12].

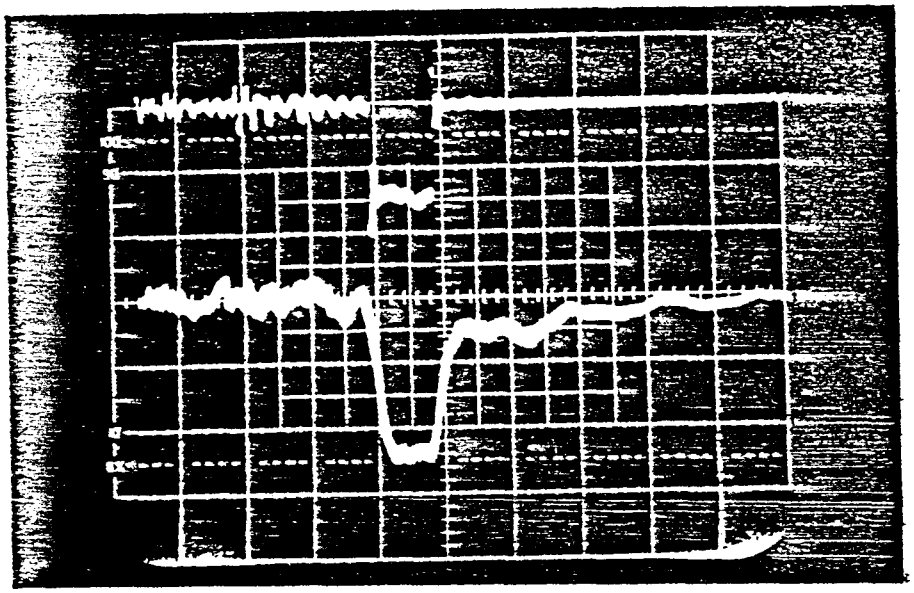

Fig. 2-11 Measured response to gamma ray pulse of about 1 μsec. The upper trace is an injection current of the accelerator and the lower one an output voltage of the electrometer. Horizontal scale : 1 μsec/div. Vertical scale : 0.2 A/div. (upper) and 2×10^{-4} A/div. (lower).

References

1) T. Iida and K. Sumita, To be submitted in Nucl. Instr. Meth.

2) H. Wakabayashi, et al., Proc. US/Japan Seminar on Fast Pulse Reactors I-2 (1976).

3) R. Subramaniam, et al., Nucl. Sci. Eng. 13 (1962) 271.

4) S Gotoh, J. Nucl. Sci. Technol. 3 [9] (1966) 359.

5) A. H. Snell, " Nuclear Instruments and their Uses ", New York, John Wiley & Sons (1962)

6) Y. Fujita, et al., Proc. Symp. On Intense Pulsed Neutron Sources in Japan III-p-2 (1975).

7) T. Iida, et al., To be published in Nucl. Instr. Meth.

8) L. Colli, et al., Rev. Sci. Instr. 23 (1952) 39.

9) T. E. Bortner, et al., Rev. Sci. Instr. 28 (1957) 103.

10) A. Van der Ziel, "Noise", Chapman & Hall (1955).

11) C. E. Cohn, Nucl. Sci. Eng. 7 (1960) 472.

12) J. Wakabayashi, Proc. US/Japan Seminar on Fast Pulse Reactors I-3 (1976).

Chapter III Fast Response Electrometer[1)]

3-1. Introduction

Pulse reactor experiments, which contribute to the investigation of reactor safety, always require a stable and fast response electrometer with a long detector cable. In practical experiments, however, stability and response speed of an electrometer are often degraded by the long detector cable, in other words, by a large input capacitance. A fast response electrometer for pulse reactor experiments, therefore, should be designed in consideration of the effect of such large input capacitance.

With respect to the improvement of the response speed of electrometers, Pelchowitch and Zaalberg Van Zelt , Dever and Sickle[2)] and Brookshier[3)] suggest the method of reducing a feedback stray capacitance which limits the response speed in small current ranges. However, this method is not applicable in large current ranges, since the stability condition of the electrometer usually requires a larger feedback capacitance than the feedback stray capacitance in this region. On the other hand, Presley[4)] describes a guard technique which prevents the input cable capacitance from reducing the response speed. This technique must be useful for pulse reactor experiments but there is a phase shift problem for high frequency signals in large current ranges.

We obtained a good result in improvement of response time of the electrometer by introducing a new guard technique and using the compensation method of the feedback capacitance. At

first this chapter clarifies the relation between stability and response speed of an electrometer and then shows the new guard technique and experimental results of a fast response electrometer to which this technique was applied.

3-2. Stability and Response Speed

With a long detector cable, the response of an electrometer is often accompanied by overshoot- and ringing- phenomena. Such instabilities of the electrometer can always be reduced by increasing a feedback capacitance, which will, however, result in reduction of response speed. It is therefore important to choose at first an adequate feedback capacitance in design of a fast response electrometer.

Figure 3-1 shows the equivalent circuit of a typical electrometer. Here C_{in} represents the total capacitance of the cable and a detector. It can be assumed that the input impedance of an operational amplifier is infinite in this discussion. Then, the transfer function of this circuit is described as follows :

$$G_1(S) = \frac{E_1(S)}{I_1(S)} = \frac{-R_f}{1 + (\tau_0 + R_f C_f + \frac{R_f C_{in}}{A_0})S + \tau_0 R_f (C_{in} + C_f) S^2}, \qquad (3\text{-}1)$$

where

$$\tau_0 = \frac{T_0}{A_0} = \frac{1}{2\pi f_0},$$

A_0 is the open loop gain of the operational amplifier,

T_0 the open loop time constant of the operational amplifier,

f_0 the unity-gain-crossover-frequency of the operational amplifier,

R_f a feedback resistance,

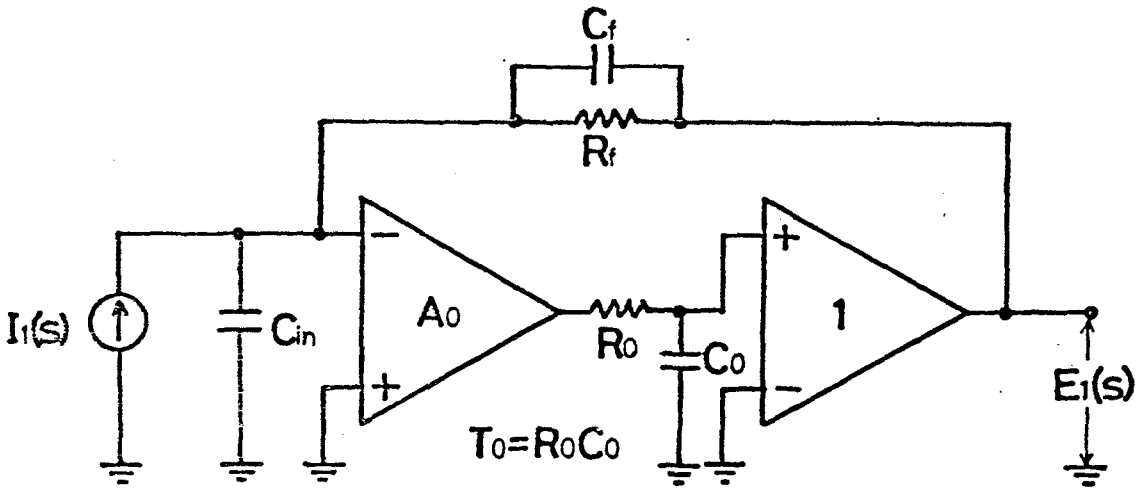

Fig 3-1 Equivalent circuit of a typical electrometer.

C_f a feedback capacitance and

s the Laplace transform variable, respectively.

Then, the stability condition of this circuit, in other words, the condition that the poles of Eq.(3-1) are all negative, can be expressed by

$$C_f \geq \frac{\tau_0}{R_f} - \frac{C_{in}}{A_0} + 2\sqrt{\frac{\tau_0 C_{in}}{R_f}} = C_{f0} \qquad (3\text{-}2)$$

For $C_f < C_{f0}$ the electrometer is underdamped and a pulsed input, having high frequency components, must cause overshoot- and ringing- phenomena. The underdamped condition should be avoided in measurements of transient phenomena. The critical damping condition is realized when C_f is equal to C_{f0}. This relation gives the fastest response of the electrometer within the stable condition. If we substitute the relation $C_f = C_{f0}$ into Eq.(3-1), the time constant at critical damping becomes

$$T = \tau_0 + \sqrt{\tau_0 R_f C_{in}} \fallingdotseq \sqrt{\tau_0 R_f C_{in}} \,. \qquad (3\text{-}3)$$

Equation(3-3) shows the limit of the obtainable response speed of a stable electrometer is determined not by C_f but τ_0 , R_f and C_{in}. For $C_f > C_{f0}$ the electrometer is overdamped. For $C_{f0} < 0$ the electrometer is therefore overdamped even if C_f may be reduced to zero. In this case, the critical damping condition can be easily realized by using a negative capacitance technique[5) 6)].

Table 3-1 gives the critical damping condition of a typical electrometer and an electrometer to which the negative capacitance technique was applied.

Table 3-1 Critical damping condition of a typical electrometer and an electrometer with a negative capacitance.

	Range condition	Equivalent circuit	Feedback capacitance Cf or Cp	Time constant T
Typical electrometer	$Rf \leq \frac{4A_0T_0}{Cin}$	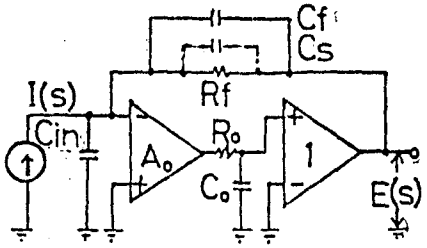	$\frac{\tau_0}{Rf} - \frac{Cin}{A_0} + 2\sqrt{\frac{\tau_0 Cin}{Rf}} - Cs$	$\tau_0 + \sqrt{\tau_0 Rf Cin}$
Electrometer With negative capacitance	$Rf > \frac{4A_0T_0}{Cin}$	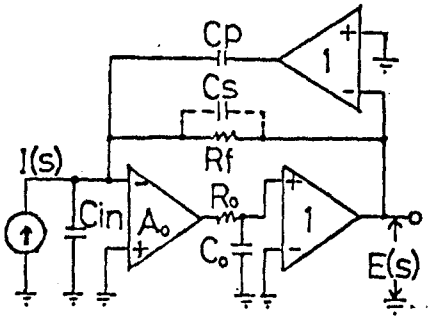	$\frac{Cin}{A_0} - 2\sqrt{\frac{\tau_0 Cin}{Rf}} + Cs$	$\sqrt{\tau_0 Rf Cin}$

3-3. Improvement of the Response Speed

The response speed of an electrometer with a long detector cable can be markedly improved by reducing an effective cable capacitance, which is easily expected from Eq.(3-3). The effective cable capacitance can be reduced using a guard amplifier to equalize cable-sheath potential to center conductor potential of the detector cable.

Figure3-2 shows the block diagram of an electrometer with such a guard amplifier designed by Presley. This electrometer has good response speed in the low current ranges. In large current ranges, however, the response speed cannot be particularly improved because the guard emitter follower with a heavy capacitive load cannot reduce the effective cable capacitance in high frequency regions. An electrometer of this type may also be apt to become unstable because of the degradation of phase stability of a feedback circuit

In order to solve these problems, a new guard technique was introduced as shown in Fig.3-3. This guard method differs in the following ways from that used by Presley. First, a guard amplifier is connected to the input terminal of a current amplifier. This is effective in preventing extra phase lag of the guard amplifier from resulting in reduction of the stability of the electrometer. Secondly, the open loop gain of the guard amplifier is adjustable in respective current ranges. This gain adjustment of the guard amplifier is very useful for controlling the effective cable capacitance and obtaining a best transient response without any instability. Thirdly, a low capacitive coaxial cable is employed apart from the ground to mini-

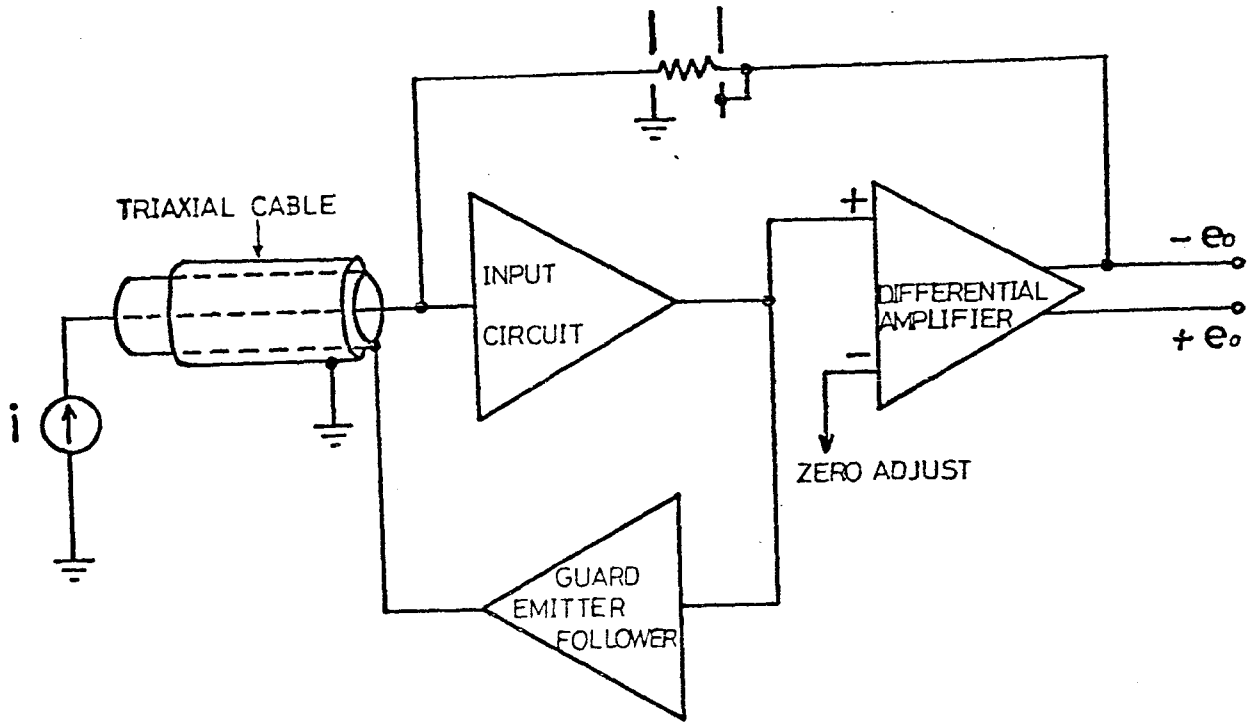

Fig. 3-2 Block diagram of the electrometer designed by Presley [4].

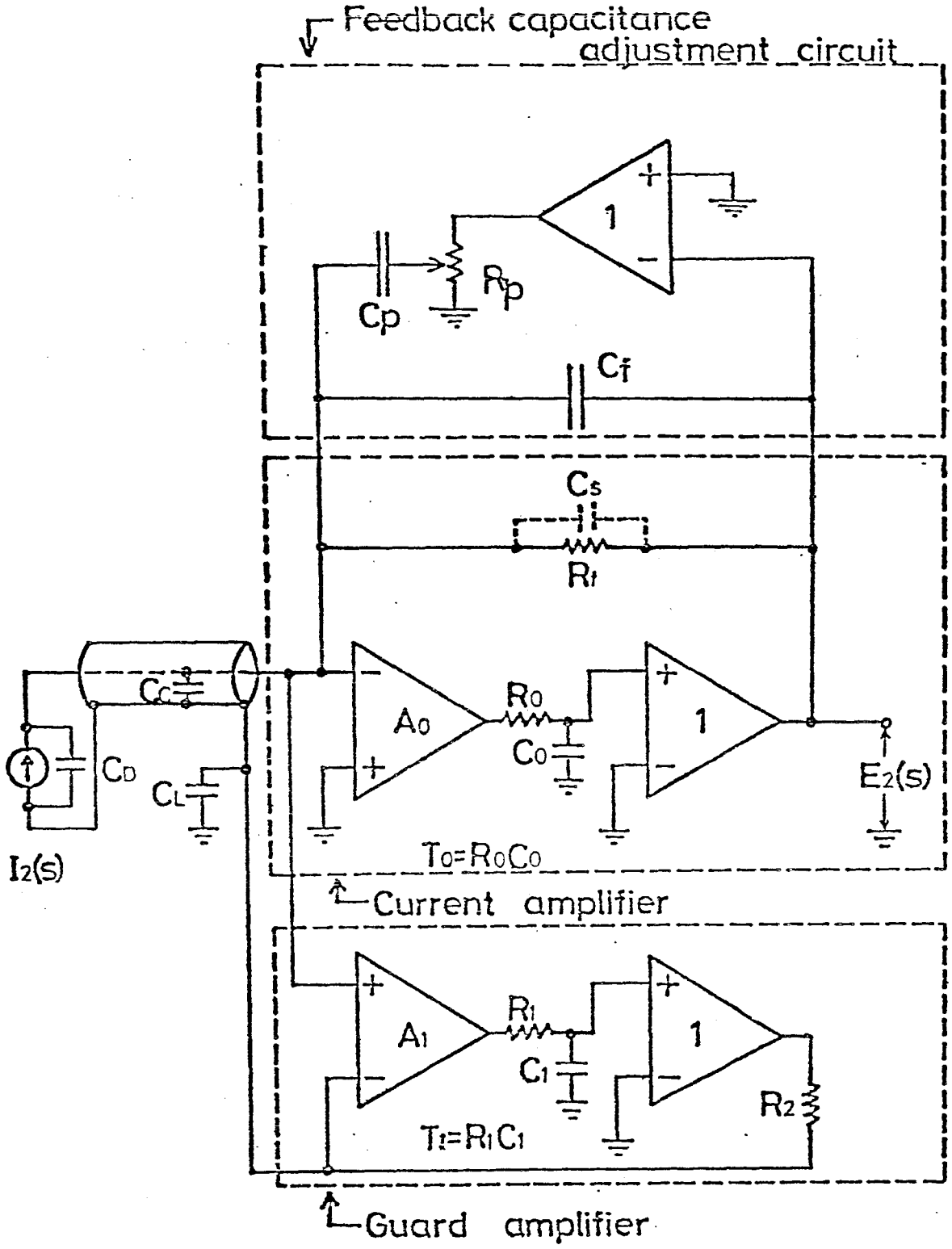

Fig.3-3 Equivalent circuit of a newly designed electrometer.

mize the capacitive load of the guard amplifier. This is effective in maintaining phase stability of the guard amplifier in the high frequency regions. Furthermore the circuit shown in Fig.3-3 has a feedback-capacitance adjustment circuit, which can add an equivalently negative or positive capacitance in parallel with a feedback resistor R_f.

The transfer function of this circuit can be written as follows :

$$G_2(S)=\frac{E_2(S)}{I_2(S)}=\frac{-R_f}{1+(\tau_0+R_fC_F+\frac{R_fC_{in}'}{A_0})S+\tau_0R_f(C_{in}'+C_F)S^2,} \quad (3\text{-}4)$$

where

$$C_{in}'=\frac{C_C+C_D}{A_1+1}\cdot\frac{(1+T_1S)(1+R_2C_LS)}{1+\left\{\frac{T_1+R_2(C_C+C_D+C_L)}{A_1+1}\right\}S+\left\{\frac{R_2(C_C+C_D+C_L)T_1}{A_1+1}\right\}S^2,} \quad (3\text{-}5)$$

A_1 is the open loop gain of the guard amplifier,

T_1 the open loop time constant of the guard amplifier,

R_2 the output resistance of the guard amplifier,

C_C a cable capacitance

C_D a detector capacitance,

C_F an equivalent feedback capacitance of the feedback-capacitance adjustment circuit and

C_L the capacitive load of the guard amplifier, respectively.

It is evident from Eq.(3-5) that the input capacitance C_C+C_D is effectively reduced to $\frac{C_C+C_D}{A_1+1}$ for the frequency much lower than both $\frac{1}{2\pi T_1}$ and $\frac{1}{2\pi R_2C_L}$. If the values of both T_1 and R_2 C_L are much smaller than the time constant of this electrometer, $G_2(S)$ becomes approximately equal to the expression(3-1) with C_{in}

replaced by $\frac{C_c + C_D}{A_1 + 1}$. Consequently, the time constant of this electrometer at critical damping becomes

$$T' = \tau_0 + \sqrt{\frac{\tau_0 R_f (C_c + C_D)}{A_1 + 1}} \fallingdotseq \frac{T}{\sqrt{A_1 + 1}} \qquad (3\text{-}6)$$

The response speed can be improved by a factor of $\sqrt{A_1 + 1}$ beyond the usual limit.

3-4. Practical Circuit and Experimental Results

A practical electrometer circuit is shown in Fig. 3-4 A model 1430 FET operational amplifier (OP. Amp. 1) is used for the current amplifier. A unity-gain-crossover-frequency of the operational amplifier is about 100 MHz. The guard amplifier is made up of a junction FET model 2SK19 (Q_1) and a model 1430 operational amplifier (OP. Amp. 2). The FET Q_1 has a nominal transconductance of 6 m℧ at 200 MHz (V_{GS}= 0). The open loop gain of the guard amplifier is given by

$$A_1 = g_m R_L \ , \qquad (3\text{-}7)$$

where g_m is the transconductance of Q_1 and R_L is the feedback resistance of OP. Amp. 2. The time constant T_1 of the guard amplifier is mainly determined by the product of feedback resistance R_L and the stray capacitance of the resistor R_L. Hence T_1 may be considered to be of the order of 10 nano-seconds. The output resistance R_2 is generally several tens of ohms and C_L may be of the order of several thousands of pico-farads in practical experiments. Then the time constant R_2 C_L becomes of the order of 100 nano-seconds. Therefore, it may be considered that R_2 C_L is much larger than T_1 and mainly determines the frequency bandwidth of the guard amplifier. Two transistors, model 2SA495 (Q_2) and 2SC372 (Q_3) are used for a negative capacitance circuit to give an adequate feedback capacitance for critical damping.

Table 3-2 indecates the measured results of response speed of this electrometer with a signal cable (RG-59/U), whose length was 45 meters, laid on the floor. The feedback resistor R_{f_i} was adjusted in order to obtain a best transient response for

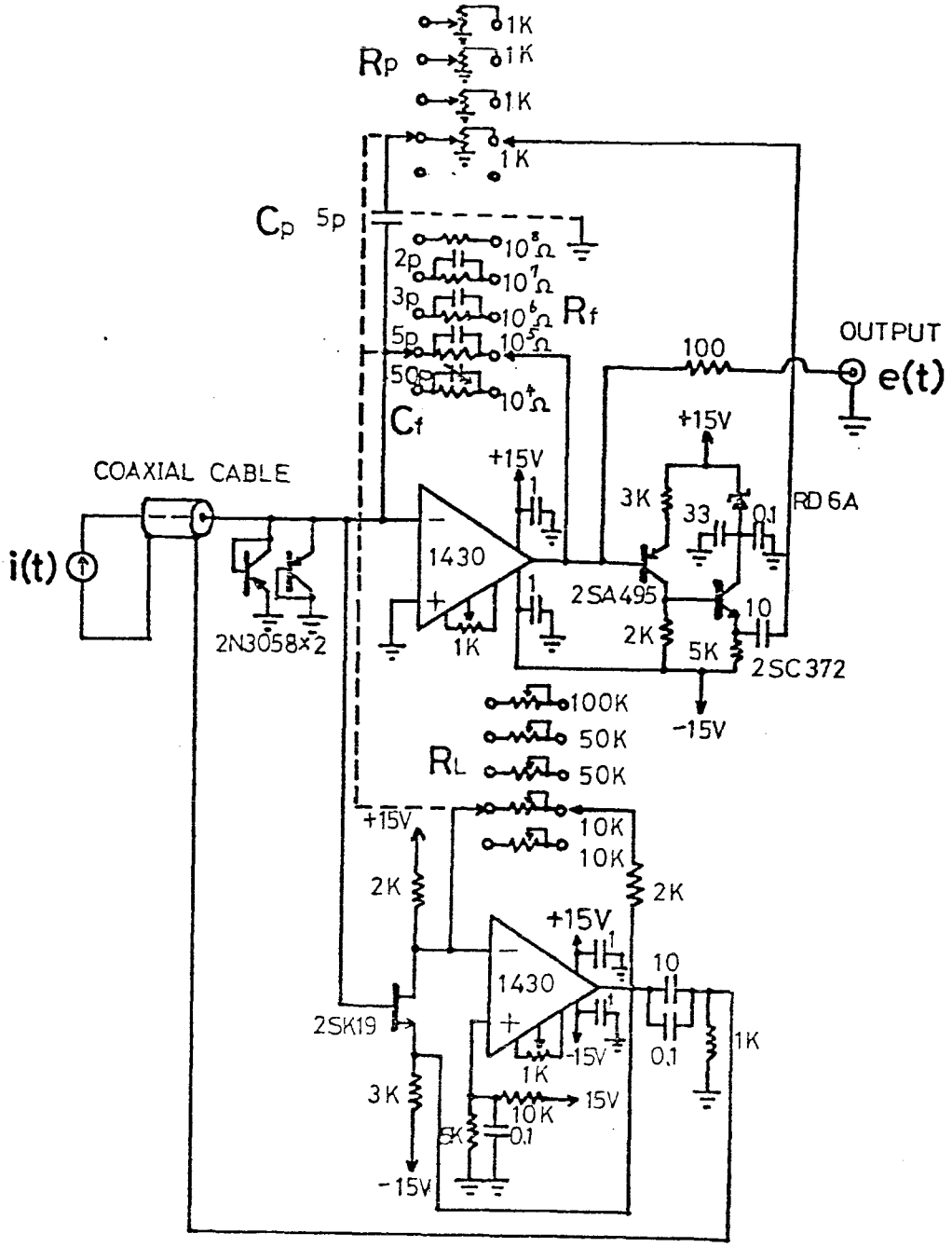

Fig.3-4 A practical electrometer circuit.

Table 3-2 Measured response speed of the electrometer circuit shown in Fig. 4 f_o = 100MHz ; Cin = Cc = 3100 pF.

Feedback resistance Rf (ohm)	Measured risetime (10-90 % μsec)	Calculated open loop gain A_1
10^4	0.2	14
10^5	0.5	23
10^6	1	58
10^7	3	64
10^8	9	71

each current range. The increment of R_L shortened the risetime, but for too large R_L the electrometer became unstable. Hence the maximum value of R_L was selected considering the stability and then an adequate feedback capacitance for critical damping was adjusted by a variable resistor R_p. Table3-2 also gives the open loop gain A_1 calculated from Eqs. (3) and (6) by using the measured risetime, and A_1 shows the degree of improvement of the response speed.

Measured noise of this electrometer is shown in Table3-3 and a discussion on the noise problem of the electrometer with a long detector cable is shown in the Appendix.

Figure3-5 shows an example of observed results of power shapes of the one shot pulse reactor "YAYOI " [6] with this electrometer and a current chamber WL-6377.

Figure3-6 shows an example of measured burst shapes of gamma rays generated by the linear accelerator " KUR LINAC " [7] with this electrometer and a current chamber WL-8074. The response is noisy because of many intense noise sources in the target room where the current chamber was set up, but no overshoot- and ringing- phenomena are observable.

3-5. Conclusion

The limit of the obtainable response speed of a stable electrometer with a long detector cable is determined by the following three factors : [1] The unity-gain-crossover-frequency of an operational amplifier, [2] a feedback resistance and [3] the detector cable capacitance. In order to obtain fast response of the electrometer, it is, therefore, necessary to use

Table 3-3 Measured noise characteristics of the electrometer circuit shown in Fig. 4 Cin = 3100 pF.

Feedback resistance (ohm)	Measured noise voltage (rms mV)
10^4	4
10^5	12
10^6	35
10^7	63
10^8	130

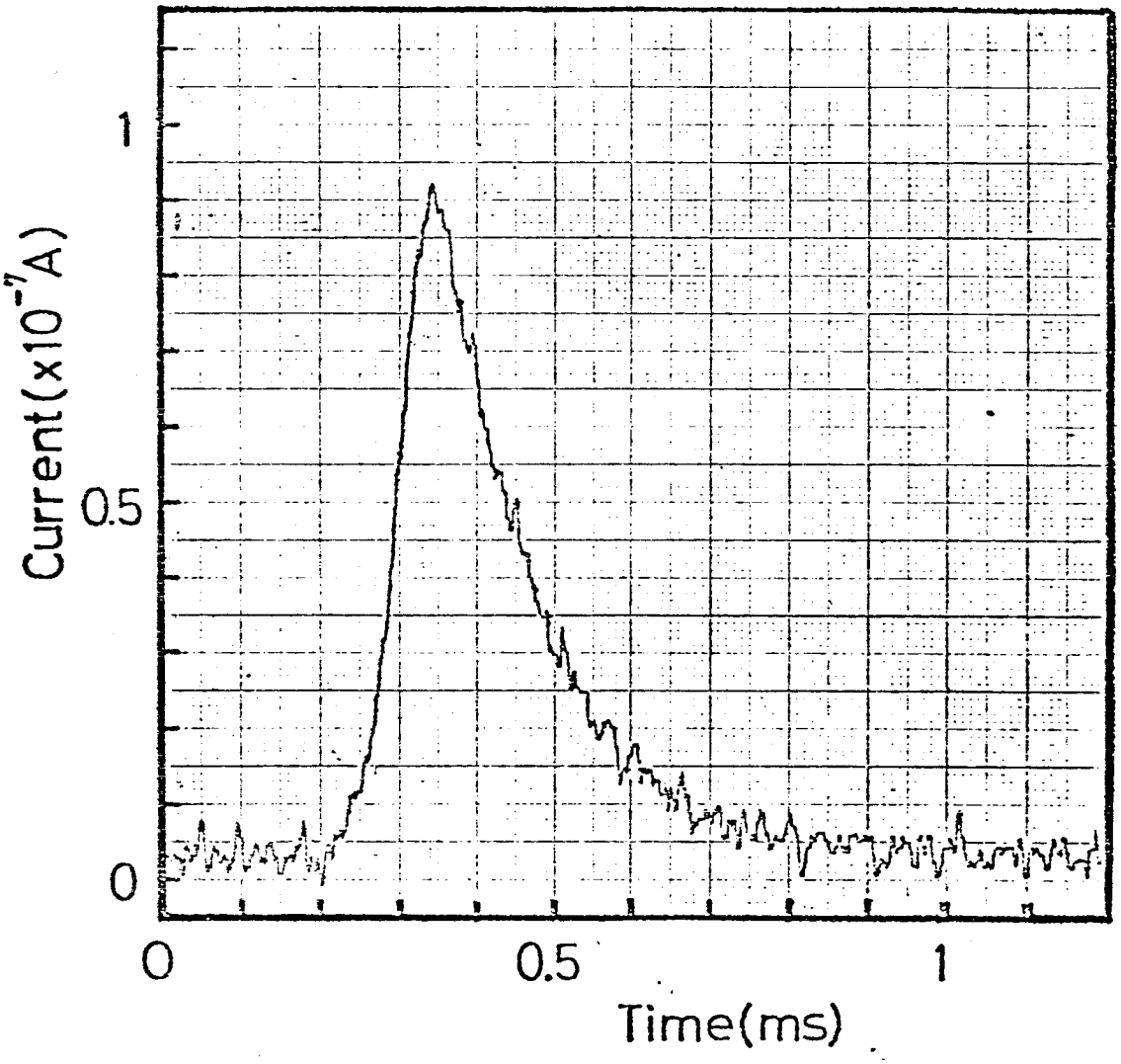

Fig.3-4 An example of observed results of power shapes of the " YAYOI ".

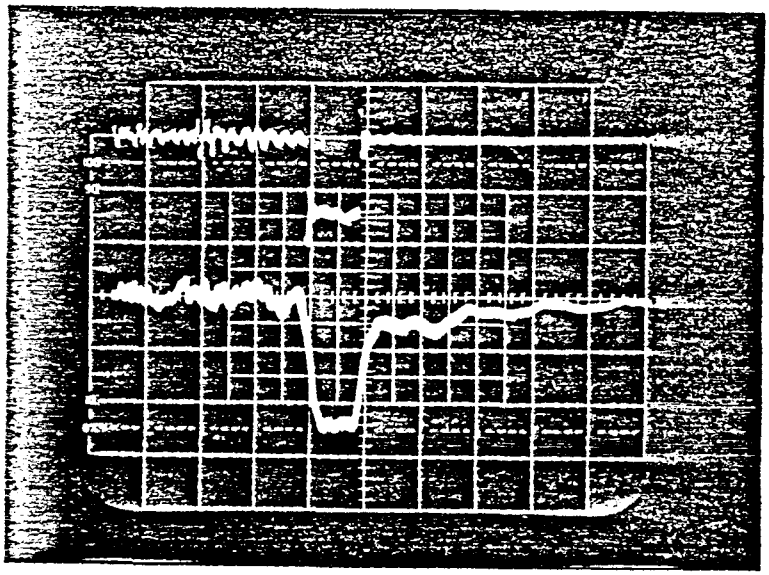

Fig.3-6 An example of measured burst shapes of gamma rays generated by "KUR LINAC". The upper trace is an injection current of the accelerator and the lower one an output voltage of the electrometer in the 10^{-4} A range. Horizontal scale : 1μs/div. Vertical scale : 200 mA/div. (upper) and 2×10^{-4} A/div. (lower).

an operational amplifier with a sufficiently high unity-gain-crossover-frequency or to reduce an effective cable capacitance. Until such operational amplifiers become generally available, we have to improve the response speed by reducing an effective cable capacitance. For this purpose, a new guard technique was developed and a fast response and stable electrometer was made. The response speed of this electrometer with a detector cable of 45 m long was improved about ten times compared with conventional ones [5) 6)]. A feasibility test of this electrometer system was also carried out using the one shot pulse reactor "YAYOI" and the linear accelerator "KUR LINAC", and satisfactory results were obtained in transient measurements of those devices.

Appendix 3-A Noise Characteristics

When a long detector cable is connected to an electrometer, a considerable output noise voltage is present even under the ideal condition where there are no external noise sources. This noise voltage is due to the internal noise sources of an electrometer and its magnitude is related to the construction of the electrometer circuit. Sources contributing to the internal noise of a typical electrometer circuit are as follows :

[1] Johnson noise of a feedback resistor.

[2] Equivalent input noise current of an operational amplifier.

[3] Equivalent input noise voltage of the operational amplifier.

Johnson noise of a feedback resistor may be represented in Fig. 3-A1 as a voltage source e_{n1}. Equivalent input noise current and voltage of an operational amplifier may be represent as i_n and e_{n2}. In large current ranges, the value of both e_{n1} and $i_n R_f$ are much smaller than that of e_{n2}. The output noise voltage is, therefore, mainly determined by equivalent input noise voltage of an operational amplifier.

The mean square voltage of the output noise of the electrometer circuit of Fig. A1 is approximately given by

$$\langle e_n^2 \rangle \doteq \int_0^\infty \phi_{vv}(\omega) \left| \frac{G_1(j\omega)}{R_f} \cdot \left\{ 1 + j\omega R_f (C_{in} + C_f) \right\} \right|^2 d\omega \ , \qquad (3\text{-A1})$$

where $\phi_{vv}(\omega)$ is the power spectral density of the equivalent input noise voltage of an operational amplifier. At critical damping, we get by substituting the relation $C_f = C_{f0}$ into Eq.(3-A1)

$$\langle e_n^2 \rangle = \int_0^\infty \phi_{vv}(\omega) \left| \frac{1 + j\omega T_N}{(1 + j\omega T)^2} \right|^2 d\omega \qquad (3\text{-A2})$$

where $T_N = (\sqrt{\tau_0} + \sqrt{R_f C_{in}})^2 \fallingdotseq R_f C_{in}$

If one adopts an approximate condition that $\phi_{vv}(\omega) = k$ (constant), which is reasonable in large current ranges*, Eq. (3-A2) becomes

$$\langle e_n^2 \rangle \fallingdotseq \frac{\pi K}{4} \sqrt{\frac{R_f C_{in}}{\tau_0^3}} \qquad (3\text{-A3})$$

Equation (A3) shows that the output noise voltage at critical damping is determined by the following three factors alike on the response speed : [1] The unity-gain-crossover-frequency of an operational amplifier, [2] a feedback resistance and [3] an input capacitance. It is also evident from Eqs. (3-3) and (3-A3) that it is effective in the design of a fast response, low noise electrometer to reduce an input capacitance.

Figure3-A2 shows the equivalent circuit of the electrometer of Fig3-4 for the aid of noise analysis. Equivalent input noise voltage of the guard amplifier may be represented as e_{n3}. The mean square voltage of the output noise at critical damping is similarly given by

$$\langle e_n'^2 \rangle \fallingdotseq \int_0^\infty \phi_{vv}(\omega) \left| \frac{1 + j\omega T_N'}{(1 + j\omega T')^2} \right|^2 d\omega + \int_0^\infty \phi_{vv}'(\omega) \left| \frac{j\omega T_N}{(1 + j\omega T')^2} \right|^2 d\omega, \qquad (3\text{-A4})$$

where $T_N' \fallingdotseq \frac{R_f C_{in}}{A_1 + 1}$,

---

* It is necessary to consider the excessive 1/f noise characteristics in small current ranges.

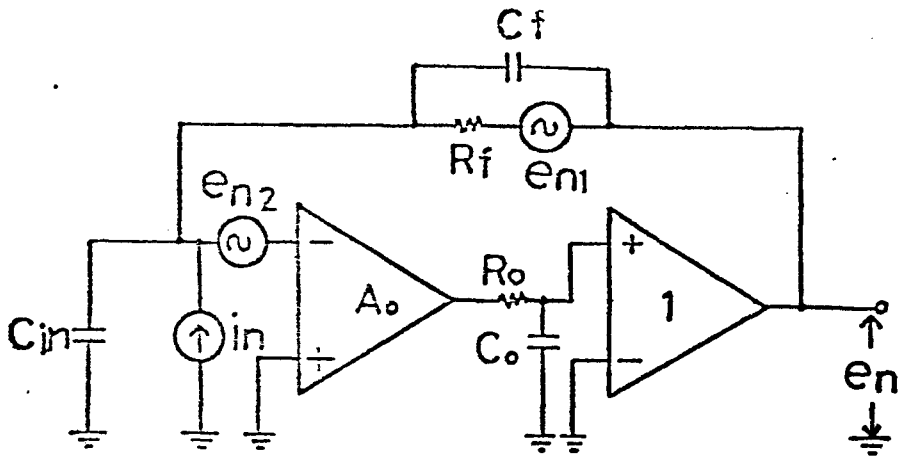

Fig.3-A1 Noise equivalent circuit of a typical electrometer.

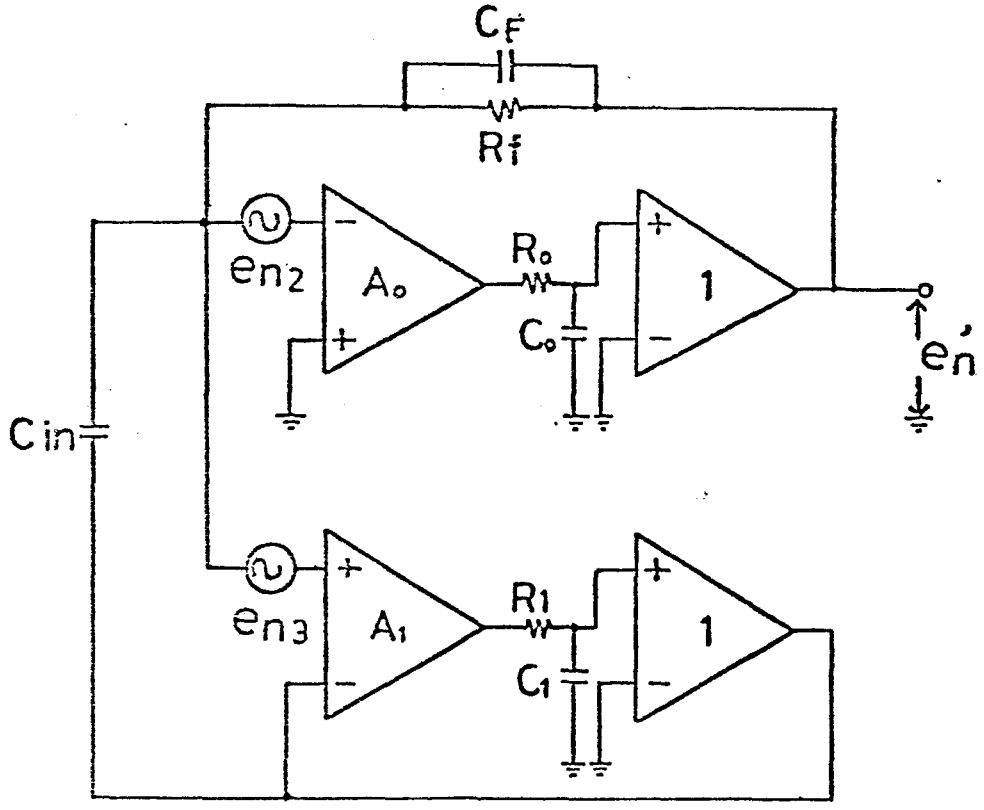

Fig.3-A2 Noise equivalent circuit of the newly designed electrometer.

$\phi'_{vv}(\omega)$ is the power spectral density of the equivalent input noise voltage of the guard amplifier. If we assume $\phi'_{vv}(\omega)$ = k' (constant), Eq.(3-A4) becomes

$$\langle e_n'^2 \rangle = \frac{\pi k}{4}\sqrt{\frac{R_f C_{in}}{\tau_0^3}}\cdot(A_1+1)^{-\frac{1}{2}} + \frac{\pi k'}{4}\sqrt{\frac{R_f C_{in}}{\tau_0^3}}\cdot(A_1+1)^{\frac{3}{2}} \quad . \qquad (3\text{-}A5)$$

The output noise voltage due to e_{n2} decreases with an effective cable capacitance, but on the other hand the output noise voltage due to e_{n3} increases. Assuming k = k', we obtain

$$\langle e_n'^2 \rangle \fallingdotseq \langle e_n^2 \rangle \cdot (A_1+1)^{\frac{3}{2}} \qquad \text{for} \quad A_1 \gg 1 \quad . \qquad (3\text{-}A6)$$

This shows that reducing an effective cable capacitance is approximately equivalent to extending the unity-gain-crossover-frequency of an operational amplifier.

References

1) T. Iida, Y. Kokubo, K. Sumita, N. Wakayama and H. Yamagishi, To be published in Nucl. Instr. Meth.

2) J. A. Dever and L. Sickles, Proc. Nucl. Eng. and Sci. Conf. Paper V - 15 (1959).

3) W. K. Brookshier, Nucl. Instr. Meth. 25 (1964) 317.

4) S. P. Presley, Rev. Sci Instr. 37 (1966) 5.

5) N. Wakayama and T. Iida, JAERI-M 5955 p.p. 127-130 (1975).

6) K. Sumita, T. Iida and N. Wakayama, Proc. US/Japan Seminar on Fast Pulse Reactors III - 1 (1967).

7) Y. Fujita, Y. Kimura, K. Takami, S. Yamamoto, T. Kozuka, S. Hayashi, K. Kobayashi and T. Shibata, Proc. Symp. on Intense Pulsed Neutron Sources in Japan III - P - 2 (1975).

Chapter IV Fast Response Logarithmic Electrometer [1)]

4-1. Introduction

Many experiments have been carried out for the investigation of reactor safety at the pulsed reactors of the " NSRR " [2)], the "YAYOI"[3)] and others. The logarithmic electrometer, which covers a very wide current range, is useful for those pulsed reactor experiments. Its response time has been generally limited on account of instability caused by the input capacitance of a detector and a cable. It requires a large feedback capacitance to obtain the stability at high current levels. Therefore, its response time is severely degraded at low current levels. In the case that a small feedback capacitance is selected to obtain a fast response, the response of the logarithmic electrometer is often accompanied by overshoot- and ringing- phenomena at high current levels. Such contraries between the response time and the stability of a logarithmic electrometer are caused by the marked change of the current dependent resistance of a logarithmic element. This has made it difficult to design a fast response logarithmic electrometer for pulsed reactor experiments.

In order to solve this problem, we proposed a phase compensation technique which was realized by inserting a resistor between a detector cable and the input terminal of the circuit[4)]. This technique made it possible to improve the response time at low current levels. However, at high current levels, the logarithmic electrometer with this technique has poor response time which is determined by the product of the inserted resistor and an input capacitance.

A new phase compensation technique was developed to overcome this problem and the marked improvement of the response time of the logarithmic electrometer was obtained. At first, the relation between the stability and the response time of a logarithmic electrometer shall be generally discussed and then the new phase compensation technique and experimental results of a fast response logarithmic electrometer shall be introduced.

4-2. Stability and Response Time

Figure 4-1 shows the equivalent circuit diagram of a conventional logarithmic electrometer. Here C_{in} represents the total capacitance of a detector and a cable. An operational amplifier has smooth 6 dB/octave roll off providing stable operation at all values of gain. Semiconductor diodes or silicon planar transistors have been recently employed for the logarithmic element D [5)6)]. The relation between a current i_d, flowing through the p-n junction and a voltage v_d across it is given by

$$i_d = i_s \cdot \{ \exp(q v_d / nkT) - 1 \} \quad , \tag{4-1}$$

where i_s is the saturation current and is temperature dependent,

q the electronic charge,

n a factor which depends on the density of the recombination centres in the junction region,

k Boltzmann's constant and

T the absolute temperature, respectively.

When $i_d \gg i_s$, Eq. (1) is approximated by

$$v_d = \frac{nkT}{q} \ln \frac{i_d}{i_s} \quad , \tag{4-2}$$

which shows good logarithmic characteristics.

Figure 4-2 shows the measured $i_d - v_d$ characteristics of a diode-connected model 2N3058, which was used for a newly designed logarithmic electrometer. The result gives the following values :

$n = 1.0$, $i_s = 6.0 \times 10^{-14}$ A ($T = 300^{\circ}$K).

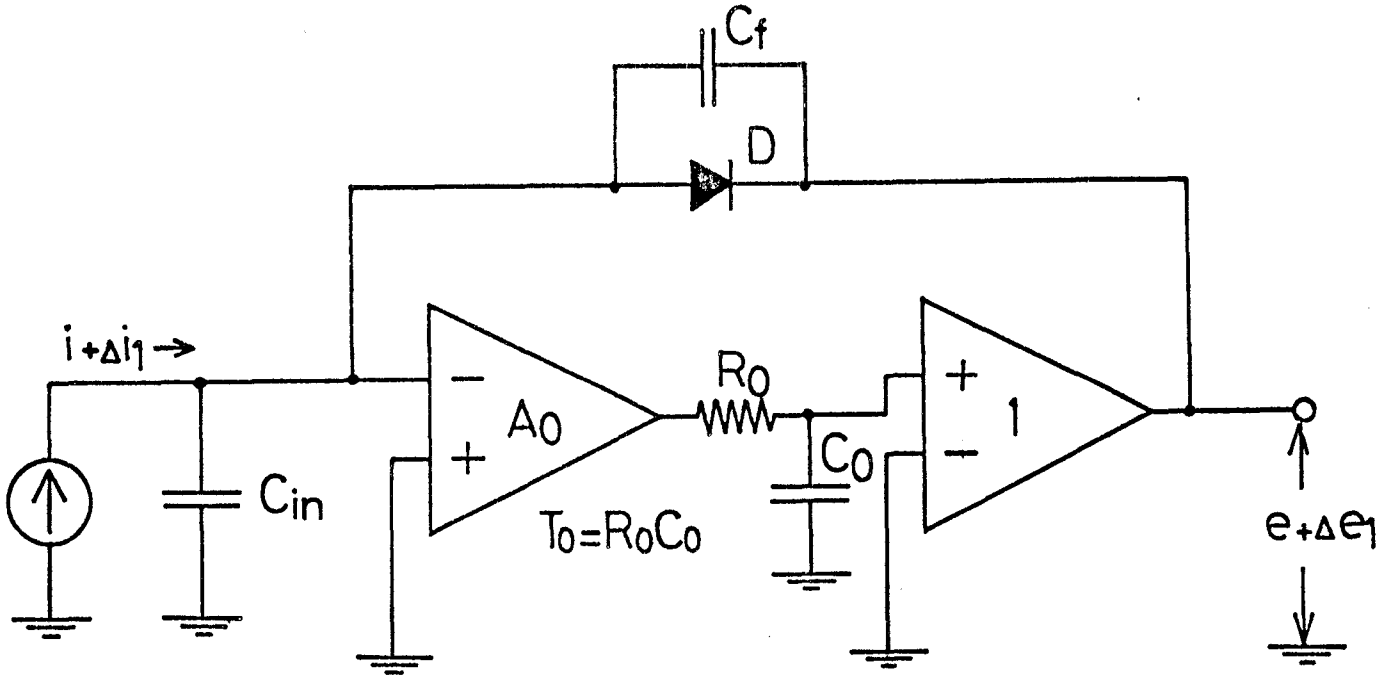

Fig.4-1 Equivalent circuit diagram of a conventional logarithmic electrometer.

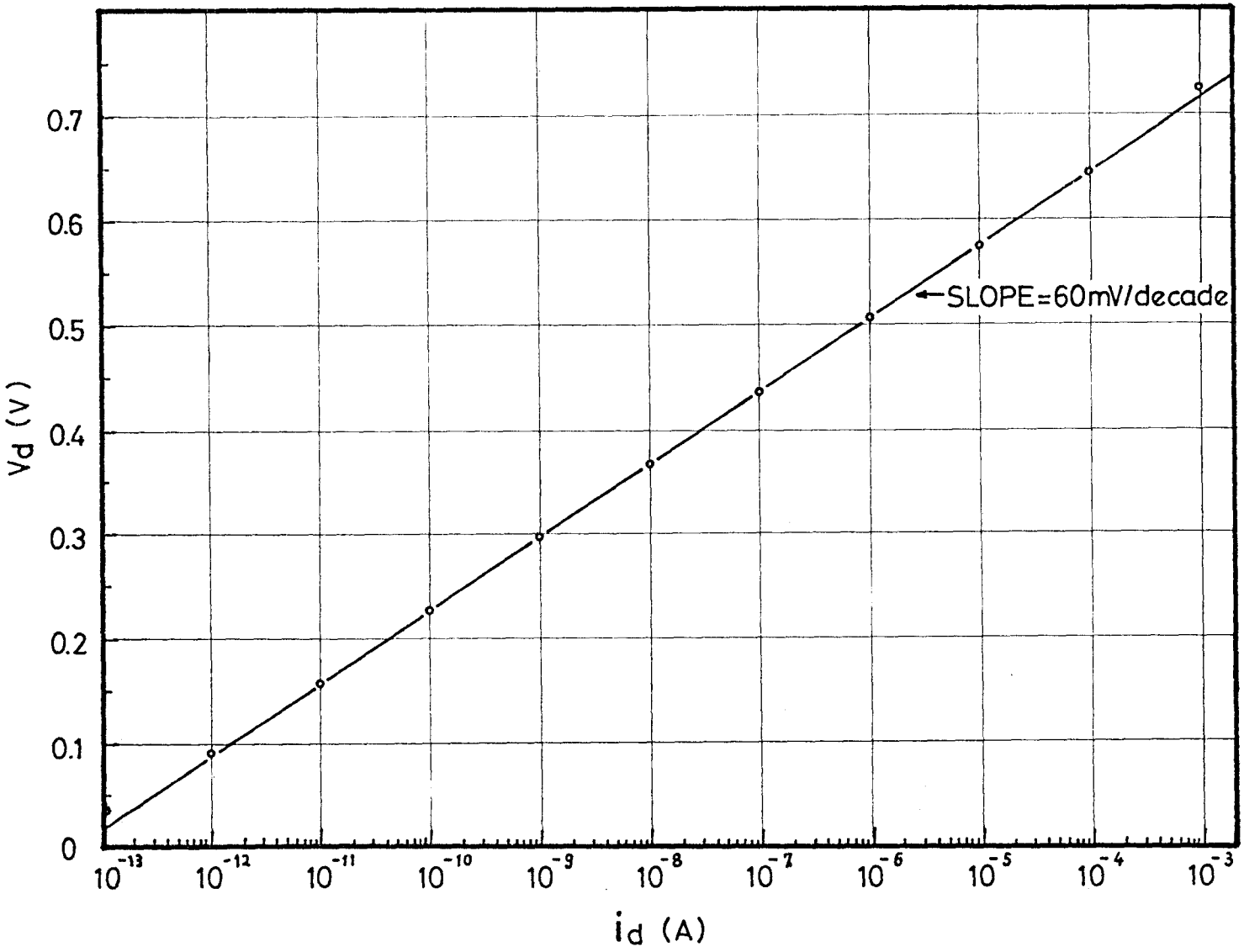

Fig.4-2 Logarithmic characteristics of a diode-connected 2N 3058 for T = 300°K.

The transient response of a logarithmic electrometer can be generally expressed by a non-linear differential equation with respect to time[7]. It is troublesome to solve the differential equation, so that it is difficult to obtain the simplified relation between the response time and the stability of a logarithmic electrometer. For present purpose, a small signal response analysis was adapted and it makes easy to evaluate the relation between the response time and the stability of a logarithmic electrometer. It is evident from experimental results which shall be shown in section 4-4 that this analysis is applicable to our purpose.

The transfer function of the logarithmic electrometer circuit shown in Fig.4-1 can be described as follows :

$$G_1(S) = \frac{\Delta E_1(S)}{\Delta I_1(S)} = \frac{-r_D}{1 + \left(\frac{r_D C_{in}}{A_0} + r_D C_f + \tau_0\right) S + r_D (C_{in} + C_f) \tau_0 S^2} , \tag{4-3}$$

where
$$\tau_0 = \frac{T_0}{A_0} = \frac{1}{2\pi f_0} , \tag{4-4}$$

$$r_D = \frac{nRT}{q} \cdot \frac{1}{i} , \tag{4-5}$$

A_0 is the open loop gain of the operational amplifier,

T_0 the open loop time constant of the operational amplifier,

f_0 the unity-gain-crossover-frequency of the operational amplifier,

r_D the linear resistance of the logarithmic element

for the small signal and it increases proportionately with decreasing bias current,

C_f a feedback capacitance and

s the Laplace transform variable, respectively.

Then, the stability condition of this circuit, in other words, the condition that the poles of Eq.(4-3) are all negative can be expressed by

$$C_f \geq \frac{\tau_0}{r_D} - \frac{C_{in}}{A_0} + 2\sqrt{\frac{\tau_0 C_{in}}{r_D}} = C_{f0} \,. \tag{4-6}$$

For $C_f < C_{f0}$ the logarithmic electrometer is underdamped and a pulsed input, having high frequency components, must cause overshoot- and ringing phenomena. Such underdamped condition should be avoid in measurements of transient phenomena. The critical dampimg condition is realized when C_f is equal to C_{f0}. This relation gives the fastest response of the logarithmic electrometer within the stable condition. If we substitute the relation $C_f = C_{f0}$ into Eq.(4-3), the time constant T_1 at critical damping becomes

$$T_1 = \tau_0 + \sqrt{\tau_0 r_D C_{in}} \fallingdotseq \sqrt{\tau_0 r_D C_{in}} \,, \tag{4-7}$$

which shows the limit of the obtainable response time of the logarithmic electrometer is determined not by C_f but τ_0, r_D and C_{in}. For $C_f > C_{f0}$ the logarithmic electrometer is overdamped, not to mention of stable. A logarithmic electrometer should be overdamped for pulsed reactor experiments.

As shown by Eq.(4-5), the resistance r_D of the logarithmic element varies according to a bias current flowing through it.

Consequently the damping coefficient of the logarithmic electometer depends on the level of an input current. Hence, it is necessary in the design of a logarithmic electrometer to ensure the stability all over the measuring current range.

The critical damping condition of the logarithmic electrometer shown in Fig.4-1 was calculated varying an input bias current. Here input capacitance C_{in} was estimated at 3000 pF, which is nearly equivalent to the total capacitance of a detector and a cable of about 40 meters. A MOS FET operational amprifier which is easily available also has the following features : A_o = 100dB, f_o = 1 MHz. The feedback capacitance and the time constant at critical damping were calculated from Eqs. (4-5) ,(4-6) and(4-7) using above values. The results are shown in Fig.4-3. In the design of a linear electrometer, it is possible to select an adequate feedback capacitance for each current range, but in the case of the logarithmic electrometer such a selection is impossible. When measurements of the maximum current of 10^{-3} A are assigned to the logarithmic electrometer shown in Fig. 1, it needs a feedback capacitance of 14700 pF (= C_{f1}) for the stability, which is shown in Fig.4-3 (curve A). The response time of the logarithmic electrometer with that feedback capacitance C_{f1} is nearly determined by the product of γ_D and C_{f1} , so that it is inversly proportional to the input bias current. This is shown in Fig.4-3 (curve C). Consequently that logarithmic electrometer suffers from the severe degradation of the response time at low current levels. For example, the response time becomes about 3.8 sec at 10^{-10} A level (= 0.026V

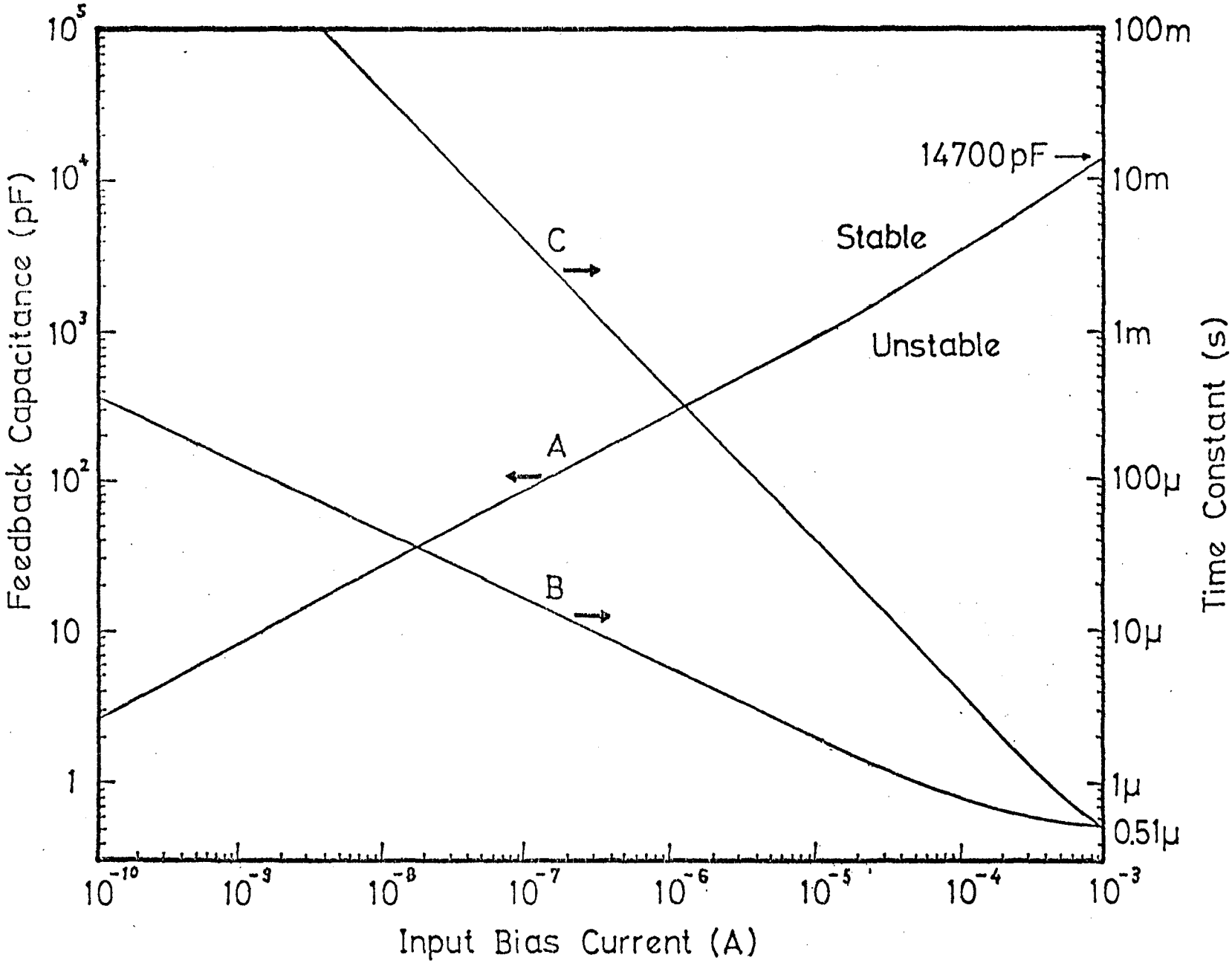

Fig. 3 The critical damping condition of the logarithmic electrometer shown in Fig. 1. Curve A shows the feedback capacitance for critical damping, curve B the time constant at critical damping and curve C the time constant of a conventional logarithmic electrometer. f_0 = 1MHz ; A_0 = 100dB ; C_{in} = 3000 pF ; nkT/q = 26 mV.

$\div 10^{-10}$ A × 14700 pF). Thus, the conventional logarithmic electrometer such as shown in Fig.4-1 cannot be applicable to the wide range instrumentation of pulsed reactors of which powers widely change with very short reactor period. It is important in design of the logarithmic electrometer for pulsed reactor experiments to improve the response time especially at low current levels without any instability.

4-3. Improvement of the Response Time

If the feedback capacitance of a logarithmic electrometer can be regulated along the curve A in Fig.4-3 , the response time will be markedly improved without any instability. Such improvement is shown as the change from curves C to B in the same Fig.4-3. The curve B shows the time constant of the logarithmic electrometer at critical damping. Such conception, using a variable impedance element for the phase compensation should be valuable in the improvement of the response time of a logarithmic electrometer. It is difficult to obtain a suitable feedback capacitor corresponding to the voltage across the logarithmic element. Thereupon, a new phase compensation technique was developed in place of the conventional method, which was using the feedback capacitance in parallel with the logarithmic element. The equivalent circuit of a logarithmic electrometer with the new technique is shown in Fig.4-4. This technique is based on that a resistance r_x inserted between a detector cable and the input terminal of the logarithmic electrometer recovers the phase lag caused by the input capacitance [4) 8)]. Moreover such inserted variable resistance r_x can be regulated according to the level of input current and is easily available to adapt this phase compensation technique.

The transfer function of the logarithmic electrometer circuit shown in Fig.4-4 is expressed by

$$G_2(S) = \frac{\Delta E_2(S)}{\Delta I_2(S)} = \frac{-r_D}{1 + \left(\frac{r_D C_{in}}{A_0} + r_x C_{in} + \tau_0\right) S + \tau_0 (r_D + r_x) C_{in} S^2} \quad (4\text{-}8)$$

The stability condition of this circuit can be given by

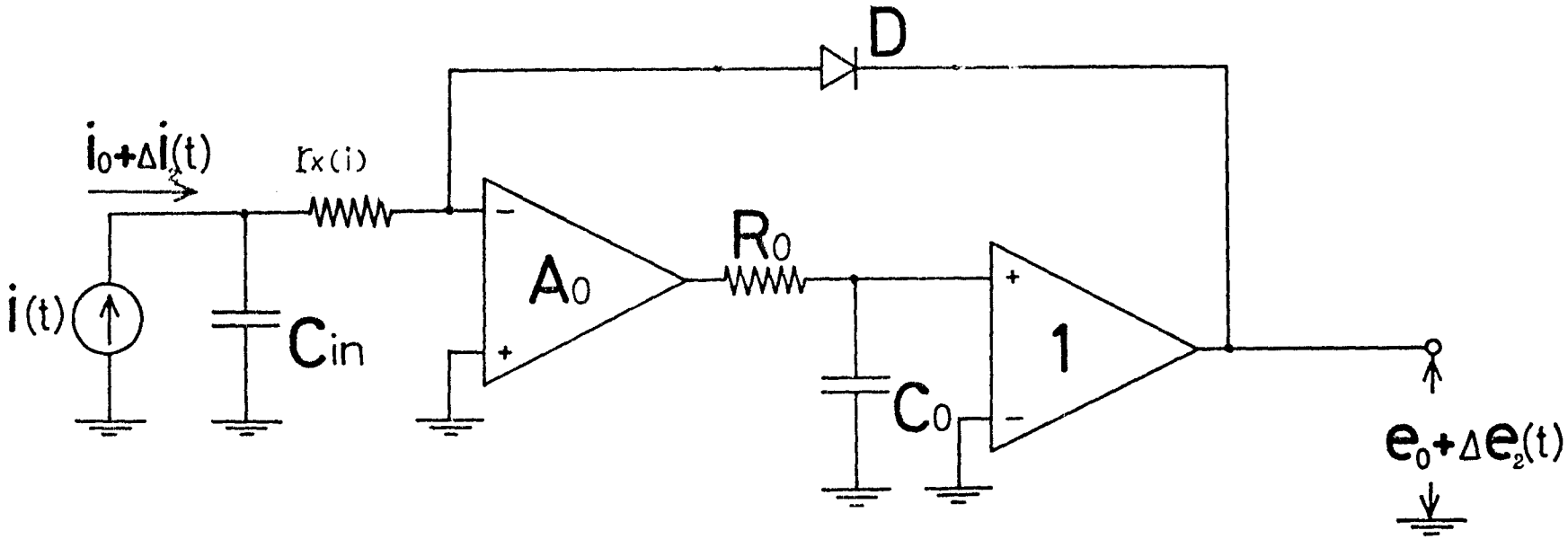

Fig. 4-4 The equivalent circuit of a newly designed logarithmic electrometer.

$$r_x \geq \frac{\tau_0}{C_{in}} - \frac{r_D}{A_0} + 2\sqrt{\frac{\tau_0 r_D}{C_{in}}} = r_0 \quad . \tag{4-9}$$

For $r_x > r_0$ The logarithmic electrometer is overdamped and for $r_x < r_0$ it is underdamped. Substituting the relation $r_x = r_0$ into Eq.(4-8), we obtain the time constant T_2 at critical damping as follows :

$$T_2 = \tau_0 + \sqrt{\tau_0 r_D C_{in}} \fallingdotseq \sqrt{\tau_0 r_D C_{in}} \quad , \tag{4-10}$$

which is the same as Eq. (4-7) It is evident from this that the new phase compensation technique is effective in obtaining stable response as well as the conventional method.

The values of r_x depending on input bias current to obtain the critical damping condition of the logarithmic electrometer with this technique is shown in Fig.4-5 (curves D). If the inserted resistance r_x can be regulated along the curves D in Fig.4-5 , the response time of the logarithmic electrometer will be ideally improved. Although it is impossible to obtain such an ideal resistor, a current variable resistor suitable for this technique can be easily obtained by the use of some resistors and a semiconductor diode, and hence the response time of the logarithmic electrometer with this technique can be markedly improved.

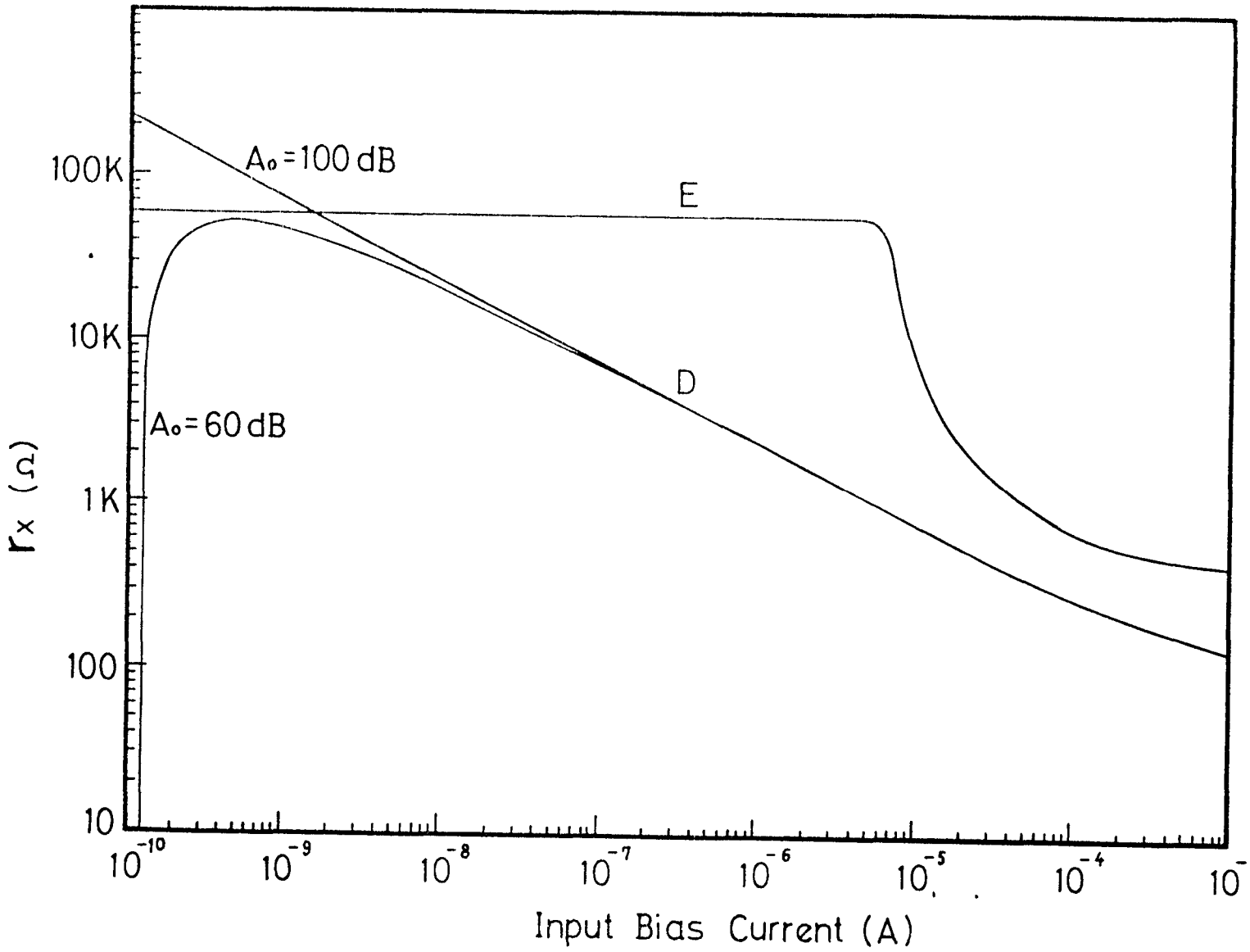

Fig.4-5 The critical damping condition of the logarithmic electrometer shown in Fig. 4. Curves D show the inserted resistance for critical damping and curve E that of the logarithmic electrometer shown in Fig. 6.

4-4. A Practical Circuit and Experimental Results

A newly designed logarithmic electrometer circuit is shown in Fig.4-6. A model μpc 152 A MOS FET operational amplifier with a unity-gain-crossover-frequency of 1 MHz and a bias current of 10^{-13} A is used for the input stage (Amp. 1). The open loop gain of the operational amplifier is fixed at 60 dB by a source feedback technique [9]. This is effective in suppressing the maximum value of the inserted resistance as shown in Fig.4-5 (curves D). But it will cause a steady-state off-set positional error to fix the gain too low. A model 2N 3058, having a saturation current of 6×10^{-14} A, is used for the logarithmic element. The inserted current variable resistor is composed of a current variable element D_1 and two resistors R_1 , R_2 . The same diode mode 2N 3058 is used for D_1 . The calculated resistance of the inserted resistor for small signal is shown in Fig.4-5 (curve E). A logarithmic output is amplified by next amplifier (Amp. 2) built up with a model μA 741A operational amplifier. The gain of 16.7 magnifications (= 1V ÷ 60 mV) was adjusted by a variable resistor R_3 and hence the gain per decade for this logarithmic electrometer was chosen as 1V/decade of input current. In order to fix an output voltage to 0 V at an input cuttent of 10^{-10} A, a bias voltage of 220 mV was applied to the Amp. 2. The zero adjustment was made by a variable resistor R_4 . The temperature influence for the logarithmic element is also compensated by two thermistors R_A , R_B used in this amplifier stage. The fundamental principles are shown in reference 10).

The input current signal for testing was prepared from

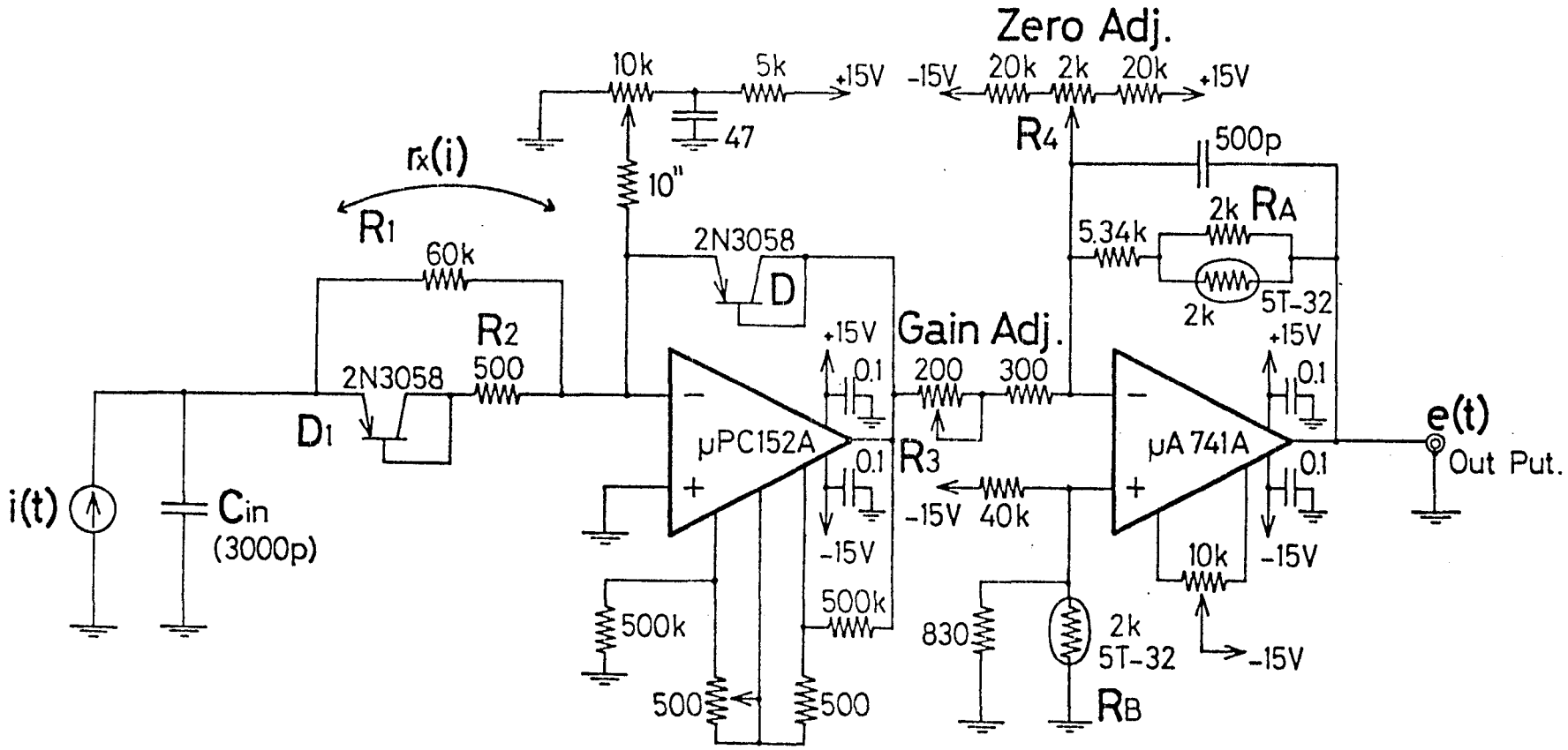

Fig. 4-6 A newly designed logarithmic electrometer circuit.

a bias current i_b and a square pulse current with an amplitude of about $0.05\, i_b$. As expected from the stability condition shown in Fig.4-5 the observed output waveforms were accompanied by no overshoot- and ringing- phenomena in the whole current range from 10^{-10} A to 10^{-3} A. The measured results of the rise time of this logarithmic electrometer are shown in Fig.4-7. The measured data agree nearly with curve F calculated from Eq.(4-8) using the curve E in Fig.4-5. A curve G in Fig.4-7 shows the rise time of the conventional logarithmic electrometer. It is evident from these results that at low current levels the response time of the logarithmic electrometer with this new phase compensation technique has been improved two decade compared with the comventional one.

Power shapes of the one-shot pulsed reactor " YAYOI " were measured by the use of this logarithmic electrometer, an ionization chamber Westinghouse type 6377 and a transient memory Iwatsu type DM 701. Figures 4-8 and 4-9 show examples of the observed power shapes of the " YAYOI " in the pulse operation below and above prompt critical state, respectively.

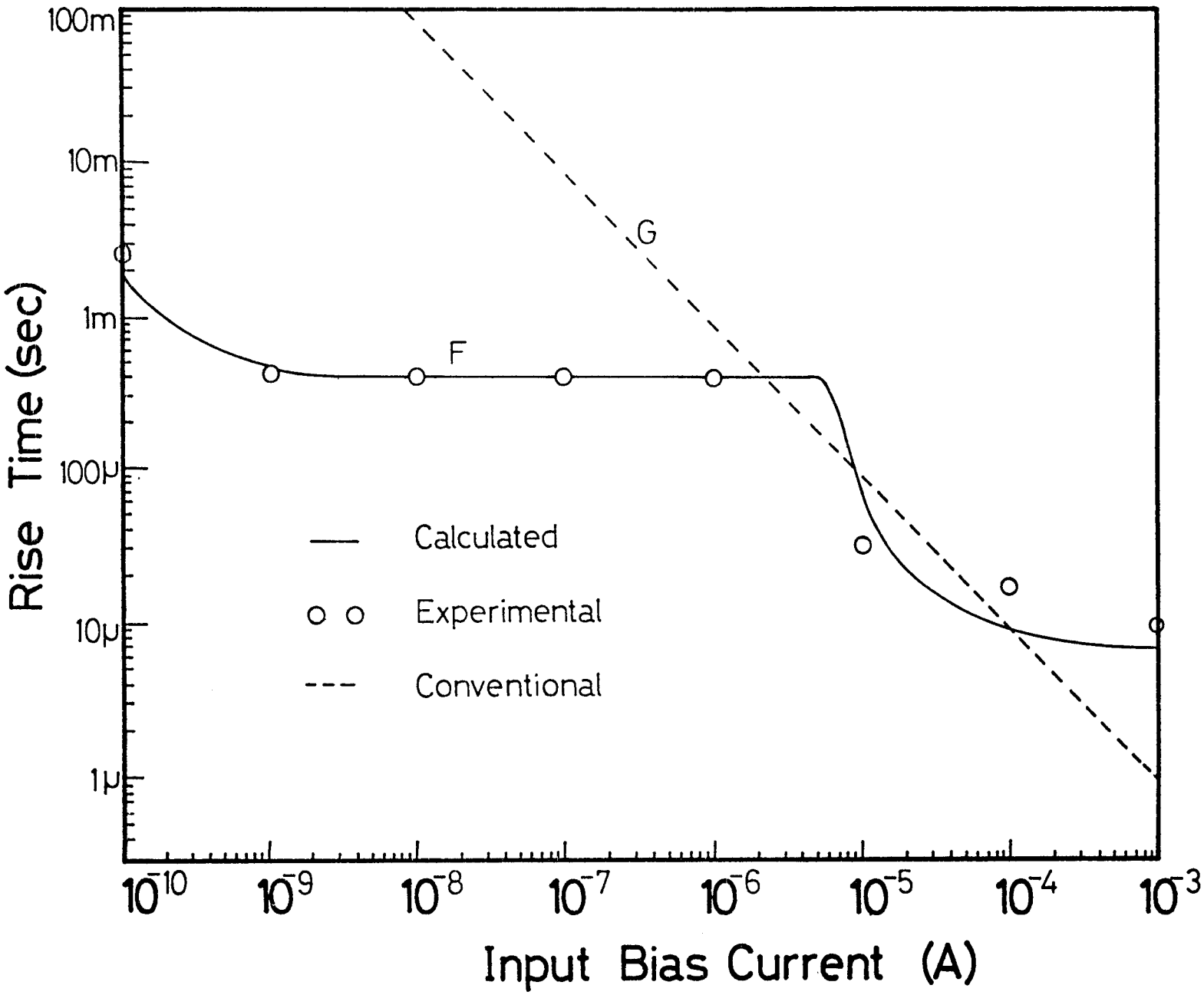

Fig.4-7 Rise times of the logarithmic electrometer shown in Fig. 6 and the conventional one

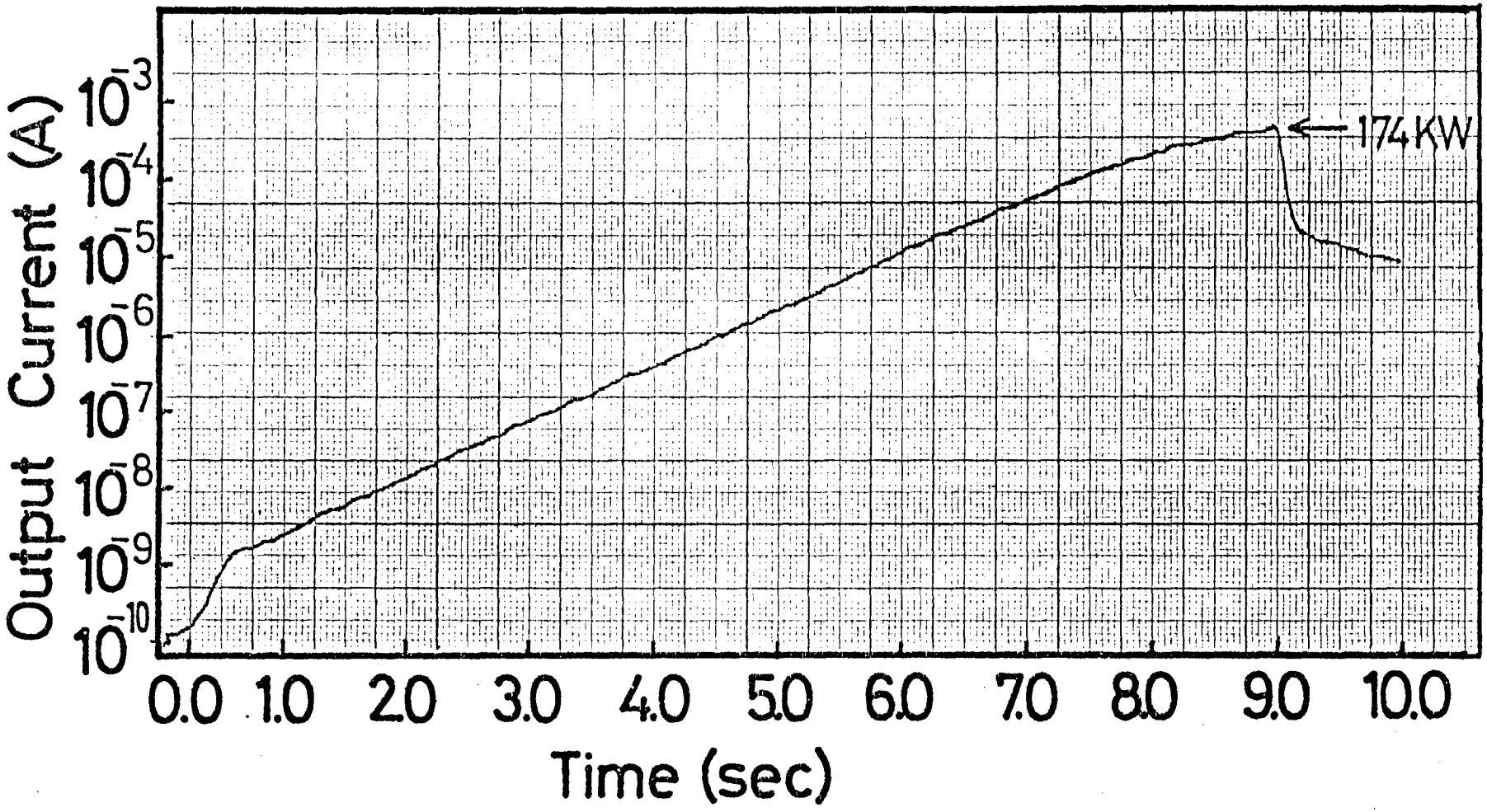

Fig.4-8 An example of the observed power shapes of the " YAYOI " in the pulse operation below prompt critical state.

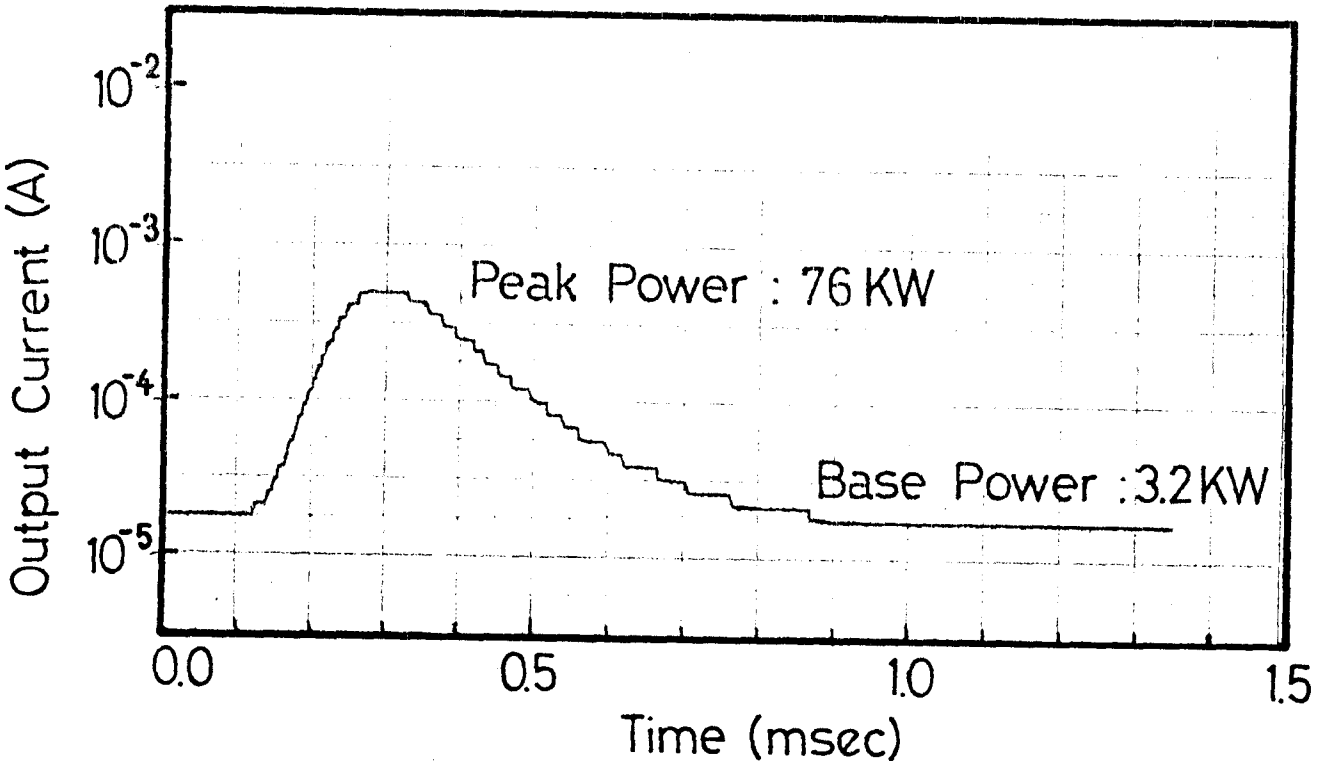

Fig.4-9 An example of the observed power shapes of the " YAYOI " in the pulse operation above prompt critical state.

4-5. Conclusion

It has been difficult to obtain a stable and fast response logarithmic electrometer with large input capacitance of a detector and a cable. At high current levels the stability of the logarithmic electrometer requires a large feedback capacitance, by which its response time is severely degraded at low current levels. This is due to the marked change of the current-dependent resistance of the logarithmic element. In order to cope with this problem, a new phase compensation technique was developed and a stable and fast response logarithmic electrometer was made. For example, the response time of this logarithmic electrometer with input capacitance of 3000pF was improved about two decades compared with the conventional one at low current levels. This logarithmic electrometer circuit is based on clear transient analysis and requires no skilful adjustment. A feasibility test of this logarithmic electrometer system was also carried out by the one-shot pulsed reactor " YAYOI " and satisfactory results were obtained.

Appendix 4-A Compensation of the Trmperature Influence

The logarithmic characteristics shown in Eq.(4-2) can be rewritten as

$$v_d = A(T) \ln i_d - B(T) , \tag{4-A1}$$

where $A(T) = \frac{nRT}{q}$ and $B(T) = \frac{nRT}{q} \ln i_s$.

The saturation current i_s is temperature dependent and is given by

$$i_s = i_o \exp\left(-\frac{B}{T}\right) , \tag{4-A2}$$

where i_o is a constant and B is 12000 for Si. It is evident from Eq.(4-A1) that the temperature sensitive v_d can be compensated by balancing the $A(T)$ and the $B(T)$ with an amplifier having a gain and a bias voltage which are dependent on temperature[9]. The simplified diagram is shown in Fig. 4-A1. Here, $R(T)$ is a temperature dependent resistor and $E_b(T)$ the temperature dependent bias voltage. The temperature dependent gain $\alpha(T)$ of the amplifier built up with an Op. Amp. 2 is given by

$$\alpha(T) = -\frac{R(T)}{R_c} . \tag{4-A3}$$

If we ignore temperature drifts of the Op. Amp. 1 and the Op. Amp. 2 , the temperature dependent output voltage $E_o(T)$ of the logarithmic electrometer shown in Fig.4-A1 can be expressed by

$$E_o(T) = \left\{ \frac{nRT}{q} \ln \frac{i_d}{i_s} - E_b(T) \right\} \alpha(T) . \tag{4-A4}$$

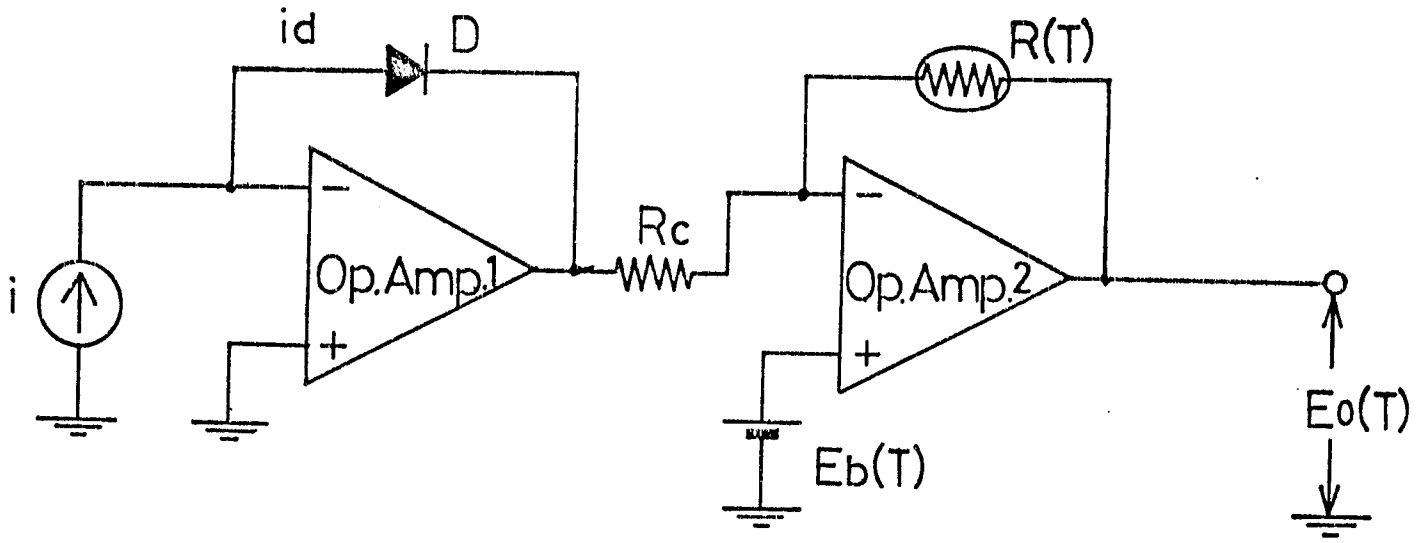

Fig.4-A1 Principle of compensating the temperature sensitive diode.

Differentiating Eq.(4-A4) with respect to T, we obtain the temperature coefficient of $E_0(T)$ as follows:

$$\frac{\partial E_0}{\partial T} = U\alpha\left(\frac{\alpha}{T} + \frac{\partial \alpha}{\partial T}\right) - \left(E_b \cdot \frac{\partial \alpha}{\partial T} + \frac{\partial E_b}{\partial \alpha} \cdot \alpha - \frac{\eta k B \alpha}{T \beta}\right) . \qquad (4\text{-}A5)$$

The first term and the second term of the right hand of Eq. (4-A5) should be zero for exact temperature compensation. From the first term, the temperature coefficient of α becomes

$$\frac{1}{\alpha} \cdot \frac{\partial \alpha}{\partial T} = -\frac{1}{T} = -0.0033\ /^\circ K \quad \text{at } 300^\circ K . \qquad (4\text{-}A6)$$

From the second term and Eq.(4-A6), the temperature coefficient of E_b becomes

$$\frac{1}{E_b} \cdot \frac{\partial E_b}{\partial T} = \frac{1}{T} - \frac{\eta k B}{\beta T E_b} = -0.012\ /^\circ K \quad \text{at } 300^\circ K . \qquad (4\text{-}A7)$$

In the circuit of the newly designed logarithmic electrometer, these temperature coefficient were realized by the use of some resistors and two thermisters R_A, R_B, which had a nominal tempereature coefficient of -0.042 /°K at 300°K. Thus, variation of less than 0.1 decade was obtained in the range from 10^{-10} A to 10^{-4} A for the ambient temperature variation of 20°C.

References

1) T. Iida and K. Sumita et al., To be submitted in the IEEE Transactions on Instrumentation and Measurement.

2) N. Wakayama, H. Yamagishi, T. Iida, N. Ohnishi and S. Ohtomo, JAERI-M-6710 pp.115-118 (1976).

3) H. Wakabayashi, A. Furuhashi, S. An and T. Tamura, Proc. US /Japan Seminar on Fast Reactors I-2 (1976).

4) N. Wakayama, T. Iida and K. Sumita, Preprint 1974 Fall Meeting At. Energy Soc. Japan, (in Japanease), C21 (1974).

5) M. Y. El-Ibiary, IEEE Trans. Nucl. Sci. NS-10, 21-31 (1963)

6) W. L. Patterson, Rev. Sci. Instr. 34, 1311-1316 (1963).

7) L. S. Horn and B. I. Khasanov, Nucl. Instr. Meth. 40, 267 -271 (1966).

8) K. Sumita, T. Iida and N. Wakayama, Proc. US/Japan Seminar on Fast Pulse Reactors III-1 (1976).

9) NEC Electron Device Data Book '72, 818 (1972).

10) T. Furukawa and N. Wakayama, Nuclear Electronics IAEA, 141-155 (1965).

Chapter V. Fast Response Log N & Period Meter

5-1 Introduction

Various applications of this system can be expected in transient neutronic measurements in reactor operations. One of the typical examples is the instantaneous measurement of the time dependent reactivity. Such the measurement is needed urgently for determination of pulse shape control of a pulsed reactor. Other application is to obtain the safety scram signal in rapid transient situation of a steady reactor.

In kinetic studies on pulsed reactors, it is often useful to characterize dynamic behavior by instantaneous reciprocal period or instantaneous $\alpha(t)$ $(\equiv \dot{n}(t)/n(t))$. Major response characteristics can be determined if $\alpha(t)$ is clearly known. Excess prompt reactivity in a pulsed reactor is evaluated by measuring the value of $\alpha(t)$ with power excursion[1)2)]. As the simplified treatment, the excess prompt reactivity is obtained from one group, one point reactor kinetic equation with delayed neutron neglection as follows.

$$\rho(t) - \beta = \ell \cdot \alpha(t) = \ell \frac{d}{dt}\{\ell n n(t)\},$$

where $\rho(t)$ is the reactivity at time t.

There is the proportional relationship between the instantaneous excess prompt reactivity and the value of $\alpha(t)$, that is, the inverse of the prompt period. Then the time dependent excess prompt reactivity can be observed directly as the output of a fast response log N & period meter.

Of course, the integral time constant of the log N & period meter should be much less than the reactor period itself; the time constant in a reactor power increasing, and the effect of the ion transit time of the ionization chamber should be neglected by the suitable correction method.

T. Furukawa[3] pointed out that the log N & period meter for steady reactors was liable to trip spuriously due to inverse period overshoot of the period meter output, resulting from exponentially increasing reactor power from beyond the range of the log N channel. He also obtained data sheets[4] which were effective in designing the optimum time constant of the log N & period meter for steady reactors. However, his data sheets are not applicable to the design of the log N & period meter for pulsed reactors, since the log N & period meter for pulsed reactors requires very fast responsiveness and therefore a new circuit design which is different from one for steady reactors.

A fast response log N & period meter was developed for pulse reactor operation.[5] A new phase compensation technique[6] was applied to the logarithmic electrometer circuit in the log N & period meter, and the response time and the overshoot error of the log N & period meter were markedly reduced. At first, the transient response of a log N & period meter shall be discussed in this chapter and then the new phase compensation technique and experimental results of the fast response log N & period meter shall be shown.

5-2 Transient Response

The instantaneous prompt $\alpha(t)$, i. e. the inverse of the prompt reactor period, is given by

$$\alpha(t) = \frac{d}{dt} n(t)/n(t) = \frac{d}{dt}\{\ell n\, n(t)\} \quad . \tag{5-1}$$

The value of $\alpha(t)$ can be, therefore, observed as the output of an ideal log N & period meter, which has no time lag. However, a real log N & period meter, whose equivalent circuit diagram is shown Fig. 5-1, causes an inevitable error due to the following two effects in the measurement of $\alpha(t)$ value. One is due to the lag of the response time of an analog differentiator which is built up with an operational amplifier. The transfer function of the differentiator shown in Fig. 5-1 is given by

$$G_D(S) = \frac{E_0(S)}{E_1(S)} = \frac{-R_d C_d S}{1 + (\tau_1 + R_d C_{fd} + \frac{R_d C_d}{A_1})S + \tau_1 R_d (C_d + C_{fd}) S^2} , \tag{5-2}$$

where $R_d C_d$ is the gain of the differentiator.

The fastest response of the differentiator is realized when C_{fd} is equal to C_{f_0} $\left(= \frac{\tau_1}{R_d} - \frac{C_d}{A_1} + 2\sqrt{\frac{\tau_1 C_d}{R_d}}\right)$ like as discussed in section 3-2. If we substitute that relation into Eq. (5-2), the integral time constant of the differentiator becomes

$$T_D = \tau_1 + \sqrt{\tau_1 R_d C_d} \quad . \tag{5-3}$$

It is important in the desigen of a fast response analog differentiator to make this time constant T_D sufficiently small. Such design of the time constant is not so difficult and a fast response differentiator can be easily obtained. Hence it is assumed that the error due to the lag of the response time of the differentiator is negligible in further

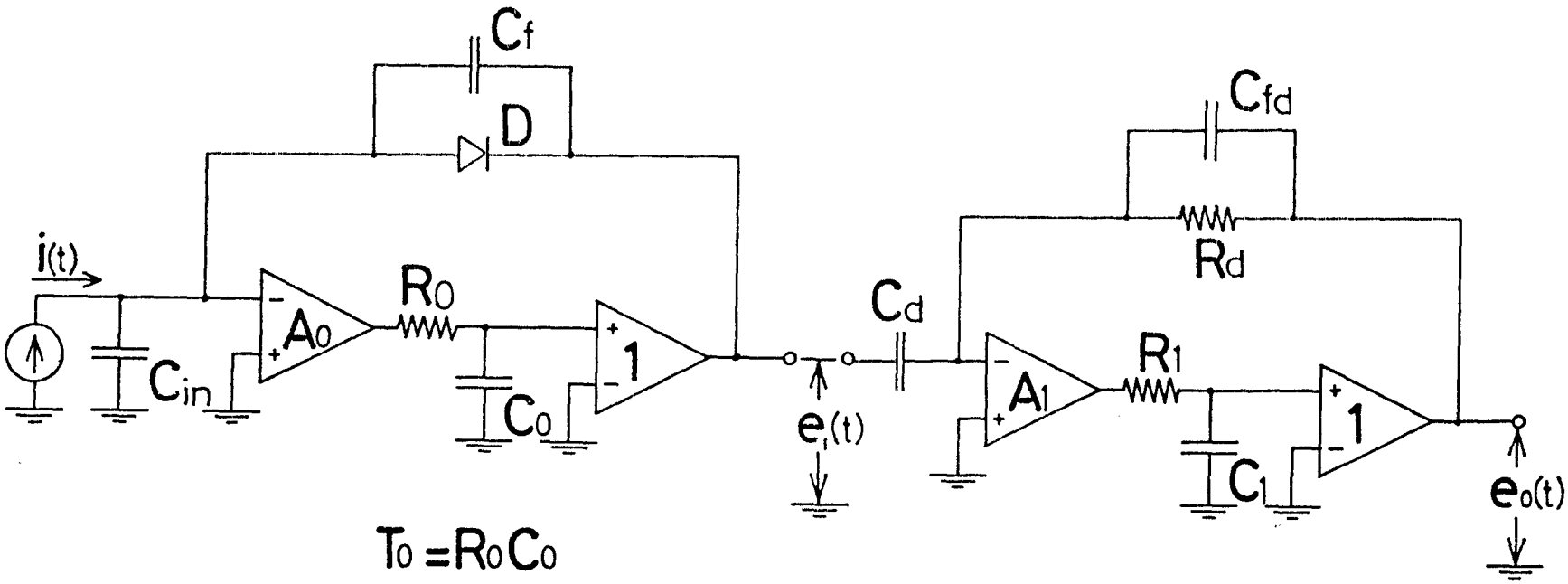

Fig.5-1 Equivalent circuit diagram of a fundamental log N period meter.

discussions. The other is due to the lag of the response time of a logarithmic electrometer. This makes it difficult to observe the precise $\alpha(t)$ value.

From circuit analysis, the transient response of the log N & period meter circuit shown in Fig. 5-1 can be generally expressed by

$$e_o(t) = \frac{R_d C_d}{C_f} i(t) - \frac{nkTR_dC_d}{q_e} \frac{\exp\{\beta(t)\}}{\int_0^t \exp\{\beta(t)\}dt + \frac{nkTC_fC_I}{q_e}}, \quad (5-4)$$

where $\beta(t) = \frac{q_e}{nkTC_f} \int i(t)\,dt$,

and C_I is an integral constant.

Here, the following assumption is introduced to simplify the analysis on the transient response of the circuit.

$$i(t) = i_0 \exp\left(\frac{t}{T_P}\right) . \quad (5-5)$$

where i_0 is an initial input current and T_P is a time constant corresponding to a reactor period. This assumption is effective in estimating the general response characteristics of a log N & period meter circuit and is also approximately applicable to the real situation of a transient reactor power of a pulsed reactor. In this assumption, the response of the ideal log N & period meter circuit with no time lag is easily given by

$$e_o(t) = \frac{nkTR_dC_d}{q_e} \cdot \frac{1}{T_P} \quad (= \text{constant}), \quad (5-6)$$

which shows that the output voltage is proportional to the inverse of the reactor period. On the other hand, the output voltage of the real log N & period meter circuit with some time constants gradually the constant value shown in

Eq. (5-6).

Figure 5-2 illustrates profiles of the transient response of the lag N & period meter circuit shown in Fig. 5-1. These were calculated from Eq. (5-4), varying the initial current i_0 as a parameter and using the following values; $\frac{nkT}{q_e} = 26mV$, $C_f = 14700pF$, $T_p = 1ms$. The former two values have been described in section 4-2. It is evident from the profiles that the smaller the initial current i_0 is, the larger the overshoot error of the reciprocal period is. The response characteristics which are accompanied by such overshoot error disturb the precise measurement of $\alpha(t)$ value. A fast response log N & period meter circuit for pulsed reactors should be designed not to cause such overshoot error.

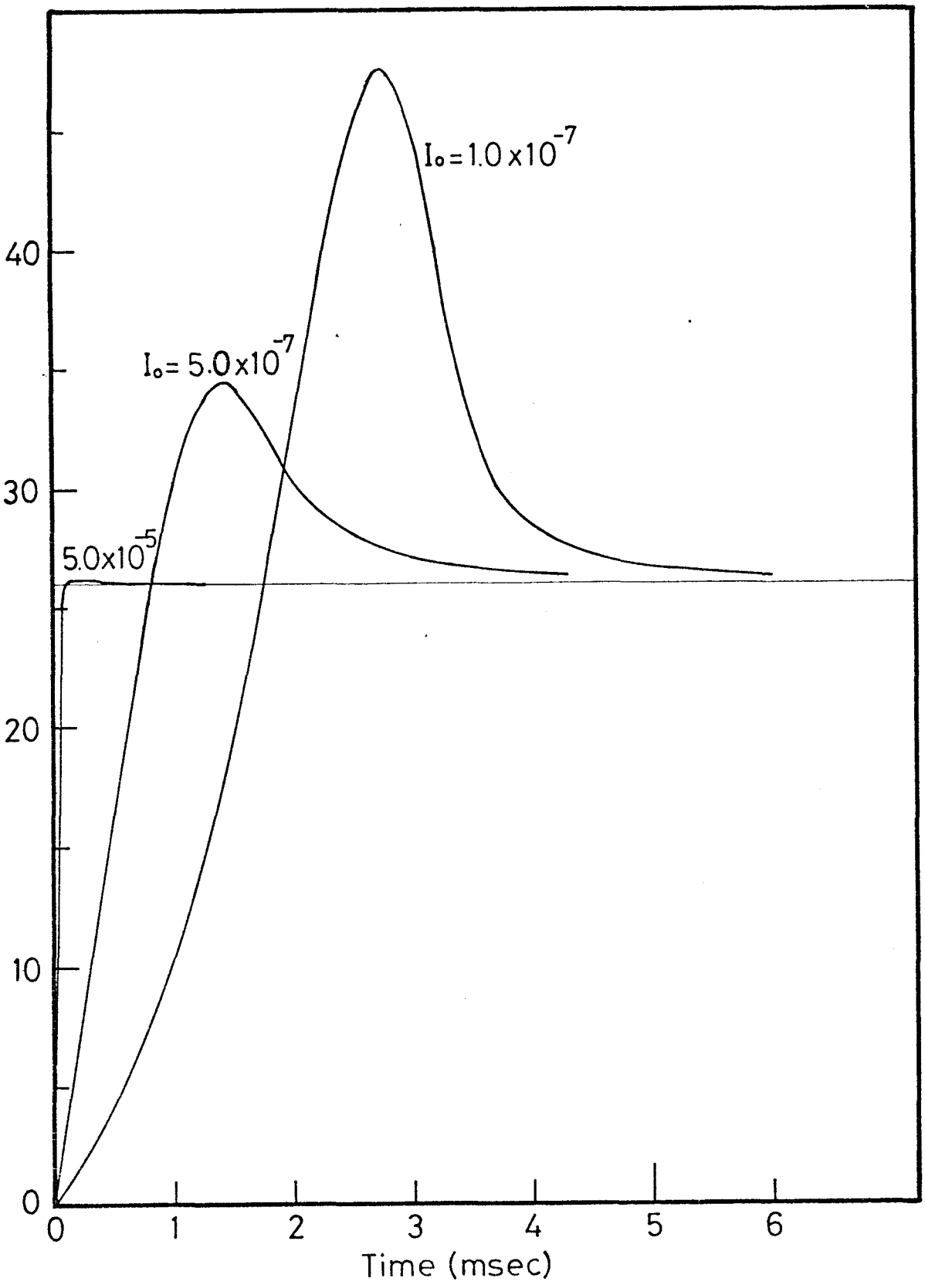

Fig. 5-2 Profiles of the transient response of the log N & period meter circuit shown in Fig. 5-1.

5 - 3 Improvement of the response characteristics

As described in previous section, the overshoot error of the log N & period meter is governed by the lag of the response time of the logarithmic electrometer. Therefore, the error can be reduced by improving the response time of the logarithmic electrometer, especially at low current levels.

Figure 5-3 shows the equivalent circuit diagram of a new type logarithmic electrometer designed by N. Wakayama etc [6]. This circuit maintains the stability based on that a resistance R_{in} inserted between a detector cable and the input terminal of the circuit recovers the phase lag caused by the input capacitance at high current levels and moreover a feedback capacitance C_f does that at low current levels.

The transfer function of this circuit for small input signal is given by

$$G_D(S)=\frac{\Delta E_o(S)}{\Delta I_o(S)}=-r_D\left[1+\left(\frac{r_D C_{in}}{A_o}+C_f+R_{in}C_{in}+\tau_o\right)S+\left\{R_{in}C_{in}r_D C_f+\tau_o\left(r_D C_{in}+R_{in}C_{in}+r_D C_f\right)\right\}S^2+R_{in}C_{in}C_f r_D \tau_o S^3\right]^{-1}. \qquad (5-7)$$

Then, the stability condition of this circuit, in other words, the condition that the poles of Eq. (5-7) are all negative, can be expressed by

$$\left.\begin{aligned} &b^2-3ac \geq 0 \\ &a^2b^2+18abc-4a^3c-4b^3-27c^2 \geq 0 \end{aligned}\right\}, \qquad (5-8)$$

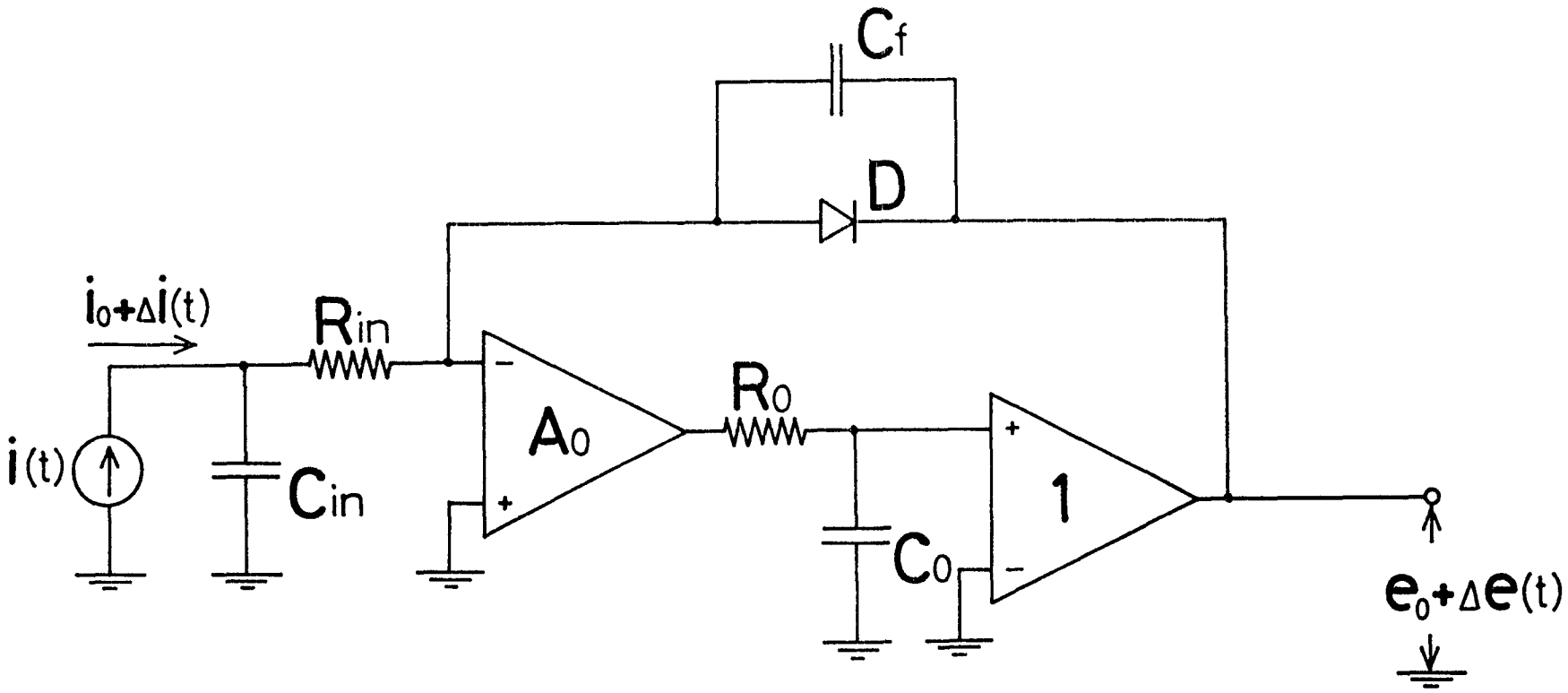

Fig. 5-3 Equivalent circuit diagram of a newly designed logarithmic electrometer for the log N period meter.

where $$a = \frac{r_D C_{in}}{A_0} + r_D C_f + R_{in} C_{in} + \tau_0 ,$$

$$b = R_{in} r_D C_{in} C_f + \tau_0 (r_D C_{in} + R_{in} C_{in} + r_D C_f) ,$$

$$c = R_{in} r_D C_{in} C_f \tau_0 .$$

It is troublesome to obtain the exact relation between R_{in} and C_f at critical damping from above equations. Thereupon, a simplified method is here proposed to estimate roughly the relation. The summary of this method is shown in Fig. 5-4. A curve A shows the time constant of the logarithmic electrometer at critical damping. In the case that a small feedback capacitance C_f' is selected, a conventional logarithmic electrometer, whose equivalent circuit diagram is shown in Fig. 4-1, becomes unstable at the current levels above I_x in Fig. 5-4, which is easily from the discussion in section 4-2. Consequently, it becomes necessary that a resistance is inserted between a detector cable and the input terminal of the amplifier to suppress too fast response at such high current levels. Hence, the resistance R_{in} can be approximately determined by the following relations.

$$R_{in} > \sqrt{\frac{nkT\tau_0}{qC_{in}I_x}} = \sqrt{\frac{\tau_0}{C_f'^2}} \qquad (5-9)$$

The time constant of this type logarithmic electrometer is shown as a curve C in Fig. 5-4. A curve B shows the time constant of the conventional logarithmic electrometer. It is evident

from the comparison of the two curves B and C that the response time of the new type logarithmic electrometer is markedly improved at low current levels. Needless to say, the time constant of the new type logarithmic electrometer is reduced to $R_{in}\,C_{in}$ at high current levels and it should be sufficiently small than the reactor period.

Figure 5-5 shows the profiles of the transient response of the log N & period meter with the new type logarithmic electrometer. Those were approximately calculated from Eq. (5-4) using the following equation

$$i(t)=i_0\exp\left(-\frac{t}{R_{in}C_{in}}\right)+\frac{i_0 T_p}{T_p+R_{in}C_{in}}\exp\left(\frac{t}{T_p}\right)\left[1-\exp\left\{1-\left(\frac{1}{T_p}+\frac{1}{R_{in}C_{in}}\right)t\right\}\right] \tag{5-11}$$

and the following values ; R_{in} = 6.6 KΩ ; C_f' = 30 pF ; T_p = 1 ms. It is evident from the comparison of the profiles in Figs. (5-2) and (5-5) that the overshoot error of the new type log N & period meter is markedly reduced at low current levels.

Figure 5-6 shows the relation between the reactor period T_p and the minimum initial current i_0 when the overshoot error becomes less than 1 per cent. A curve D shows the minimum initial current of the new type log N & period meter and a curve E does that of the conventional one. It is evident from the comparison of the two curves D and E that the new type log N & period meter can cover the current range much more widely than the conventional one.

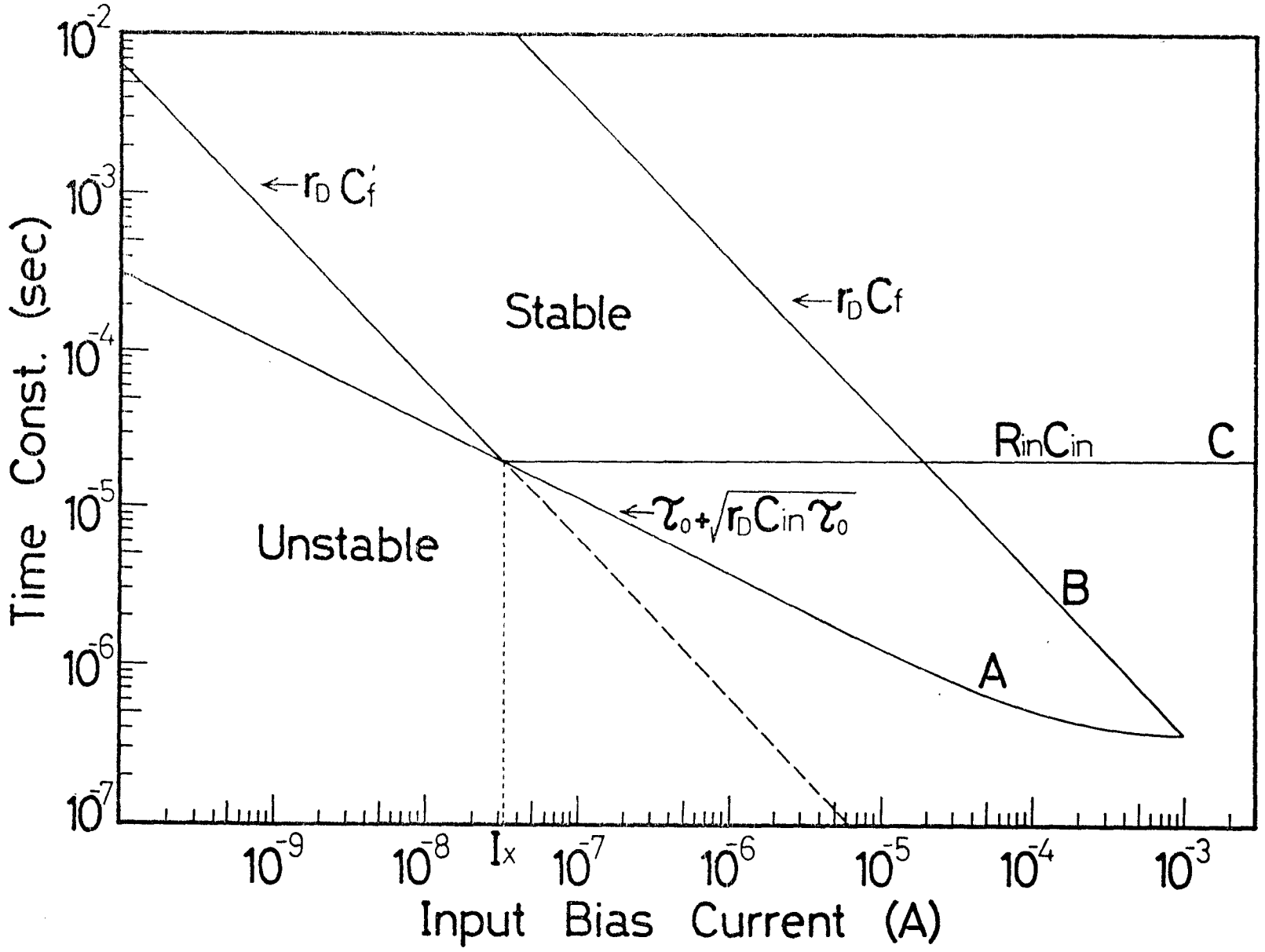

Fig. 5-4 A simplified method to obtain roughly the stability condition of the logarithmic electrometer circuit shown in Fig. 5-3.

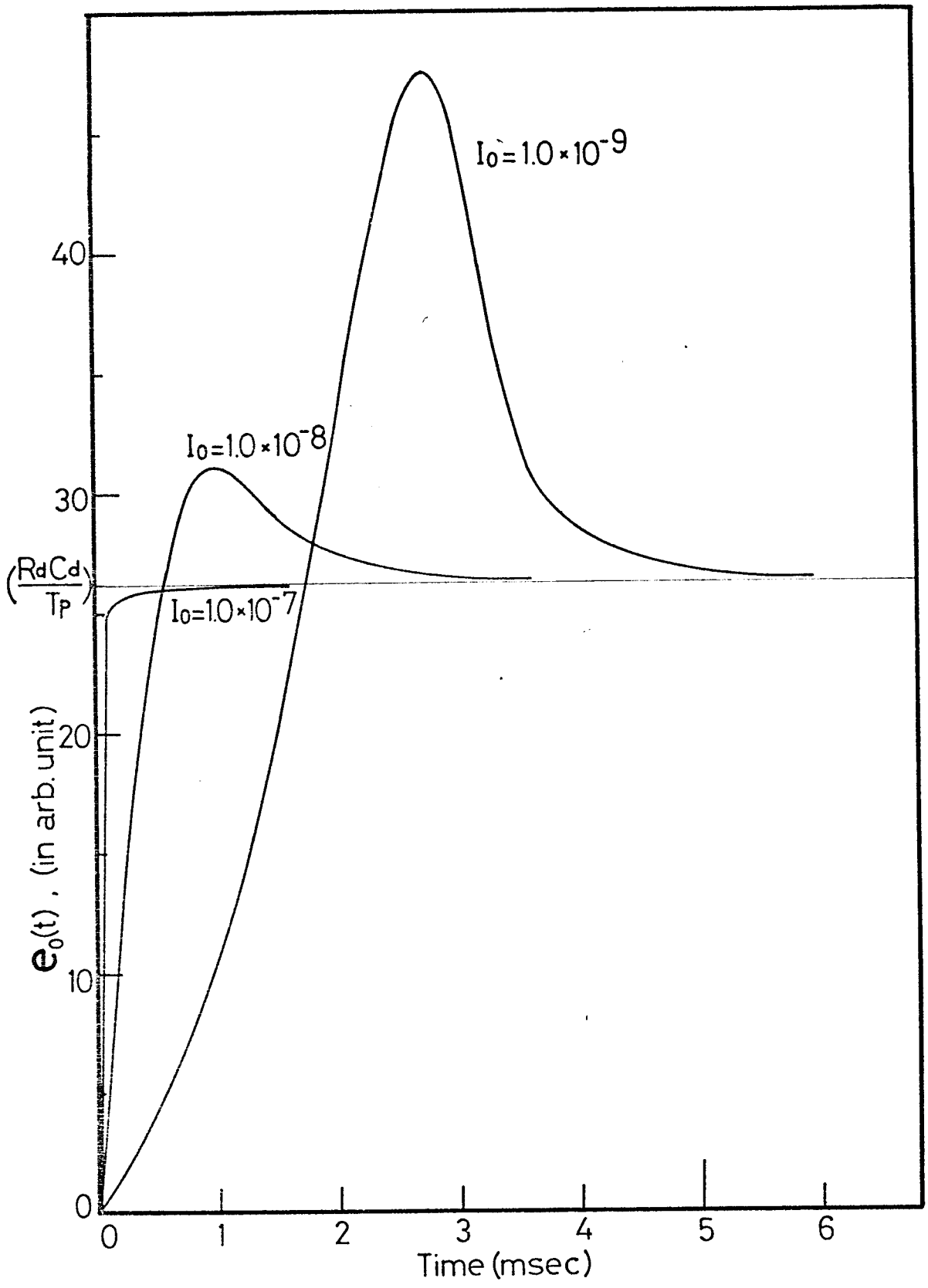

Fig. 5-5 Profiles of the transient response of a newly designed log N & period meter circuit.

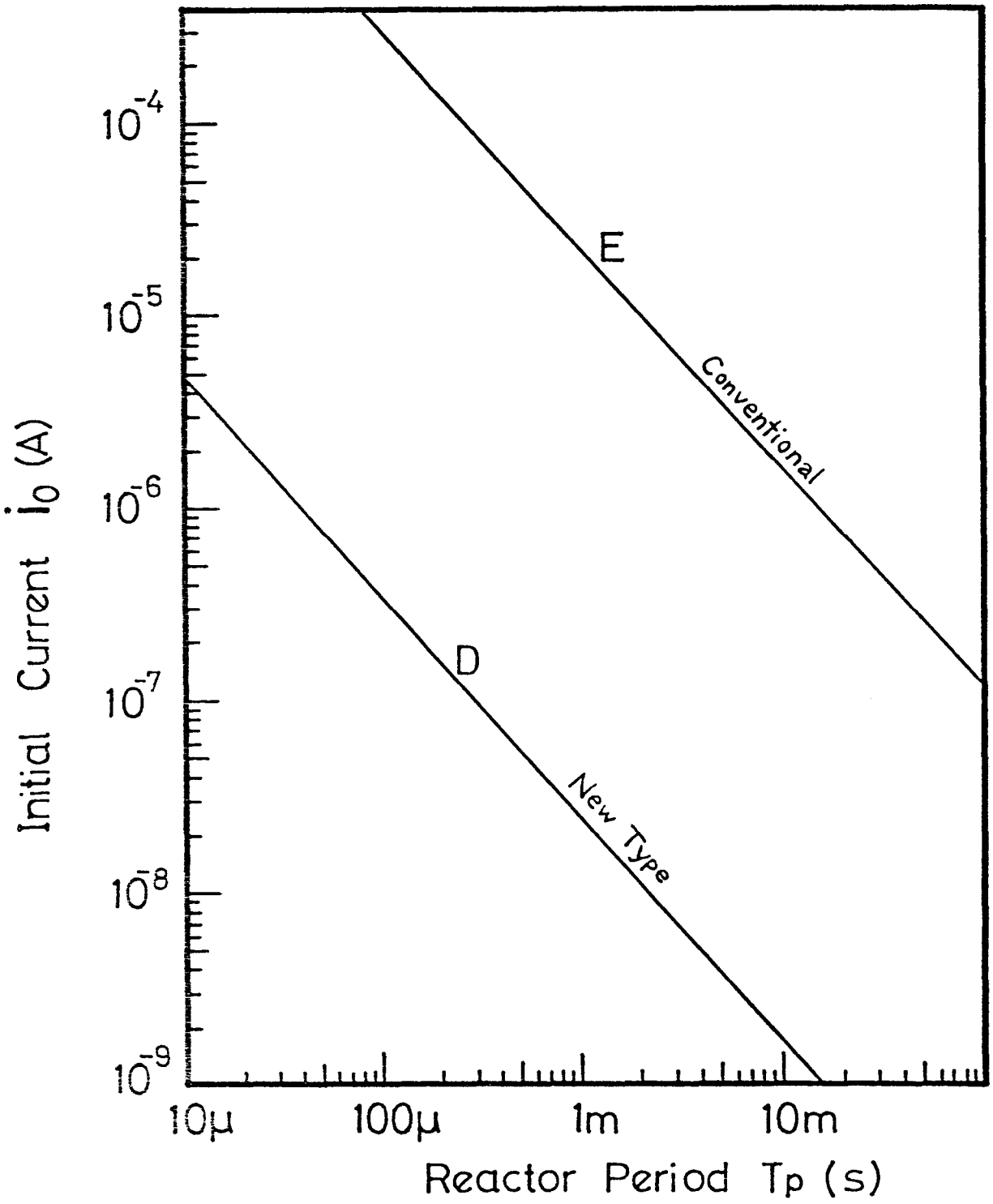

Fig. 5-6 The relation between the reactor period T_p and the minimum initial current i_0 when the overshoot error becomes less than 1 per cent.

5-4 A Practical Circuit and Experimental Results

A practical logarithmic electrometer circuit with the new phase compensation technique is shown in Fig. 5-7. Two model 1430 FET operational amplifiers with a unty-gain-crossover-frequency of about 100 MHz are used in the circuit. A silicon planar transistor model 2N3058, having a saturation current of 6×10^{-14} A, is used for a logarithmic element. A detailed design on temperature compensation, zero adjustment and so on is described in chapter IV. The inserted resistance R_{in} and the feedback capacitance C_f' should be adjusted according to measuring conditions, that is, a cable capacitance and a reactor period. A practical period meter circuit is shown in Fig. 5-8. A model 1430 FET operational amplifier is used for the analog differentiator. The gain $R_d C_d$ of the differentiator is fixed to the magnitude of a period range of 230 magnifications. Consequently, the reactor period T_p is given by

$$T_p = \frac{T_{P.R.}}{e_o} \qquad (5\text{-}10)$$

where $T_{P\ R}$ is the period range and e_o the output voltage of the log N & period meter (volt.).

Figure 5-9 shows some examples from the observed results in the pulse operation of the NSRR with this log N & period meter. In this experiment, the inserted resistance of 5 kΩ and the feedback capacitance of 40 pF were selected based on the principle described in previous section. The measured results are apparently accompanied by no overshoot phenomena shown in section 5-2.

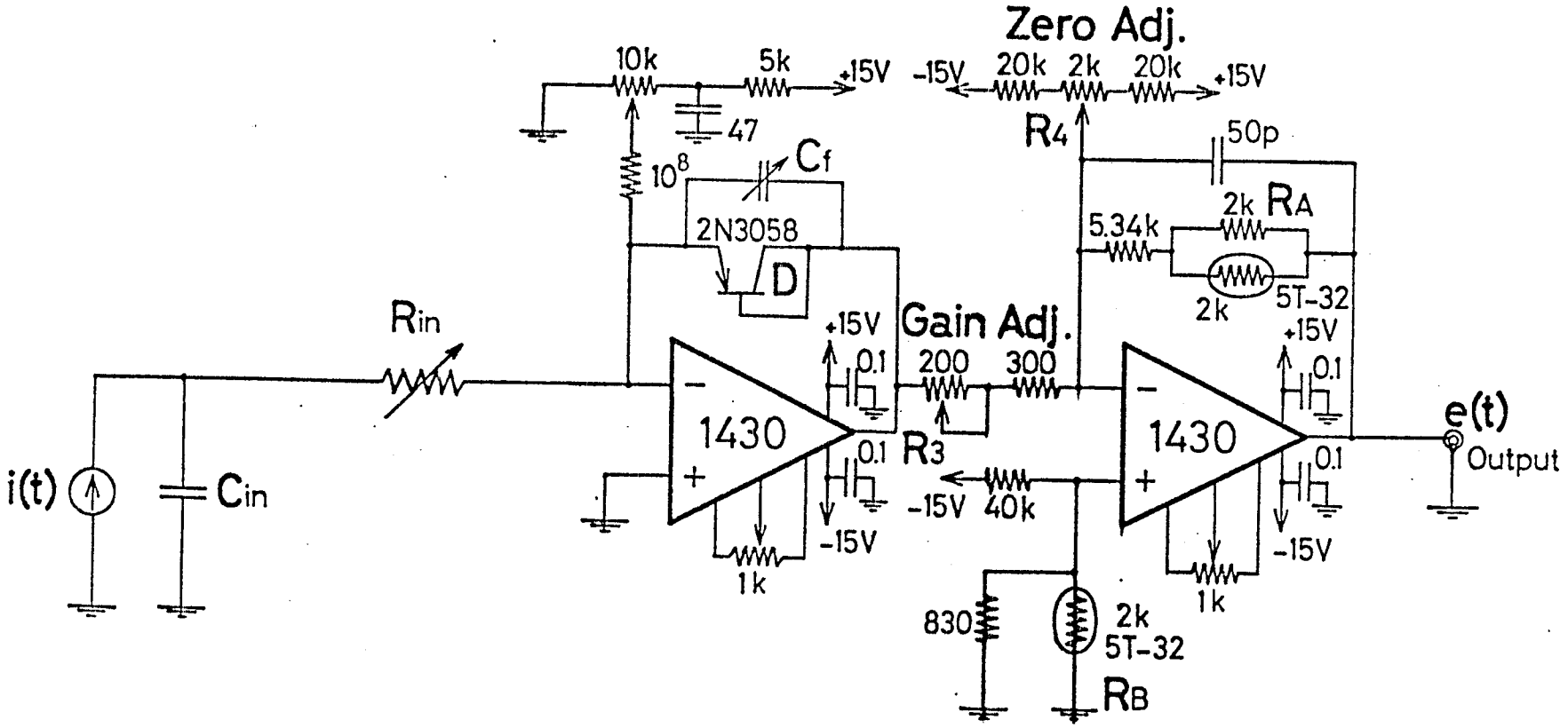

Fig. 5-7 A practical logarithmic electrometer circuit with a new phase compensation technique.

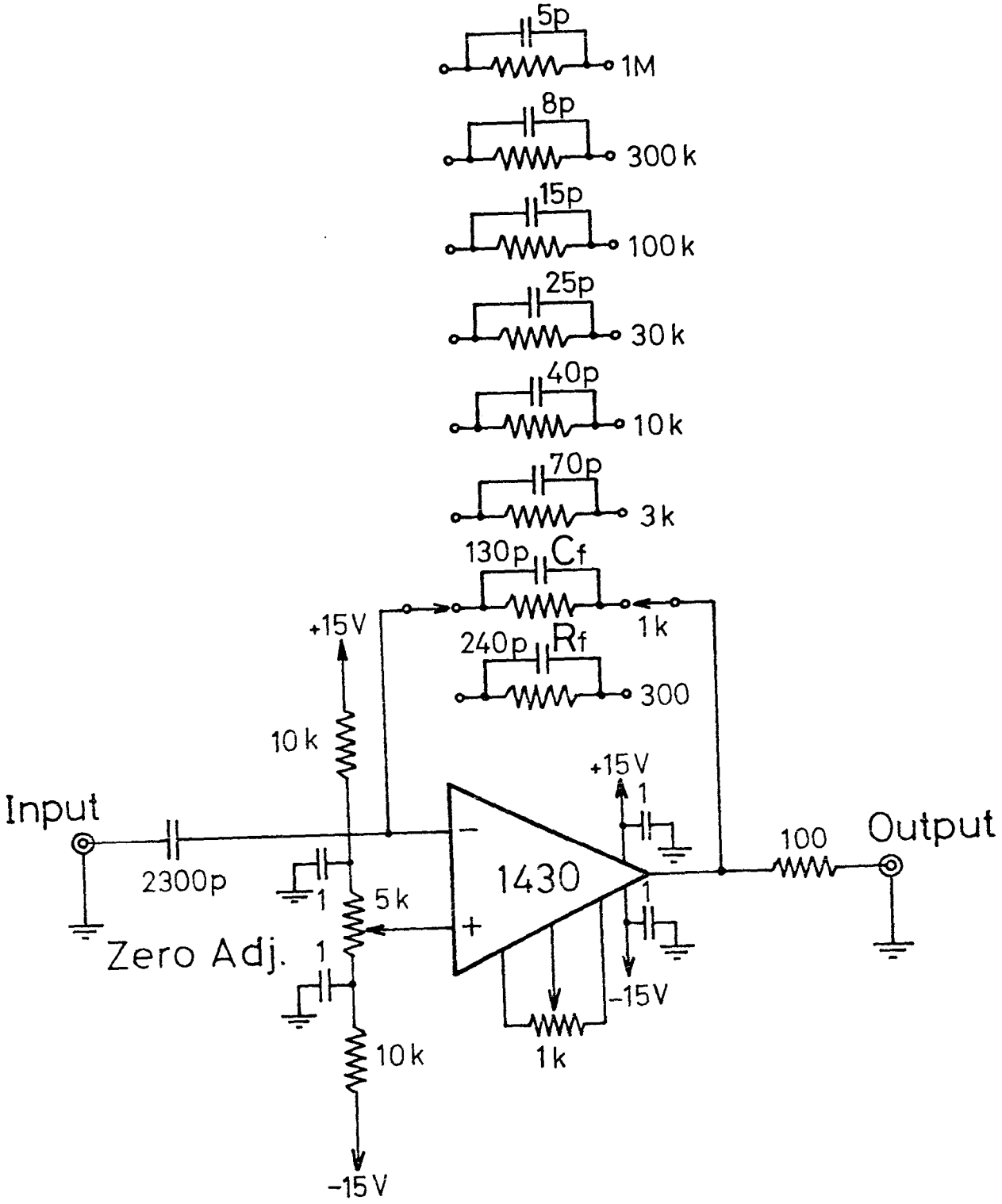

Fig. 5-8 A practical period meter circuit.

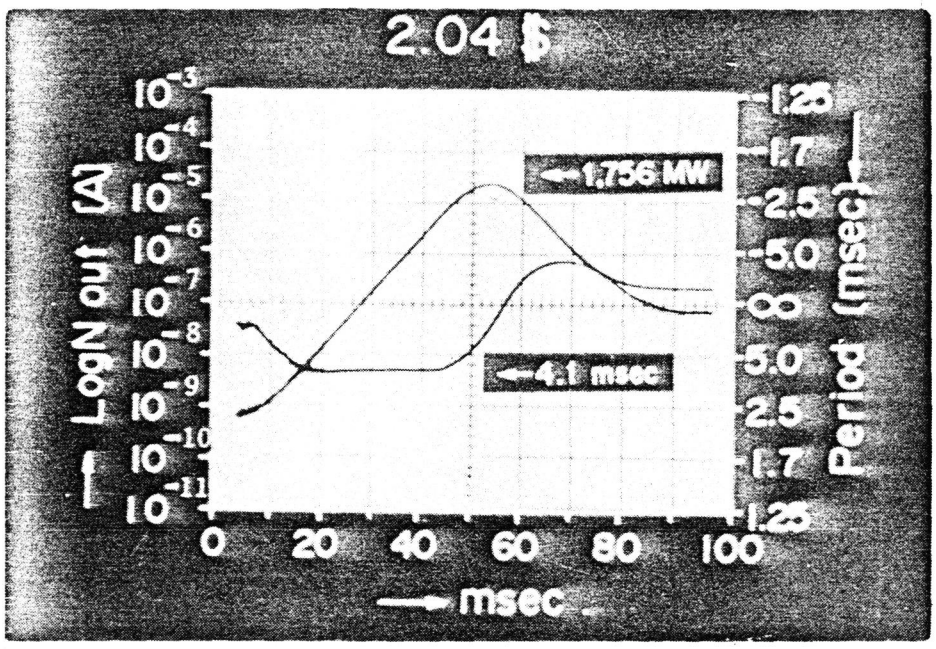

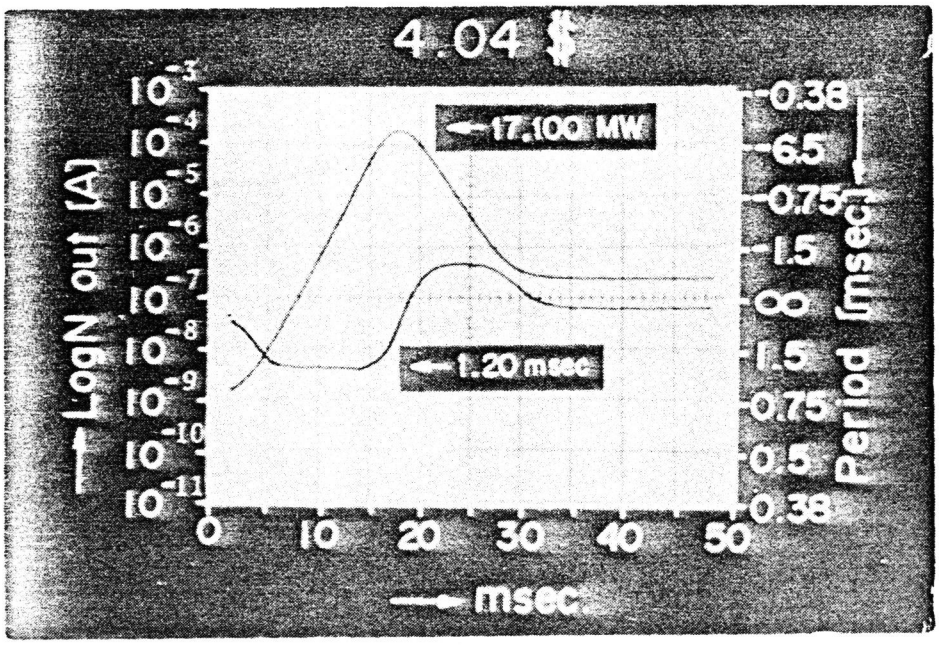

Fig. 5-9 Some examples from the observed results in the pulse operation of the " NSRR " with our systems.

Figure 5-10 shows an example from the observed results in the pulse operation of the YAYOI. In this experiment, very fast responsiveness was required for measuring systems and an inserted resistor of 350 Ω and a feedback capacitor of 25pF were selected in the new logarithmic electrometer circuit. Thus, the time constant of the logarithmic electrometer was reduced to about 1 μsec at the current levels above 10^{-7} A. Therefore, the measured result is hardly accompanied by such an overshoot error as described in section 5-2.

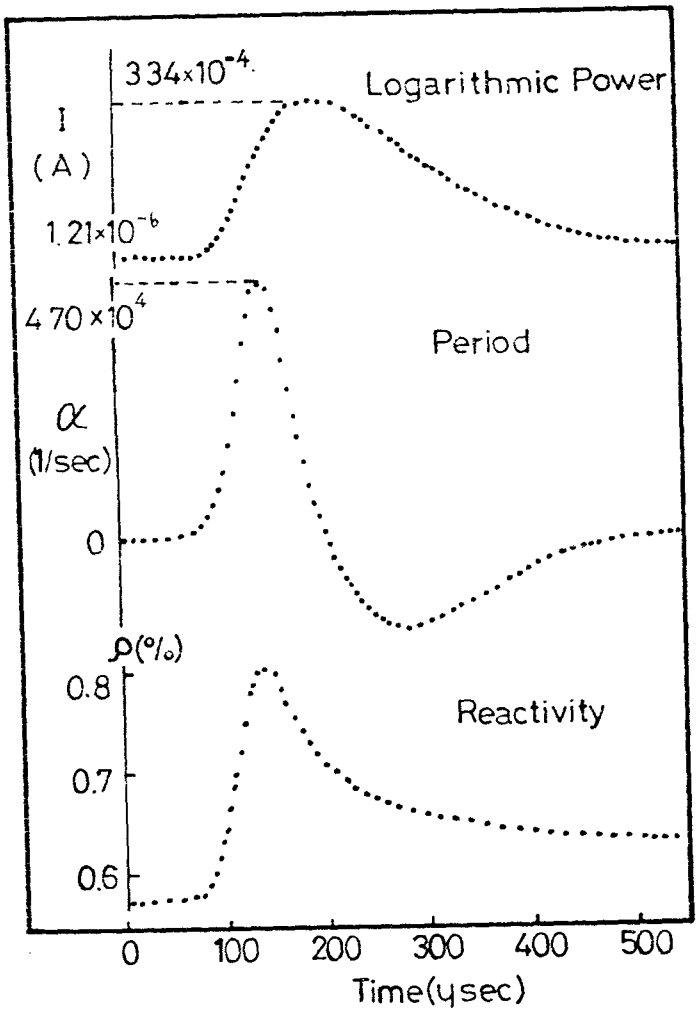

Fig. 5-10 An example from the observed results in the pulse operation of the " YAYOI " with our systems.

5-5 Conclusion

It has been difficult to design and manufacture a stable and fast response log N & period meter for pulsed reactors. At low current levels, it often produces an overshoot error, which is caused by the lag of the response time of the logarithmic electrometer. In order to overcome this problem, a phase compensation technique reported by N. Wakayama etc.[6] was applied to the logarithmic electrometer circuit and a stable and fast response log N & period meter was made. The range which could be covered by this new type log N & period meter was extended about two decades as wide as the commercially supplied, conventional one. This log N & period meter circuit is based on clear transient analysis and requires no skilful adjustment. A feasibility test of this log N & period meter was also carried out by utilizing the one shot pulse reactors "NSRR" and "YAYOI". Satisfactory results were obtained in the instantaneous $\alpha(t)$ meausrements and the precise values of reactivity inserted into the reactors were determined.

References

1) H. Wakabayashi, etc., J. of the Fuc. of Eng., the U. of Tokyo (B) Vol. XXXIV, No.1 (1977).

2) N. Wakayama, H. Yamagishi, T. Iida, etc., JAERI - M - 6710 pp. 115-118 (1976).

3) T. Furukawa, J. of the At. Energy Soc. Japan, Vol. 12, No. 2 62 (1970).

4) T. Furukawa, J. of the At. Energy Soc. Japan, Vol. 11, No. 6 347 (1969).

5) K. Sumita, T. Iida and N. Wakayama, Proc. US/Japan Seminar on Fast Pulse Reactors III - 1 (1976).

6) N. Wakayama, T. Iida and K. Sumita, Preprint 1974 Ann. Meeting At. Energy Soc. Japan, (in Japanese), C - 21 (1974).

Chapter VI Summary

In chapter I, requirements for the nuclear instrumentation of pulsed reactors have been discussed.
The ionization chamber-electrometer system is much superior to the pulse counting one in the view point of statistical accuracy, and it is evident that the former system should be applied to a power shape monitor for pulsed reactors. The response time of the former system must be improved to be successfully applied to a power shape monitor for pulsed reactors.

In chapter II, the transfer function of ionization chambers has been investigated. The impulse response of an ionization chamber was measured using intense gamma ray pulses produced by a linear accelerator, by varying the applied voltage as a parameter. The results obtained clarified the following points. First the transfer function of the ionization chamber is mainly expressed by the transit times of positive ions and electrons. Secondly the positive ion transit time decreases proportionately with increasing applied voltage and the electron transit time does consistently with that. The fluctuation current of the ionization chamber, set up in the thermal column of a reactor, was also measured by varying the time constant of a current amplifier system as a parameter. The results show that the power spectral density of the fluctuation current is not perfectly white but dependent on these transit times in the very high frequency region. These experiments should be useful to select detectors for pulsed reactors and to develope newly a new fast response one.

In chapter III, a fast response electrometer for pulsed reactors has been developed. The response speed of an electrometer with a long detector cable was markedly improved by reducing the effective cable capacitance. In the circuit of the electrometer, a new guard technique was used to reduce an effective cable capacitance and a negative capacitance technique to obtain the critical damping condition. Stability of this electrometer is ensured by adjustment of the open loop gain of the guard amplifier and the feedback capacitance. This stable and fast response electrometer was successfully applied to transient power measurements of the one shot pulse reactor " YAYOI ".

In chapter IV, a fast response logarithmic electrometer has been developed. The response time of a logarithmic electrometer was improved by introducing a new phase compensation technique. It is based on that a current variable resistance inserted between a detector cable and the input terminal of the logarithmic electrometer recovers the phase lag caused by the input capacitance. This stable and fast response logarithmic electrometer was successfully applied to transient power measurements of the one shot pulse reactor "YAYOI ".

In chapter V, a fast response log N & period meter has been examined. The covering range of a log N & period meter was markedly extended by improving the response time of the logarithmic electrometer. The logarithmic electrometer maintains the stability based on the fact that a current variable resistance inserted cable and the input terminal of the circuit recovers the phase lag caused by the input capacitance at high current levels and

moreover a feedback capacitance does that at low current levels. These resistance and capacitance are adjusted according to measuring conditions in a cable capacitance and a reactor period. This fast response log N & period meter was successfully used to determine the precise values of reactivity inserted into the pulsed reactors "NSRR" and "YAYOI".

The fast response amplifier system shown in this paper has been used for the nuclear instrumentation of the "NSRR" and the "YAYOI" and should be also useful for that of the JLB. Consideration for the response time of an ionization chamber should be also useful to develope a fast response one as a detector for the JLB.

Acknowledgment

The author would like to express his greatest appreciation to Prof. Kenji Sumita who has guided the author to the present study and has been giving the continuous encouragement and criticisms. Many thanks should go to Prof. Tamotsu Sekiya, Prof. Masaharu Kawanishi and Prof. Toshihiko Namekawa of Osaka University for their critical reading the manuscript and instructive advices.

Most works contained in this thesis had been carried out at the nuclear instrumentation laboratory of the Department of Nuclear Engineering, Faculty of Engineering, Osaka University. The author wishes to show the sincere gratitude to Mr. S. Makino (Osaka University, now NAIG), Mr. Y. Kokubo, Mr. H. Kamimura and Mr. Y. Maekawa (Osaka University) for their kind suggestions and discussions in the experiments and analyses.

The author is great thankful to Mr. N. Wakayama and Mr. H. Yamagishi (JAERI) for their very useful suggestions and discussions in designing the amplifier circuits and carrying out the experiments at the "NSRR". The author is also great thankful to Dr. H. Wakabayashi (the University of Tokyo), Dr. Y. Fujita and Dr. K. Kanda (Kyoto University) for their helpful suggestions and discussions in carrying out the experiments at the "YAYOI", the "KUR-LINAC" and the "KUR", respectively. The author wishes to thank the Japan Atomic Energy Research Institute, the University of Tokyo and Kyoto University for their kind permissions to refer the experimental results. This work was partially supported by the

Grant-in-Aid for the Scientific Research Promotion of the Ministry of Education.

List of Publications by the Author

1. T. Iida, N. Wakayama and K. Sumita : Proceedings for the Symposium on Intense Pulsed Neutron Sources in Japan (Tokai) (1975) p. 205-223 (1975).
" Rapid Neutron Flux Monitering System for Pulsed Reactor ".

2. K. Sumita, T. Iida, et al. : Proceedings of US/Japan Seminar on Fast Pulse Reactors, (Tokai) (1976), p. 183-204 (1976).
" Rapid Response and Wide Range Neutronic Power Measuring Systems for Fast Pulsed Reactors ".

3. T. Iida, Y. Kokubo, K. Sumita, et al. : To be published in Nuclear Instruments and Methods.
" A Fast Response Electrometer for Pulse Reactor Experiments ".

4. T. Iida and K. Sumita : To be submitted in Nuclear Instruments and Methods.
" Transfer Function Measurement of Ionization Chambers ".

5. T. Iida and K. Sumita, et al. : To be submitted in the IEEE Transactions on Instrumentation and Measurement.
" A Fast Response Logarithmic Electrometer for Pulse Reactor Experiments ".